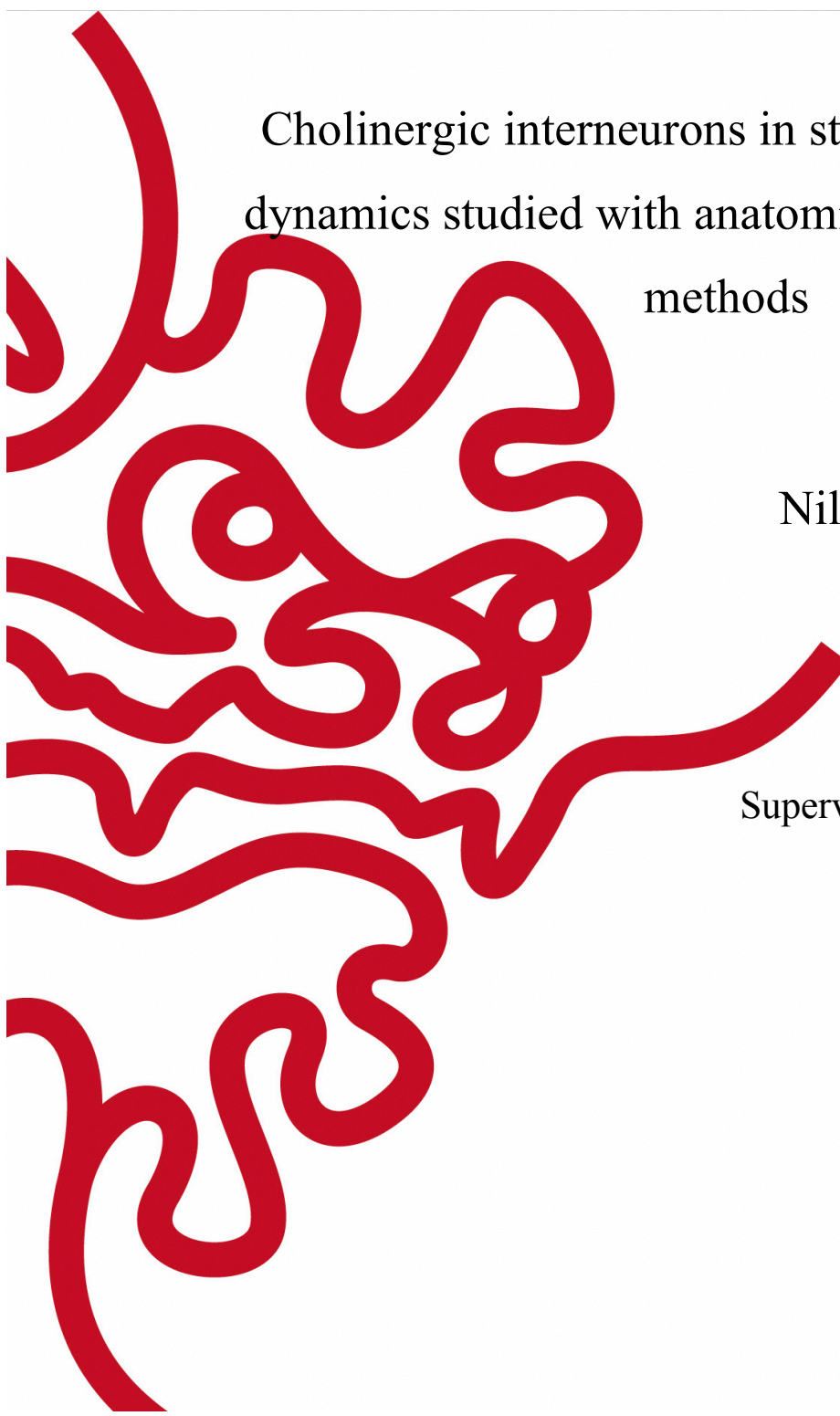


Okinawa Institute of Science and Technology Graduate  
University

Thesis submitted for the degree

Doctorate of Philosophy



Cholinergic interneurons in striatal microcircuit  
dynamics studied with anatomical and behavioral  
methods

by

Nilupaer Abudukeyoumu

Supervisor: Gordon W Arbuthnott

October, 2018



## Declaration of Original and Sole Authorship

I, **Nilupaer Abudukeyoumu**, declare that this thesis entitled “*Cholinergic interneurons in striatal microcircuit dynamics studied with anatomical, and behavioral methods*” and the data presented in it are original and my own work.

I confirm that:

- No part of this work has previously been submitted for a degree at this or any other university.
- References to the work of others have been clearly acknowledged. Quotations from the work of others have been clearly indicated, and attributed to them.
- In cases where others have contributed to part of this work, such contribution has been clearly acknowledged and distinguished from my own work.
- None of this work has been previously published elsewhere, with the exception of the following:

1. **N. Abudukeyoumu**, M. Garcia-Munoz, Y. Nakano, G. W. Arbuthnott (2018). " Impaired reach-to-grasp responses in mice depleted of striatal cholinergic interneurons." Society for Neuroscience, San Diego, USA (**Poster of the Year Award**).
2. **N. Abudukeyoumu**, Hernández-Flores T, M. Garcia-Munoz and G. Arbuthnott (2018). "Cholinergic modulation of striatal microcircuits." *European Journal of Neuroscience*.
3. Mekhail, S. P, **N. Abudukeyoumu**, J. Ward, G. Arbuthnott and S. N. Chormaic (2018). "Fiber-bundle-basis sparse reconstruction for high resolution wide-field microendoscopy." *Biomed Opt Express* **9**(4): 1843-1851.
4. **N. Abudukeyoumu**, Y. Nakano, M. Garcia-Munoz, G. W. Arbuthnott (2017). " Partial Deletion of Cholinergic Interneurons from Dorsolateral Striatum and its Role in Behavioral Responses." 12th International Basal Ganglia Society Meeting, Mérida, Yucatán. México.

5. **N. Abudukeyoumu**, M. Garcia-Munoz, O. P. Jaidar, G. W. Arbuthnott (2016). "Striatal cholinergic interneurons: their depletion and its progression." Society for Neuroscience, San Diego, USA.
  
6. **N. Abudukeyoumu**, M. Garcia-Munoz, Y. Nakano, O. P. Jaidar and G. Arbuthnott (2015). "Cholinergic interneurons sprouting in striatum?." British Neuroscience Association, Festival of Beuroscience, 23<sup>rd</sup> Meeting, Edinburgh, UK.
  
7. M. Garcia-Munoz, **N. Abudukeyoumu**, O. P. Jaidar, Lopez-Huerta, V. G, Y. Nakano and G. Arbuthnott (2014). "Cortical bursting activity is enhanced by blockade of astrocytic glutamate transporter." Astrocytes in Health and Neurodegenerative Disease. A joint Biochemical Society/British Neuroscience Association Focused Meeting. University College London, Institute of Child Health, UK.

Signature:

Date: October, 2018

## Acknowledgements

I would like to extend thanks to the many people in our research Unit, who so generously offered help to the work presented in this thesis.

Special mention goes to my enthusiastic supervisor, Gordon Arbuthnott. My PhD has been an amazing experience with peaks and valleys and I thank Gordon wholeheartedly, not only for his tremendous academic support, patient guidance, encouragement and valuable discussion which contributed greatly to the development of my research but also for giving me wonderful opportunities to participate many international conferences around the world to extend my knowledge in the field. His supervision and great scientific guidance were always helpful.

I am also hugely appreciative to Marianela Garcia-Munoz, especially for sharing her writing and proof-reading expertise willingly, and for being so dedicated to her role as academic editor for all of my manuscripts during publishing.

Similar profound gratitude goes to former postdoc Omar Jaidar, who has been a truly dedicated mentor and technical support to learn many experimental procedures, data analysis and how to efficiently design experiments. I am particularly indebted to Omar for his constant faith in my lab work, I have very fond memories of my time there.

I would like to express my special thanks of gratitude to my colleague Teresa Hernandez Flores for the golden opportunity to work together on the topic of “Cholinergic modulation of striatal microcircuits” which was published recently.

I am also very thankful to the technicians of Brain Mechanism for Behaviour Unit, Yoko Nakano and Maria Carter who contributed greatly to the experiments presented in this thesis. Other unit members special mention goes to Teresa Hernandez Flores for teaching me new calcium imaging method, Violeta Gisselle Lopez Huerta and Esther Lai for giving me feedback for presentations and valuable questions regarding my research.

To professor Jeff Wickens, for allowing me to attend Neurobiology Research Unit Neuroscience journal club, and for providing me with a fantastic discussion on many topics.

Also, Andrew liu, a technician in the same lab who guided loyally at the beginning of my research by teaching immunohistochemistry and answering my all of the questions. Sho Aoki and Masakazu Igarashi, for going far beyond the call of duty.

I also would like to thank professor Paul Bolam and Kenji Doya, the external and internal examiners at my PhD proposal defence. Paul Bolam made the long trip possible from UK to Okinawa and gave me insightful comments and feedbacks in regard to my proposal and research progress after the examination. Many thanks to professor Kenji Doya whom always ready to help and his constructive suggestions which were available during and after the proposal defence.

Many thanks also go to my thesis committee members Gail trip, Bern Kuhn and Mitsuhiro Yanagida whom were supported me throughout my PhD. Spending extra time to schedule the meetings and give me fully support and valuable discussions during each research progress report.

I appreciate the great supports from our lab administrator Hiroko Chinone, as well as the great supports from OIST student support section staffs and the Dean (Jeff Wickens and Ulf Skoglund). The financial support from government of Japan and Graduate school made it possible my stay in Japan and fully focus on research.

Finally, but by no means least, I would like to thank the great support and love of my parents, siblings, extended family members and friends made it possible for me to undertake my PhD. Their great supports once more proved the eternal truth of a proverb: *It takes a village to raise a child*. Especially thanks to my mom, **Talaykiz**, for her continued unbelievable support and encouragement who experienced all of the ups and downs of my research and without her I would not have come this far.

## List of abbreviations and acronyms

A list of all abbreviations that were used throughout this thesis and their full names provided in alphabetical order presented below:

<b>5-HT</b>	Serotonin
<b>A<sub>1</sub></b>	G protein coupled adenosine receptor type 1
<b>A<sub>2A</sub></b>	G protein coupled adenosine receptor type 2A
<b>AAVrh10</b>	adeno associated virus serotype 10
<b>AC</b>	Adenylate cyclase/Adenylyl cyclase
<b>ACh</b>	Acetylcholine
<b>AChE</b>	Acetylcholinesterase
<b>AMPA</b>	$\alpha$ -amino-3-hydroxy-5-methyl-4-isoxazolepropionic acid
<b>BG</b>	Basal ganglia
<b>BK</b>	Potassium current
<b>cAMP</b>	Cyclic adenosine monophosphate
<b>C<sub>v</sub></b>	Voltage gated calcium channel
<b>CCK</b>	Cholecystokinin
<b>CE</b>	Coefficient of error
<b>ChAT</b>	Choline acetyltransferase
<b>ChIs</b>	Cholinergic interneurons
<b>CRIs</b>	Calretinin expressing interneurons
<b>DA</b>	Dopamine
<b>DAPI</b>	4',6-diamidino-2-phenylindole
<b>DAT</b>	Dopamine transporter
<b>DLS</b>	Dorsolateral striatum
<b>DMS</b>	Dorsomedial striatum
<b>eCB</b>	endocannabinoid
<b>EnK</b>	Enkephalin
<b>EP</b>	Entopeduncular nucleus
<b>FAIs</b>	Fast adapting interneurons
<b>FSIs</b>	Fast-spiking interneurons
<b>GABA</b>	Gamma-aminobutyric acid
<b>GAD</b>	Glutamic acid decarboxylase
<b>GFAP</b>	Glial fibrillary acidic protein

<b>Glu</b>	Glutamate
<b>GP</b>	Globus pallidus
<b>GPe</b>	External globus pallidus
<b>GPi</b>	Internal globus pallidus
<b>HD</b>	Huntington's disease
<b>LDT</b>	Laterodorsal tegmental nucleus
<b>LTSIs</b>	Low threshold-spiking interneurons
<b>mAChRs</b>	Muscarinic acetylcholine receptors
<b>MG</b>	Myasthenia gravis
<b>MSNs</b>	Medium spiny neurons
<b>NAc/NAcc</b>	Nucleus accumbens
<b>nAChRs</b>	Nicotinic acetylcholine receptors
<b>NGFIs</b>	Neurogliaform interneurons
<b>NMDA</b>	N-Methyl-D-aspartic acid or N-Methyl-D-aspartate
<b>NOS</b>	Nitric oxide
<b>NPY</b>	Neuropeptide Y
<b>OFT</b>	Open field test
<b>P</b>	Postnatal age
<b>PD</b>	Parkinson's disease
<b>pDMS</b>	Posterior dorsomedial striatum
<b>Pf</b>	Parafascicular nucleus
<b>PKC</b>	Protein Kinase C
<b>PLC</b>	Phospholipase
<b>PPN</b>	Pedunculopontine nucleus
<b>PV</b>	Parvalbumin
<b>PVIs</b>	Parvalbumin-containing interneurons
<b>SABIs</b>	Spontaneously active bursty interneurons
<b>SK</b>	Small conductance calcium activated potassium channels
<b>SNc</b>	Substantia pars compacta
<b>SNr</b>	Substantia nigra pars reticulata
<b>SOMs</b>	Glutamate decarboxylase expressing somatostatin interneurons
<b>SP</b>	Substance P
<b>STN</b>	Subthalamic nucleus
<b>TAN</b>	Tonically active neurons



<b>THIs</b>	Tyrosine hydroxylase-expressing interneurons
<b>VA</b>	Ventral anterior nucleus
<b>vAChT</b>	Vesicular acetylcholine transporter
<b>vGLUT1</b>	Vesicular glutamate transporter type 1
<b>vGLUT2</b>	Vesicular glutamate transporter type 2
<b>VL</b>	Ventral lateral nucleus
<b>VMAT1</b>	Vesicular monoamine transporter 1
<b>VTA</b>	Ventral tegmental area

## List of Figures

Figure 1.1 The schematic diagram of direct and indirect pathways in basal ganglia circuits.	21
Figure 1.2 Schematic showing different cell types of striatal microcircuits and major inputs to the striatum that contribute to local microcircuit dynamics. ....	23
Figure 1.3 Classification of neuronal subtypes in the striatum.....	25
Figure 1.4 The synaptic connectivity probability between different neuronal cell types within striatal circuits estimated from paired recordings in slices from transgenic mice. ....	33
Figure 1.5 ACh receptor subtypes distinct expression on striatal neurons and signal transduction pathways. ....	37
Figure 2. 1 A schematic diagram for tissue preparation process for stereological systematic random sampling. ....	50
Figure 2. 2 Histological verification of specific lesion of cholinergic interneurons in the striatum. ....	55
Figure 2. 3 The ablation of ChIs in the striatum. ....	58
Figure 2. 4 vAChT positive puncta in the striatum show transient increase after ChAT-sap treatment. ....	61
Figure 2. 5 Histological verification of specific lesion of ChIs in transgenic mice striatum. .	63
Figure 2. 6 Histological verification of cholinergic neurons in PPN. ....	65
Figure 2. 7 Striatal volume comparison in control and ChAT-sap treated groups. ....	67
Figure 2. 8 Control groups volume. ....	68
Figure 2. 9 CE for ChIs counting. ....	70
Figure 2. 10 CE for terminal counting. ....	72
Figure 3. 1 Gradients of function and the subdivision of the striatum. ....	78
Figure 3. 2 Experimental time line. ....	81
Figure 3. 3 Schematic diagram for tissue preparation process for stereological systematic random sampling. ....	84
Figure 3. 4 Two behavior tests used for animals. ....	88
Figure 3. 5 The confirmation of ChIs depletion in ChAT- sap injected animals after behavioral training. ....	91
Figure 3. 6 The reach to grasp task performance. ....	93
Figure 3. 7 Shaping paw preference. ....	95

Figure 3. 8 Percentage of paw preferences of mice assessed by reach-to-grasp task. ....	98
Figure 3. 9 Paw preferences changes during the training sessions. ....	99
Figure 3. 10 The distinct reach to grasp task approach in lesioned and control group. ....	100
Figure 3. 11 The various reaching approaches of ChIs lesioned mice. ....	101
Figure 3. 12 Different levels of learners within intact control group. ....	103
Figure 3. 13 Latency to retrieve pellets. ....	106
Figure 3. 14 The reach-to-grasp attempts. ....	109
Figure 3. 15 The number of pellets achieved with a single reach-to-grasp action. ....	111
Figure 3. 16 The number of animals used in task. ....	112
Figure 3. 17 The confirmation of ChIs depletion in mice trained for behavior experiment. ....	113
Figure 3. 18 The correlation analysis of ChIs and the success rate. ....	114
Figure 3. 19 The path taken by individual mouse over a 15 minute testing session in the open field based on images taken from above. ....	115
Figure 3. 20 The exploratory behavior of mice in different conditions (1). ....	116

## List of Tables

Table 1. 1 Full list of systematic articles included for synaptic connectivity.....	33
Table 1. 2 Full list of systematic articles included for ACh receptor subtypes .....	37
Table 2. 1 The ChAT-sap toxin treated group .....	47
Table 2. 2 The Control group.....	47
Table 2. 3 The Sham group.....	47

## Contents

Acknowledgements .....	7
List of abbreviations and acronyms .....	9
List of Figures .....	12
List of Tables .....	14
Chapter 1 General Introduction .....	20
1.1 Basal Ganglia .....	20
1.2 Striatum.....	21
1.3 Striatal cell types .....	24
1.3.1 Medium - sized spiny projection neurons .....	25
1.3.2 Striatal interneurons .....	27
1.3.2.1 Cholinergic interneurons .....	27
1.3.2.2 Other types of interneurons.....	30
1.4 Source of acetylcholine and cholinergic receptors in the striatum.....	34
1.5 Striatal microcircuits.....	38
1.6 Striosomes and matrix .....	39
1.7 Movement disorders related to cholinergic interneurons.....	40
Chapter 2 Partial lesion of cholinergic interneurons from dorsolateral striatum and its progression.....	45
2.1 Introduction .....	45
2.2 Materials and methods .....	46
2.2.1 Animals and groups .....	47
2.2.2 Stereotaxic Surgery .....	48
2.2.3 Perfusion.....	50
2.2.4 Sectioning.....	51
2.2.5 Histology .....	51
2.2.6 Estimation of the total number of ChIs and vAChT boutons using the optical fractionator .....	52
2.2.7 Statistical analysis.....	53

2.3 Results.....	54
2.3.1 The confirmation of lesion with dual immunolabelling: ChIs and vAChT .....	54
2.3.2 ChIs decrease in ChAT- sap immunotoxin injected striatum.....	56
2.3.3 vAChT positive sprouts in ChAT-sap immunotoxin injected striatum .....	59
2.3.4 The observation of ChIs lesion in eGFP transgenic mice .....	62
2.3.5 The examination of PPN cholinergic neurons.....	64
2.3.6 Striatal volume loss in ChAT-sap lesioned group as measured by stereology during cell counting.....	66
2.3.7 Evaluation of ChIs counting accuracy with two different CEs .....	68
2.3.8 Evaluation of vAChT counting accuracy with two different CEs.....	71
2.4 Discussion .....	73
Chapter 3 Impaired reach-to-grasp responses in mice depleted of striatal cholinergic interneurons .....	77
3.1 Introduction.....	77
3.2 Methods.....	79
3.2.1 Animals and groups .....	79
3.2.2 Behavioral habituation and training.....	80
3.2.3 Stereotaxic Surgery.....	82
3.2.4 Perfusion.....	85
3.2.5 Sectioning.....	85
3.2.6 Histology .....	85
3.2.7 Estimation of the total number of ChIs in ChAT-SAP injected and behaviorally trained animals using the optical fractionator .....	86
3.2.8 Quantitative analysis of performance.....	88
3.2.8.1 Placement of pellet.....	88
3.2.8.2 1 <sup>st</sup> attempt.....	88
3.2.8.3 Successful retrieval on the first reach-to-grasp.....	88
3.2.8.4 Success or fail .....	89
3.2.8.5 Grasp count.....	89
3.2.8.6 Failed reaches.....	89
3.2.8.7 Criteria for learning curve within intact control animals .....	89
3.2.9 Statistical analysis.....	90

3.2.10 Ethical approval .....	90
3.3 Results.....	90
3.3.1 Immunostaining for ChAT shows loss of cholinergic interneurons after ChAT-sap toxin administration.....	90
3.3.2 The quantitative analysis of reach to grasp task performance in different groups .....	91
3.3.3 Paw preferences of mice in different groups.....	94
3.3.4 The variability of reaching-approaches in lesioned and non-lesioned group.....	99
3.3.5 The different levels of performance within intact control group.....	102
3.3.6 The latency to retrieve 5 pellets.....	104
3.3.7 The latency to retrieve first pellet.....	107
3.3.8 The number of reach-to-grasp attempts .....	108
3.3.10 The number of pellets achieved with a single reach-to-grasp action.....	110
3.3.11 The number of mice that did not attend to the reach-to-grasp task .....	112
3.3.12 Significant decrease of ChIs on lesioned compared to control side .....	112
3.3.12 The correlation of ChIs lesion and success rate.....	114
3.3.14 Open field test.....	115
3.4 Discussion .....	118
Chapter 4 Conclusion.....	124
4.1 Thesis summary.....	124
4.2 Impact and future work.....	124
References.....	126

# **Cholinergic interneurons in striatal microcircuit dynamics studied with anatomical and behavioral methods**

by

Nilupaer Abudukeyoumu

Submitted to the Graduate School in partial fulfillment of the requirements for the degree of  
Doctorate of Philosophy at the Okinawa Institute of Science and Technology Graduate  
University

## **Abstract**

Basal ganglia (BG) refer to a group of nuclei in the brain's subcortical regions. They are associated with cerebral cortex, thalamus and brainstem structures that perform many functions including motor control, procedural learning and memory. The largest nucleus of the BG is striatum that has two major neuronal cell types: medium spiny neurons and interneurons. This thesis focuses on one class of interneurons containing choline acetyltransferase (ChAT), the cholinergic interneurons (ChIs). This thesis investigated the role of ChIs in striatal microcircuit dynamics by anatomical and behavior approaches. ChIs participate in voluntary motor control, associated in learning, procedural memory, action selection, planning and execution of movement, through strong cholinergic inputs to other striatal neurons. However, the basic anatomical properties of ChIs after targeted lesion is poorly understood, though others have studied the behavioral consequences of toxin injection. The immunotoxin ribosome inactivating protein (saporin, sap) physically linked to choline acetyltransferase (ChAT-sap) selectively damaged striatal ChIs in toxin-treated mice monitored at 2, 4 and 6 weeks after application of the toxin. Systematic random cell counting, reach-to-grasp behavior task and open field test (OFT) was used to explore anatomical and behavioral differences in animals where the ChIs were destroyed in dorsolateral striatum (DLS). The thesis analyses yielded an unexpected outcome of specific ChIs lesion in DLS where vesicular acetylcholine transporter (vAChT) positive terminal numbers increased while the numbers of neurons themselves were reduced. The increase in vAChT positive terminals might derive from compensatory axonal sprouting from surviving ChIs, or from afferent axonal terminal fields of cholinergic mesopontine neurons. But the source was not further investigated in this study. In addition, the



study showed the decreased number of ChIs in injection site with no recovery after 2, 4, and 6 weeks' time in this study. The thesis also reports the effect of a selective depletion of ChIs from the DLS in a reach-to-grasp task. The mean percentage of successful grasps for the last 6 training sessions was almost half of the value for intact control, and sham operated mice. These results indicate that striatal depletion of ChIs impairs success rate, learning, motor skills in the reach-to-grasp task was observed. These results suggest that the participation of ChIs in striatal mediated motor learning impacts the function of the whole striatal microcircuitry. The lack of ChIs also altered rearing behavior (total number and duration), travelled distance and speed of movement in an open field. In addition, the results are consistent with an important participation of acetylcholine in striatal mediated behaviors possibly by their significant innervation from motor cortex.

# Chapter 1 General Introduction

## 1.1 Basal Ganglia

The basal ganglia (BG) are a group of highly interconnected subcortical nucleus of varied embryonic origins, located in the forebrain region of vertebrates. The main components of BG are striatum, substantia nigra pars reticulata (SNr), substantia nigra pars compacta (SNc), subthalamic nucleus (STN), internal globus pallidus (GPi) and external globus pallidus (GPe) (Albin *et al.*, 1989; Herrero *et al.*, 2002). These nuclei are involved in voluntary motor control, associated learning, cognitive functions, procedural memory, action selection, planning and execution of movement (Redgrave *et al.*, 1999; Herrero *et al.*, 2002; Kreitzer, 2009; Doig *et al.*, 2010; Stocco *et al.*, 2010; Gerfen & Surmeier, 2011).

The main components of BG form a circuit with two main input nuclei: the striatum and STN; an intermediate nucleus GP (GP, external segment or GPe in primates); and two output nuclei, the entopeduncular nucleus (EP, internal segment of GP or GPi) and the SNr. Additionally, the BG receive modulatory dopaminergic inputs from the SNc and ventral tegmental area (VTA). The former innervates the dorsal segment of the striatum while the latter nucleus sends projections to ventral striatum (Albin *et al.*, 1989; Bolam *et al.*, 2000; Herrero *et al.*, 2002; Wichmann & DeLong, 2003; Gerfen & Surmeier, 2011; Havekes *et al.*, 2011).

Basically, the striatum receives glutamatergic projections from all motor, sensory and associational cortical regions (Bolam *et al.*, 2000; Gerfen & Surmeier, 2011). Moreover, the thalamus provides a second major excitatory input to the striatum (Doig *et al.*, 2010). GP and SNr, the output gates of the BG system provide GABAergic input axons to thalamic nuclei that project back to frontal cortical areas. The input and output nuclei balance behavior initiation and planning of movement due to cortex and BG system working together as a loop. BG synapses can be modified by activity through a mechanism that depends on dopamine (DA) (Wickens *et al.*, 1996; Arbuthnott & Wickens, 2007; Gerfen & Surmeier, 2011) as well as the participation of other neurotransmitters (Lovinger, 2008). The connectivity within BG and main input into striatum can be seen in a simplified connectivity schematic diagram focused on striatum (*Figure 1.1*).

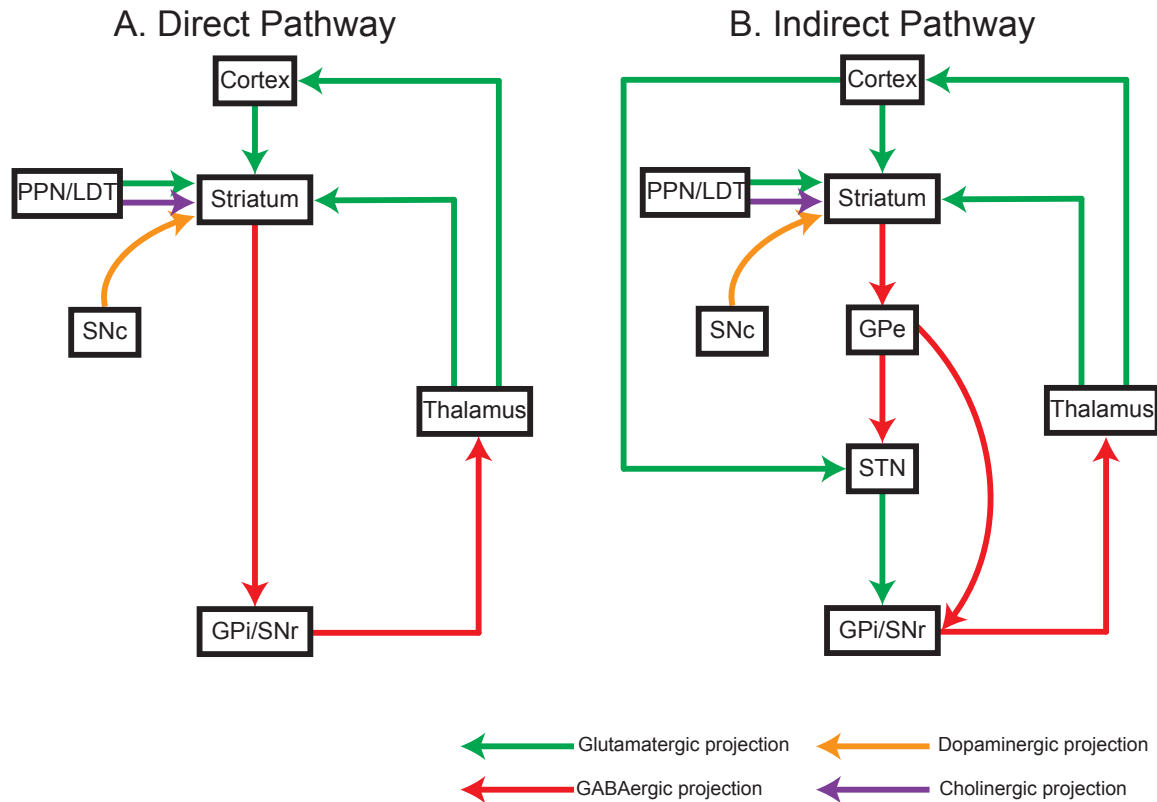


**Figure 1.1 The schematic diagram of direct and indirect pathways in basal ganglia circuits.**

**A.** In the direct pathway circuit, the striatum receives excitatory glutamatergic inputs from cortex, thalamus (ventral anterior nucleus (VA)/Ventral lateral nucleus (VL) complex) and PPN/LDT mid brain regions. Additionally, striatum also receives modulatory dopaminergic inputs from SNc and cholinergic inputs from PPN/LDT midbrain region. Transiently GABAergic inhibitory projections from the striatum project to tonically active GABAergic inhibitory neurons in the GPi and SNr, which in turn send GABAergic inhibitory projections to thalamus (VA/VL). Finally, thalamus sends glutamatergic excitatory projections to cortex. **B.** The indirect pathway includes the GPe and STN. The GPe GABAergic inhibitory neurons project to the STN, that also directly receives glutamatergic excitatory input from cortex. The STN neurons send excitatory projections to the GPi/SNr.

## 1.2 Striatum

The striatum is the biggest portion of subcortical BG nuclei, known as the neostriatum or striate nucleus is the main entrance to the BG output system that play important role in coordination of motor movement, mood, decision making, motivation cognition, memory and

procedural learning (Albin *et al.*, 1989; Graybiel *et al.*, 1994; Hikosaka *et al.*, 2000; Packard & Knowlton, 2002; Kreitzer & Malenka, 2008).

Structurally, the striatum in primates is divided by white matter (the internal capsule) into two large parts: caudate nucleus and putamen. A significant anatomical difference between primates and rodents is that this kind of separation is not present in BG circuits of rodents (Alexander *et al.*, 1986; Percheron *et al.*, 1987; Wickens, 1993). The inputs to the two compartments are different, caudate nucleus receives input from prefrontal cortex, and putamen receives input from somatosensory and motor cortex. However, even in rodent different areas have different inputs that form different functional and anatomical connections. For instance, DLS is the target of sensorimotor cortical areas, whereas the dorsomedial striatum integrates information coming from association cortices. The striatum also includes ventral striatum and the nucleus accumbens. Striatum receives two major excitatory glutamatergic inputs from layer V and VI cortical pyramidal neurons (in rat and monkey or also layer II, III in cat) (Jones *et al.*, 1977; Royce, 1982; Rakic *et al.*, 1986; McGeorge & Faull, 1989). Additional prominent inputs (**Figure 1.2**) from other parts of BG system into striatum (e.g. dopaminergic inputs from SNc, glutamatergic inputs from ventral VTA) increase complexity and diversity of striatal functions in different motor control, reinforcement learning and drug addictions (Usunoff *et al.*, 1976).

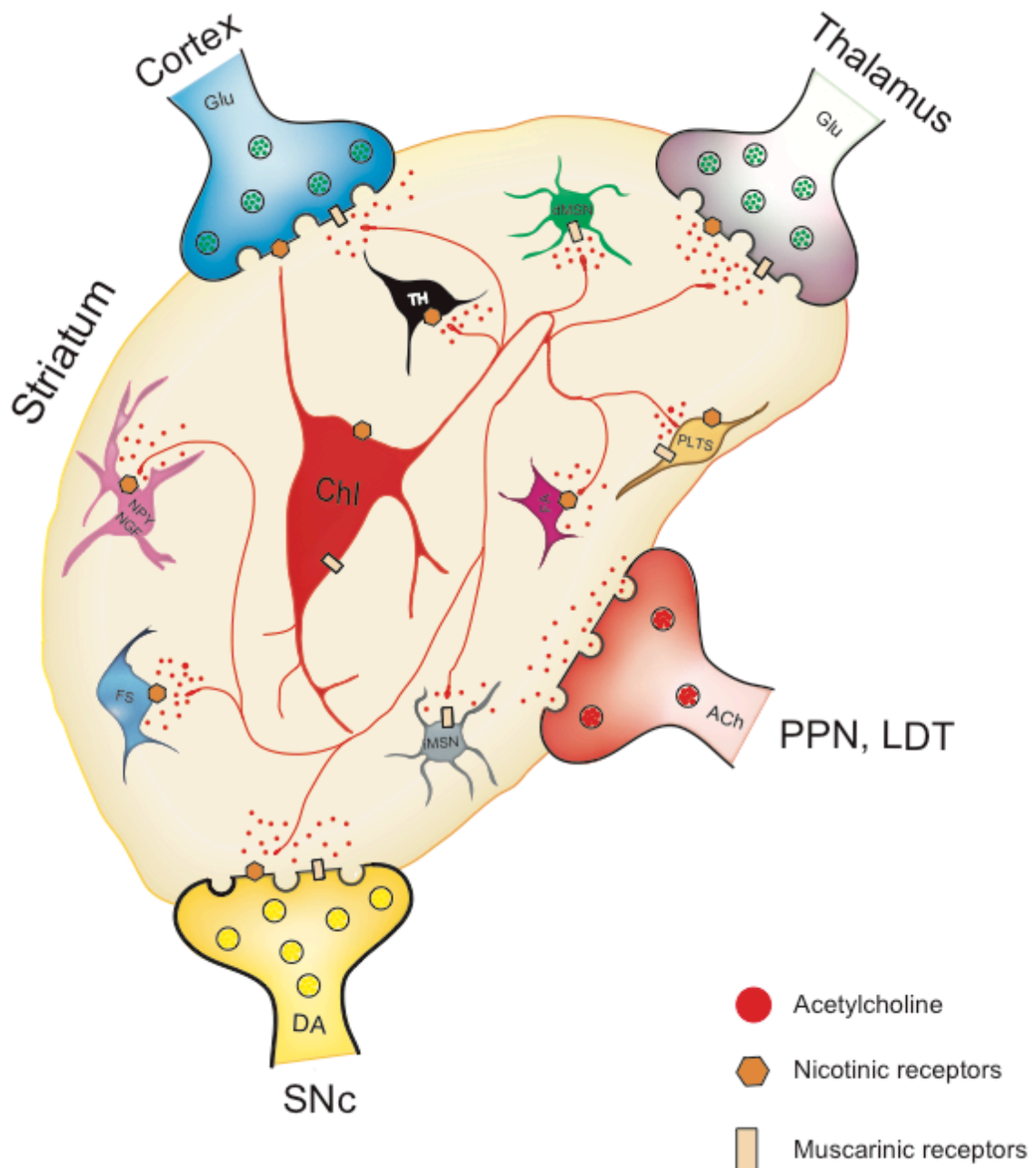


**Figure 1.2** Schematic showing different cell types of striatal microcircuits and major inputs to the striatum that contribute to local microcircuit dynamics.

### 1.3 Striatal cell types

The striatal microcircuit complexity (**Figure 1.2**) is increased by diversity of different neurons, interneurons, and a rich variety of neurotransmitters such as acetylcholine (ACh), DA, gamma-aminobutyric acid (GABA) serotonin (5-HT), substance P (SP) and glutamate (Glu) etc (Lynch *et al.*, 1972; Fonnum *et al.*, 1978).

On a macro level, there are two major cell types involved in striatal circuits (**Figure 1.3**): spiny cells/medium sized spiny projection neurons (MSNs) constitute 90-95% of striatal neurons and the remaining neurons are a neurochemically and morphologically distinct group of rarer aspiny local circuit neurons called interneurons, which are constitute 5-10% of the neuron population (Graveland & DiFiglia, 1985; Kawaguchi, 1993; Kawaguchi *et al.*, 1995; Kreitzer, 2009; Gerfen & Surmeier, 2011).

There are about 17 million corticostriatal neurons participate in the innervation of striatal microcircuits in the rat, formed from some 2.8 million neurons, that are unilaterally distributed and make GABAergic inhibitory synapses. Around half of these neurons make the direct pathway (**Figure 1.1. A**) and the other half form the indirect pathway (**Figure 1.1. B**) MSNs in rats (Oorschot, 1996; Zheng & Wilson, 2002; Wilson, 2013). Much of the literature about the basal ganglia is centered upon the differences in these two pathways, however, they are not the main focus of this thesis, nor even of the research of the unit in which these experiments were carried out. We will concentrate instead on the interneuron types including the Chi's that are our major interest in this thesis.

The second major cell type, the interneurons, are sub-divided into two groups: ChIs and GABAergic interneurons (Kawaguchi, 1993; Kawaguchi *et al.*, 1995; Silberberg & Bolam, 2015).

Interneurons (**Figure 1.3**) have been studied by [3H]-thymidine autoradiography, morphology, chemical markers expression properties, genetic deletion, optogenetic control, functional characteristics and electrophysiological properties (Steiner & Tseng, 2010). The most recent count of the individual types of interneurons includes: ChIs, tyrosine hydroxylase-expressing interneurons (THIs), low threshold interneurons (LTSIs), parvalbumin-containing interneurons (PVI) or fast spiking interneurons (FSIs), neuropeptide Y (NPY), NADPH

diaphorase, nitric oxide (NOS) and glutamate decarboxylase expressing somatostatin interneurons (SOM), calretinin expressing interneurons (CRIs) and spontaneously active bursty interneurons (SABIs) (Kimura *et al.*, 1981; Brecht *et al.*, 1991; Kawaguchi *et al.*, 1995; Figueredo-Cardenas *et al.*, 1996; Wu & Parent, 2000; Tepper & Bolam, 2004; Kreitzer, 2009; Ibanez-Sandoval *et al.*, 2010; Tepper *et al.*, 2010; Assous *et al.*, 2018). However, this list is not static; in fact, subclasses of new interneurons types are being discovered and characterized and BAC transgenic mice developed to aid their study (Silberberg & Bolam, 2015). The massive external inputs, local GABAergic MSNs and interneuron circuits work together to achieve organizational and functional physiology of striatum in different behavior tasks.

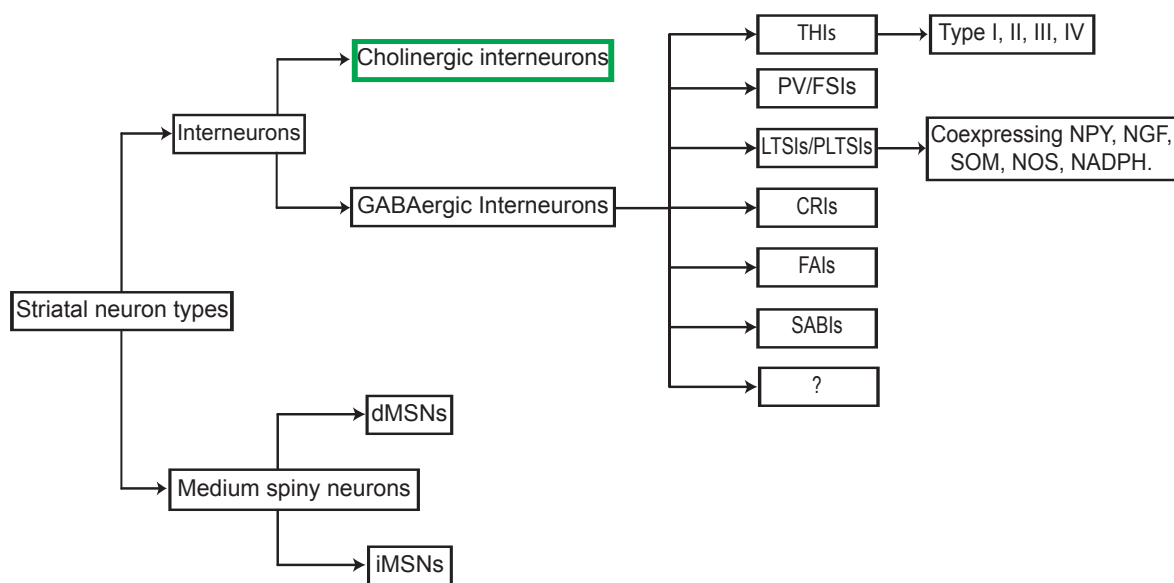


**Figure 1.3 Classification of neuronal subtypes in the striatum.**

### 1.3.1 Medium - sized spiny projection neurons

MSNs are inhibitory neurons that use GABA as their main neurotransmitter. Every MSN has glutamic acid decarboxylase (GAD) (Calabresi *et al.*, 2014) a synthetic enzyme for GABA (Kita & Kitai, 1988), GAD65 is extensively expressed by MSNs (Steiner & Tseng, 2010). MSNs make up approximately 90% of all striatal neurons (the portion of MSNs in different species varies from 90%-95%) (Kemp & Powell, 1971). The MSNs have spherical cell bodies roughly 10-20 $\mu$ m in diameter and up to 7 primary spiny dendrites that are 1.5-2.5 $\mu$ m in diameter in mammals (DiFiglia *et al.*, 1976; Bishop *et al.*, 1982; Graveland & DiFiglia, 1985). Their axons are arborized in a radius of 500 $\mu$ m and mutually inhibit other MSNs by the

release of GABA (Wilson & Groves, 1980). MSNs are the main target of cortical inputs and form the only output of striatum. Additionally, MSNs also receive inputs from thalamus and amygdala (DiFiglia *et al.*, 1976; Wilson & Groves, 1980). MSNs are subdivided into two categories: direct pathway medium spiny neurons (dMSNs) and indirect pathway medium spiny neurons (iMSNs) according to the types of receptors, G-protein expression and distinct projections targets (Abbott & Nelson, 2000).

Unlike other GABAergic interneurons, glutamatergic and dopaminergic terminals, MSNs do not exhibit large nAChRs currents (Zhou *et al.*, 2002) leaving mAChR as main target of cholinergic actions in striatal projection neurons. ACh evokes complex excitatory actions by direct modulation of several ionic currents, mainly  $K^+$ ,  $Na^+$  and  $Ca^{2+}$  (Pineda *et al.*, 1995; Perez-Rosello *et al.*, 2005; Shen *et al.*, 2007; Carrillo-Reid *et al.*, 2009b) and participates in plasticity of the striatum (Wang *et al.*, 2006).

Both dMSNs and iMSNs highly express M1 receptors (Bernard *et al.*, 1992; Yan *et al.*, 2001; Goldberg *et al.*, 2012) that are mainly found in spines on MSNs (Hersch *et al.*, 1994; Hersch & Levey, 1995; Alcantara *et al.*, 2001). M1 receptors increase neuronal excitability of both MSNs by enhancement of persistent  $Na^+$  conductance and by directly or indirectly depressing  $K^+$  currents (Akins *et al.*, 1990; Galarraga *et al.*, 1999; Figueroa *et al.*, 2002; Perez-Rosello *et al.*, 2005; Shen *et al.*, 2005; Shen *et al.*, 2007; Carrillo-Reid *et al.*, 2009b; Goldberg *et al.*, 2012; Perez-Ramirez *et al.*, 2015). Moreover, M1 receptors modulate  $Ca^{2+}$ -channels involved in neurotransmitter release and activating  $Ca^{2+}$ -dependent  $K^+$ -channels that shape MSNs firing pattern (Dolezal & Tucek, 1999; Galarraga *et al.*, 1999; Perez-Rosello *et al.*, 2005; Perez-Burgos *et al.*, 2008; Perez-Burgos *et al.*, 2010). Besides its direct modulatory actions on ionic currents, ACh also plays an important role in the regulation of synaptic transmission and striatal plasticity through the endocannabinoid (eCB) system (Oldenburg & Ding, 2011). At inhibitory synapses in MSNs, M1 receptors promote eCB production and retrograde activation of CB1 receptors resulting in suppression of this inhibitory synaptic transmission (Narushima *et al.*, 2007). While at glutamatergic synapses, M1 receptors reduce postsynaptic  $Ca_v1.3$  currents, which promote a decrease in eCB production and a decrease in activation of presynaptic CB1 receptors (Wang *et al.*, 2006).

On the other hand, M4 receptors are selectively expressed by dMSNs (Santiago & Potter, 2001; Yan *et al.*, 2001; Goldberg *et al.*, 2012) and their activation selectively increase



excitability of dMSNs by enhancing Cav1 Ca<sup>2+</sup>-channels and increase network activity (Hernandez-Flores *et al.*, 2015). In addition, M4 receptors play an important role in the plasticity of glutamatergic corticostriatal synapses (Shen *et al.*, 2015).

### 1.3.2 Striatal interneurons

#### 1.3.2.1 Cholinergic interneurons

In general, anatomical studies have revealed ChIs immunoreactive for choline ChAT, with a large multipolar cell body of 23 - 50µm in diameter with 3 to 6 primary dendrites that extend in a radial pattern (Doig *et al.*, 2014) and that arborize up to 1 mm (Kimura *et al.*, 1981; Bolam *et al.*, 1984b; Wilson *et al.*, 1990). Electron microscopy of rat striatal tissue performed by Doig *et al.* 2010; 2014, indicates that ChIs receive a prominent inhibitory input and that most of excitatory input is from thalamic afferents; a single ChI receives  $8450 \pm 694$  connections of which the majority are symmetric. Moreover, there are approximately three times more vesicular glutamate transporter type 2 (vGLUT2)-positive thalamic terminals than vesicular glutamate transporter type 1 (vGLUT1)-positive cortical terminals in an individual ChI (Doig *et al.*, 2014). It is important to mention that boutons expressing vGLUT1 (cortical) and vGLUT2 (thalamic) are the highest in the dorsal one-third in the rat striatum (Wouterlood *et al.*, 2012). In addition, the density of vGLUT1 and vGLUT2 in the striatum is highly age dependent. The expression level of vGLUT2 terminals in posterior dorsomedial striatum (pDMS) dramatically decreased in aged animals. By contrast, vGLUT1 density remained unchanged by age (Matamales *et al.*, 2016). However, since vGLUT2 is also expressed in some DA terminals in ventral striatum (Stuber *et al.*, 2010) it is harder to isolate thalamic inputs (Abudukeyoumu *et al.*, 2018).

In spite of the comparative small number of ChIs (Lehmann *et al.*, 1979; Bolam *et al.*, 1984a; Bennett & Wilson, 1999; Bennett *et al.*, 2000; Kreitzer, 2009; Girasole & Nelson, 2015), their long and many branched axons, allow a widespread release of ACh (Bolam *et al.*, 1984a; Contant *et al.*, 1996; Calabresi *et al.*, 2000; Abudukeyoumu *et al.*, 2018).

Similar to dopaminergic axon varicosities, cholinergic ones form few structurally defined synaptic connections, therefore favoring a slow cholinergic volume transmission

(Descarries *et al.*, 1997; Zhou *et al.*, 2001; Aznavour *et al.*, 2003; Coppola *et al.*, 2016; Ovsepian *et al.*, 2016; Dunant & Gisiger, 2017). The integration of a striatal cholinergic tone established by volume and synaptic transmission is considered to act within neuronal networks to change their balance of activity to possibly initiate neuronal ensembles with specific functions (Carrillo-Reid *et al.*, 2009a; Fuxe *et al.*, 2012; Abudukeyoumu *et al.*, 2018).

The spontaneously active firing characteristic of ChIs ensures the basal cholinergic tone (Kawaguchi *et al.*, 1995; Lee *et al.*, 1998; Wilson, 2005). These neurons have high input resistance, a broad action potential duration (Wilson *et al.*, 1990; Tubert *et al.*, 2016), a depolarized, and often changing, resting membrane potential that is often fixed at -60mV with a low holding current (Threlfell *et al.*, 2012). These interneurons also called “tonically active neurons or TANs” and “autonomous pacemakers”, are able to produce action potentials at 2-10 Hz in the absence of synaptic input (Bolam *et al.*, 1984a; Wilson *et al.*, 1990). Behind this tonic or pacemaking mechanism, is an interplay of several ionic conductances (Wilson *et al.*, 1990; Pisani *et al.*, 2007). Their pacemaker cycle begins with an initial tetrodotoxin-sensitive sodium current-induced depolarization, that leads to calcium influx from Cav<sub>2</sub> channels. This first calcium influx in turn, activates the calcium and voltage-activated big potassium currents (BK). This potassium influx contributes to membrane repolarization and activation of the Cav<sub>2.2</sub> current, that in turn, activates the small-conductance calcium-activated potassium current (SK). This second potassium current induces a medium duration after-hyperpolarization (mAHP) of 100 - 200 ms, that defines the spike pattern and spike width (Kawaguchi, 1992; Bennett *et al.*, 2000; Goldberg & Wilson, 2005). A decrease in intracellular calcium levels reduces the SK current and consequently the mAHP. The I<sub>h</sub> inward cyclic nucleotide-gated cation current (HCN) repolarizes the membrane to about -60 mV, with a resulting inactivation of the outward potassium A-type KV<sub>4</sub> current. At the end of the cycle, depolarization is slowed down, the persistent sodium current is activated, and the threshold for an action potential is reached, beginning a new sequence (Bennett *et al.*, 2000; Goldberg & Wilson, 2005; Deng *et al.*, 2007; Pisani *et al.*, 2007; Abudukeyoumu *et al.*, 2018).

Another feature of ChIs is a long pause in the tonic firing, that follows bursts of action potentials. Their intrinsic properties allow ChIs to fire in regular, irregular and in burst fashion interspersed with long pauses (Bennett *et al.*, 2000; Goldberg & Wilson, 2005; Wilson, 2005) (Sanchez *et al.*, 2011; Aceves Buendia *et al.*, 2017). During a burst, a subthreshold accumulation of calcium through Cav<sub>1</sub> channels recruits an additional potassium current that

in turn, produces a long-lasting (several seconds) hyperpolarization (sAHP) (Wilson & Goldberg, 2006; Tubert *et al.*, 2016; Abudukeyoumu *et al.*, 2018).

It is considered that the delta frequency activity of these interneurons results from the combination of synaptic inputs and intrinsic mechanisms (Beatty *et al.*, 2015). A muscarinic dependent coherence between motor cortex and ChIs can be established following optogenetic stimulation at both beta and low gamma frequencies (Kondabolu *et al.*, 2016). The reports on striatal oscillatory activity at different frequencies and the synchronization with other brain regions have been the topics of several recent publications (Brittain & Brown, 2014; Feingold *et al.*, 2015; Sharott *et al.*, 2017; Abudukeyoumu *et al.*, 2018).

Recordings of striatal neurons in behaving primates revealed two cellular striatal populations (Kimura *et al.*, 1984): phasic active neurons that show brief action potentials and low spontaneous activity or MSNs (Wilson & Groves, 1981; Apicella, 2017) and TANs that display a broader action potential and tonic spontaneous firing rate (<12 Hz) (Kimura *et al.*, 1984; Wilson *et al.*, 1990; Aosaki *et al.*, 1995; Apicella, 2002; Doig *et al.*, 2014; Apicella, 2017). Following electrophysiological criteria, TANs were considered as putative ChIs when antidromic stimulation from GP was unable to activate them (Kimura *et al.*, 1990; Kimura *et al.*, 1996). Moreover, in view of their morphological, electrophysiological, regional, functional and immunoreactivity similarities, TANs were identified as ChIs (Wilson *et al.*, 1990; Aosaki *et al.*, 1995; Bennett & Wilson, 1999; Reynolds *et al.*, 2004; Inokawa *et al.*, 2010; Goldberg & Reynolds, 2011; Bradfield *et al.*, 2013; Schulz & Reynolds, 2013; Atallah *et al.*, 2014; Abudukeyoumu *et al.*, 2018).

The fact that the firing properties of TANs are similar to some GABAergic interneurons has created confusion in their proper neuronal differentiation in extracellular recordings (Berke, 2008; Beatty *et al.*, 2012; Gonzales *et al.*, 2013; Gonzales & Smith, 2015; Apicella, 2017). It would be best to identify all interneurons, including cholinergic, not only associated to their extracellular electrophysiological characteristics but with other criteria. The systematic approach to interneuron research being developed (Kepecs & Fishell, 2014; Wamsley & Fishell, 2017) will provide a database of properly genetically classified interneurons (e.g., mRNA-expression profile, chemical markers expression properties). However, mRNA expression profiles can also be variable, so a single method might not be sufficient for classification. The

future will likely bring further determination of their individual electrophysiological characteristics and integrative properties (Abudukeyoumu *et al.*, 2018).

### 1.3.2.2 Other types of interneurons

The recent development in molecular technology and different types of transgenic mice has contributed immensely to the discovery of different cell types, synaptic connections and diversity of interneurons circuitry in the striatum. GABAergic interneurons are noticeably different from ChIs and GABAergic MSNs in morphology, expression of molecular markers, functional characteristics, and action potential shape. The GABAergic interneurons identified until now includes: FSI/PV<sup>+</sup>, THI, LTS/PLTS (NPY, NGF, SOM, NOS, NADPH), CRI, FAI and SABI (**Figure 1.3**).

Fast-spiking interneurons (**FSIs**) make up around 2.6% of striatal GABAergic cell population. Among the FSI, the best-characterized type is the one that express calcium-binding protein, parvalbumin (**PV**), which are characterized with a dense axonal arborization of over 600µm of diameter, display a high frequency action potential firing (200-300 Hz) with no spike adaptation and electronically coupling in groups by gap junctions (Kita *et al.*, 1990; Kawaguchi, 1993; Fukuda, 2009; Tepper *et al.*, 2010). The duration of their action potential is short and they are distributed more often in the dorsal striatal area. They receive a powerful cortical input and use GABA as neurotransmitter to form local cell connections to modulate the functional correlation between MSNs (Kubota *et al.*, 1993; Fukuda, 2009).

Tyrosine hydroxylase-expressing interneurons (**THIs**) are GABAergic neurons in striatum of different species (human, monkey, rat, and mouse) these TH<sup>+</sup> positive interneurons also express vesicular monoamine transporter 1 (VMAT1) and DA transporter (DAT) (Betarbet *et al.*, 1997). THIs use GABA as the main neurotransmitters but they do not release DA (Dubach *et al.*, 1987; Betarbet *et al.*, 1997; Meredith *et al.*, 1999; Palfi *et al.*, 2002; Lopez-Real *et al.*, 2003; Tande *et al.*, 2006; Huot & Parent, 2007; Ibanez-Sandoval *et al.*, 2010; Ibanez-Sandoval *et al.*, 2015). THIs comprise four subtypes (**Figure 1.3**): Type I, Type II, Type III, Type IV that constitute 60%, 13%, 6% and 21% of all striatal THIs in the striatum, respectively. THIs are medium sized with soma ranging from 11.4 to 24µm and the shape of soma differ such as round, ovoid and pyramidal. Aspiny and varicose dendrites are common

for all four types of THIs. Each different type of THIs has distinct electrophysiological properties such as input resistance, resting potential, action potential and firing rate for review see (Ibanez-Sandoval *et al.*, 2010; Ibanez-Sandoval *et al.*, 2015). TH<sup>+</sup> projection neurons can be found in SNc and VTA brain regions, which do use DA as neurotransmitter while the TH<sup>+</sup> interneurons of striatum do not (Kita *et al.*, 1986; Grace & Onn, 1989; Iribe *et al.*, 1999).

Low threshold-spiking interneurons (**LTSIs**) or plateau low threshold spike interneurons (**PLTSIs**) have tonic activity, low-threshold Ca<sup>2+</sup> spikes and a long calcium-dependent plateau potential (Kawaguchi, 1993; Kawaguchi *et al.*, 1995; Tepper & Bolam, 2004). They can be identified by their co-expression of NOS, NPY, the enzyme NADPH diaphorase, and SOM (Silberberg & Bolam, 2015). Among striatal interneurons, LTSIs have the least dense axonal arborization (Kawaguchi, 1993). SOM axons are distributed in the matrix area. They constitute 1-2% of the striatal cell population and vary in shape from round to triangular, with a soma of 12-33µm in diameter and long dendrites. These interneurons make symmetrical and asymmetrical synaptic contacts with other neurons. However, the symmetrical inputs are mainly situated on dendrites and spines in rats (DiFiglia & Aronin, 1982; Takagi *et al.*, 1983). Somatostatin expressing neurons are characterized electrophysiologically as having a large depolarizing plateau potential. Immunohistochemically, 20-40% of them express strong immunoreactivity for calcium binding protein D28K, a protein that buffers calcium inside of neurons (Kawaguchi *et al.*, 1995; Figueredo-Cardenas *et al.*, 1996).

Calretinin expressing interneurons (**CRIs**) are GABAergic interneurons that express the calcium binding protein, calretinin. They have a small aspiny soma of 7-20µm in diameter and are mostly immunoreactive for GAD67 (Kawaguchi *et al.*, 1995; Tepper *et al.*, 2010). In terms of their electrophysiological profile, little is known (Bennett & Bolam, 1993; Rymar *et al.*, 2004; Tepper & Bolam, 2004; Sharott *et al.*, 2012).

Recently, three newly identified interneurons have been described the FAI, NGFI and SABI (Ibanez-Sandoval *et al.*, 2011; Assous *et al.*, 2018).

Fast adapting interneurons (**FAIs**) are characterized by spike frequency adaptation during repetitive action potential firing patterns and the expression of the serotonin receptor, 5-HT<sub>3</sub> (5-HT<sub>3</sub>R) (Faust *et al.*, 2015). Nevertheless, other interneurons also co-express 5HT<sub>3</sub>R,

like PV<sup>+</sup> neurons that have both markers and show FSI electrophysiological features (Munoz-Manchado *et al.*, 2016).

Neurogliaform interneurons (**NGFIs**), as its name indicates, share similarities with cortical NPY-expressing neurogliaform cells and express NPY. Although they have NPY; they are not NPY-LTSI (Ibanez-Sandoval *et al.*, 2011; Silberberg & Bolam, 2015).

Spontaneously active bursty interneurons (**SABIs**) are medium sized GABAergic interneurons (cell body perimeter:  $73.94 \pm 15.6\mu\text{m}$ ), has 5-6 sparsely spiny dendrites of  $50\mu\text{m}$  in length and sparse axons arborized up to  $300\text{-}500\mu\text{m}$  from cell body which have been described based on morphology, intrinsic properties and highly varied burst-firing patterns recorded from 5-HT3R-Cre transgenic mice (Assous *et al.*, 2018). However, the connection (**Figure 1.4**) between SABI and MSNs is not significant (around 4.1%) indicates that SABI is not related to direct disinhibition process of MSNs, for more detailed description see (Assous *et al.*, 2018).

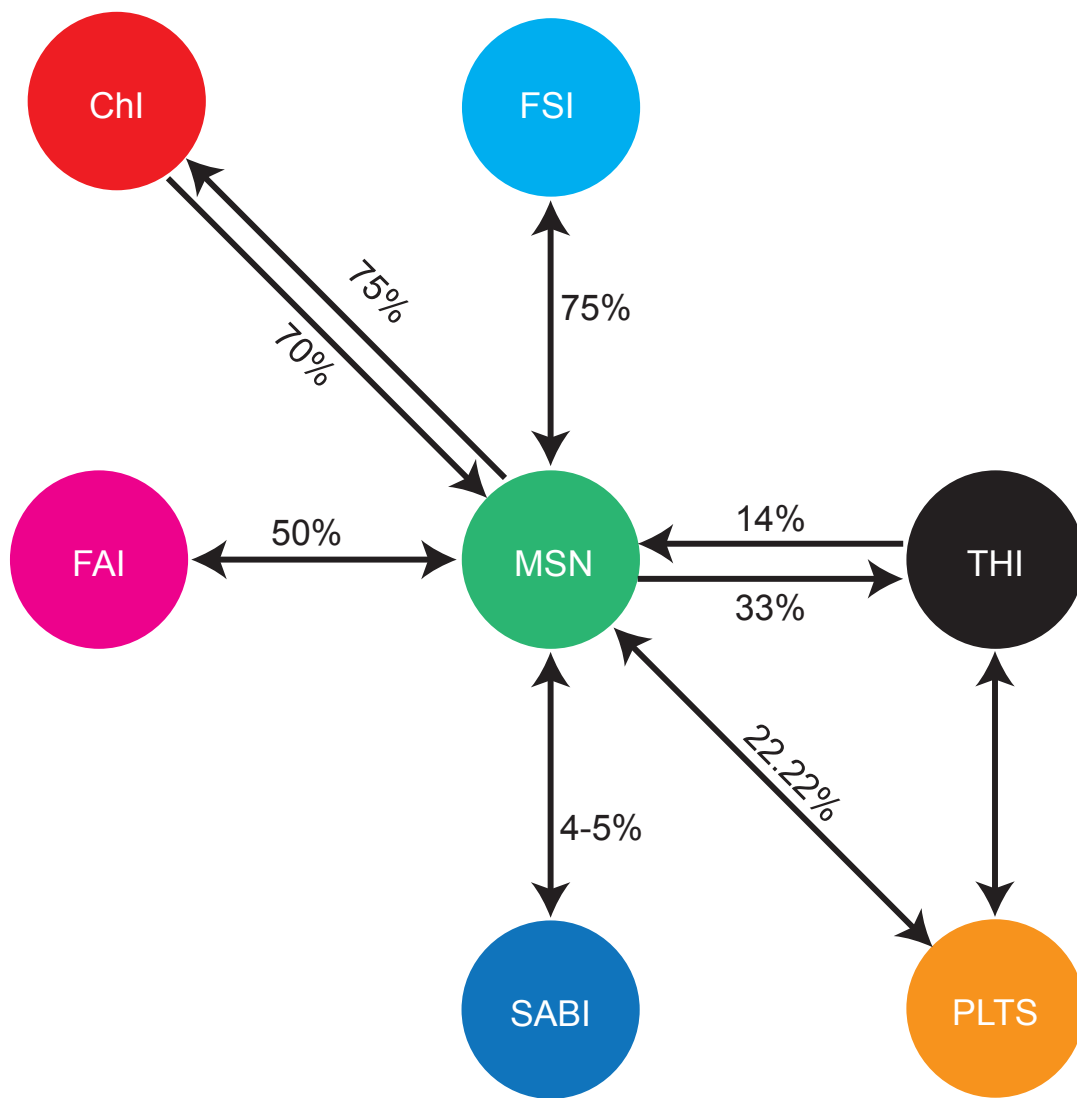


**Figure 1.4** The synaptic connectivity probability between different neuronal cell types within striatal circuits estimated from paired recordings in slices from transgenic mice.

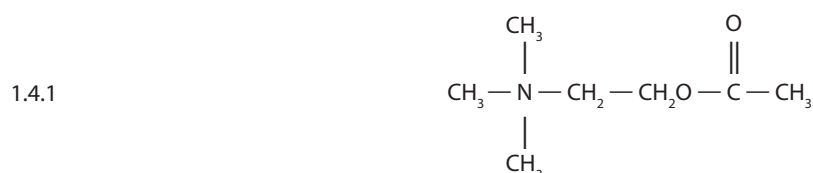
**Table 1. 1** Full list of systematic articles included for synaptic connectivity

Connections	Related references
MSN-FSI	Koos and Tepper (1999); Taverna <i>et al.</i> (2007); Chuhma <i>et al.</i> (2011)
MSN-THI	Ibanez-Sandoval <i>et al.</i> (2010); Xenias <i>et al.</i> (2015)
MSN-PLTS	Ibanez-Sandoval <i>et al.</i> (2011)

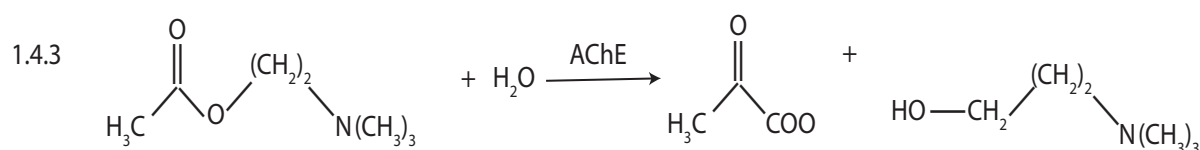
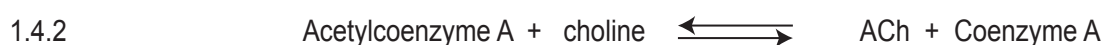
MSN-FAI	Faust <i>et al.</i> (2015)
MSN-ChI	Chuhma <i>et al.</i> (2011); Gonzales <i>et al.</i> (2013); Lim <i>et al.</i> (2014); Mamaligas and Ford (2016)
MSN-BABI	Assous <i>et al.</i> (2018)

## 1.4 Source of acetylcholine and cholinergic receptors in the striatum

Acetylcholine is an organic chemical and was the first neurotransmitter to be discovered in the mid-1920s. Most ACh is stored in nerve endings/terminals in synaptic vesicles, ACh can be an excitatory neurotransmitter or a neuromodulator (Loewi, 1921; Mellanby, 1955; Delcastillo *et al.*, 1963; Del Castillo *et al.*, 1967). The chemical structure of ACh is as follows:



ACh is synthesized by a single step reaction with choline acetyltransferase as a catalyst in reaction (1.4.2), by contrast acetylcholinesterase (AChE) catalyzes the breakdown process of ACh (1.4.3) as following chemical structure formula:



An early study indicated that destroying possible afferent pathways to striatum “cortex, thalamus, globus pallidus or ventro tegmental area”, did not affect the activity of choline acetylase nor acetylcholinesterase (AChE) or the histochemical staining within the nucleus (McGeer *et al.*, 1971; Lynch *et al.*, 1972). This led to the hypothesis that interneurons were the main source of striatal ACh. We now know external sources of ACh arrive from the pedunculo pontine (PPN) and laterodorsal tegmental nuclei (LDT) (Dautan *et al.*, 2014), nonetheless, the main source of striatal ACh still are the local spontaneously active ChIs (Kitai



& Surmeier, 1993; Pisani *et al.*, 2007; English *et al.*, 2012; Goldberg *et al.*, 2012; Abudukeyoumu *et al.*, 2018).

AChE is an enzyme that breaks down acetylcholine in the brain. Markers for cholinergic signaling such as ChAT, AChE and the vesicular acetylcholine transporter (vAChT) are the highest in the striatum, within the brain (Zhou *et al.*, 2002).

The earliest study conducted by Butcher and his colleague observed that the small area of striatum (striosome/patch) that are rich for AChE in lateral part of immature striatum but inverse in the at adult brain stage (Butcher & Hodge, 1976). In addition, opiate receptors and SP immunostaining matches the AChE- and somatostatin- poor striosomes in adult rat striatum (Herkenham & Pert, 1981). Furthermore, substantia nigra dopaminergic cell terminals in the striatum appeared to be situated in patches, and the axons mesencephalic dopaminergic cell marker cholecystokinin (CCK) was also found in patches of striatum (Hokfelt *et al.*, 1980). The discrepancy between immature and mature brains in different species and different neuronal markers (AChE, CCK, DA, opiate receptors, enkephalin, SP) indicated that the function of some neuronal structures can change as brain maturation proceeds (Butcher & Hodge, 1976; Chesselet & Graybiel, 1986; Crittenden & Graybiel, 2011).

In the adult, the matrix is the largest compartment and stains strongly for AChE, neurotensin receptors and calcium binding protein calbindin D28K. The thalamic parafascicular nucleus (pf) projections target ChI dendrites are distinctly distributed in matrix and avoid the striosomes stained for opiate receptors and poor in AChE (Herkenham & Pert, 1981). In addition, striatal ChIs are enriched in the matrix but many axons cross the border between patch and matrix (Kawaguchi, 1997; Crittenden *et al.*, 2017).

At the cellular level, ACh exerts its actions through activation of two classes of receptors, muscarinic (mAChR) and nicotinic (nAChR). Muscarinic mAChRs belong to the G-protein coupled receptor family (Caulfield, 1993). These receptors are divided into group I ( $M_1$ ,  $M_3$ , and  $M_5$ ) and group II ( $M_2$  and  $M_4$ ) (**Figure 1.5**).  $M_1$  receptors are coupled to  $G_{q/11}$  proteins via  $\alpha$  subunits that activate protein kinase C (PKC) and phospholipase C (PLC) and cause activation of inositol triphosphate and diacyl-glycerol that results in an increase in intracellular calcium.  $M_1$  receptors are found in striatal MSNs of both the direct and indirect type. In MSNs, these receptors are located presynaptically, extrasynaptically and

postsynaptically in dendritic spine necks (Hersch & Levey, 1995; Yan *et al.*, 2001). Group II receptors are coupled to  $G_i$  proteins, inhibit adenylyl cyclase (AC) activity and close  $Ca_v2$  calcium channels while opening  $K_{ir3}$  potassium channels (Caulfield, 1993; Nathanson, 2000; Eglén, 2006; Haga, 2013). Group II receptors act as autoreceptors on ChIs and are located mostly extrasynaptically, suggesting a role in volume neurotransmission (Bernard *et al.*, 1998).  $M_2$  receptors act as inhibitory heteroreceptors on striatal NPY-SOM expressing GABAergic interneurons and on corticostriatal glutamatergic terminals (Hersch *et al.*, 1994; Bernard *et al.*, 1998; Abudukeyoumu *et al.*, 2018).

The high degree of similarity of the orthosteric ligand-binding site in all five types of mAChRs (**Figure 1.5**), is the main reason it has been difficult to identify subtype-selective ligands (Eglén, 2006; Dencker *et al.*, 2012) and a reason why dissection of specific cholinergic effects on neuronal activity and release, have been difficult to achieve. Nevertheless, new pharmacological tools, such as the highly-specific antagonist peptide isolated from the green mamba snake venom are now being used (Jerusalinsky *et al.*, 2000; Karlsson *et al.*, 2000; Rowan & Harvey, 2011; Servent *et al.*, 2011). Similarly, positive allosteric modulators and allosteric agonists are becoming promising tools, even providing some therapeutic potential for several central nervous system diseases (Digby *et al.*, 2010; Bock *et al.*, 2017; Abudukeyoumu *et al.*, 2018).

ACh release is regulated by presynaptically located hetero- and autoreceptors. mAChRs ( $M_2/M_4$ ) (Hersch *et al.*, 1994; Ding *et al.*, 2006) via direct  $G_i$  mediated inhibition of presynaptic  $Ca_v2.2$  and  $Ca_v2.1$  calcium channel linked to exocytosis. Another presynaptic control of release, is regulated by the  $M_4$  auto- and hetero- receptor activation of the barium-sensitive potassium currents carried through  $K_{ir3}$  potassium channels in ChIs (Yan & Surmeier, 1996; Ding *et al.*, 2006) and corticostriatal terminals (Calabresi *et al.*, 1998; Abudukeyoumu *et al.*, 2018).

nAChRs receptors (**Figure 1.5**) are pentameric ligand-gated ion channels that consist of either heteromeric subunit combinations of  $\alpha$  subunits ( $\alpha 2-10$ ) and  $\beta$  subunits ( $\beta 2-4$ ) or homomeric  $\alpha$  subunits ( $\alpha 7$ ) (Exley & Cragg, 2008; Gotti *et al.*, 2009). The most common type of nAChR in striatum is the  $\alpha 4\beta 2^*$  type (the asterisk indicates the presence of other possible subunits in the receptor complex) (Quik & Wonnacott, 2011); this sub-composition acts as an auto-receptor in ChIs, as postsynaptic heteroreceptor in GABAergic interneurons and as

presynaptic heteroreceptor in GABA, serotonin and DA axon terminals (Eskow Jaunarajs *et al.*, 2015). The reported subunit composition on GABAergic interneurons and MSNs is proposed to have the  $\alpha 4\beta 2^*$  and  $\alpha 4\alpha 5\beta 2^*$  subtypes (Eskow Jaunarajs *et al.*, 2015; Abudukeyoumu *et al.*, 2018). In addition, nAChRs on dopaminergic axon terminals play a major role in the potentiation and shaping of DA release within the dorsolateral striatum (Exley & Cragg, 2008).

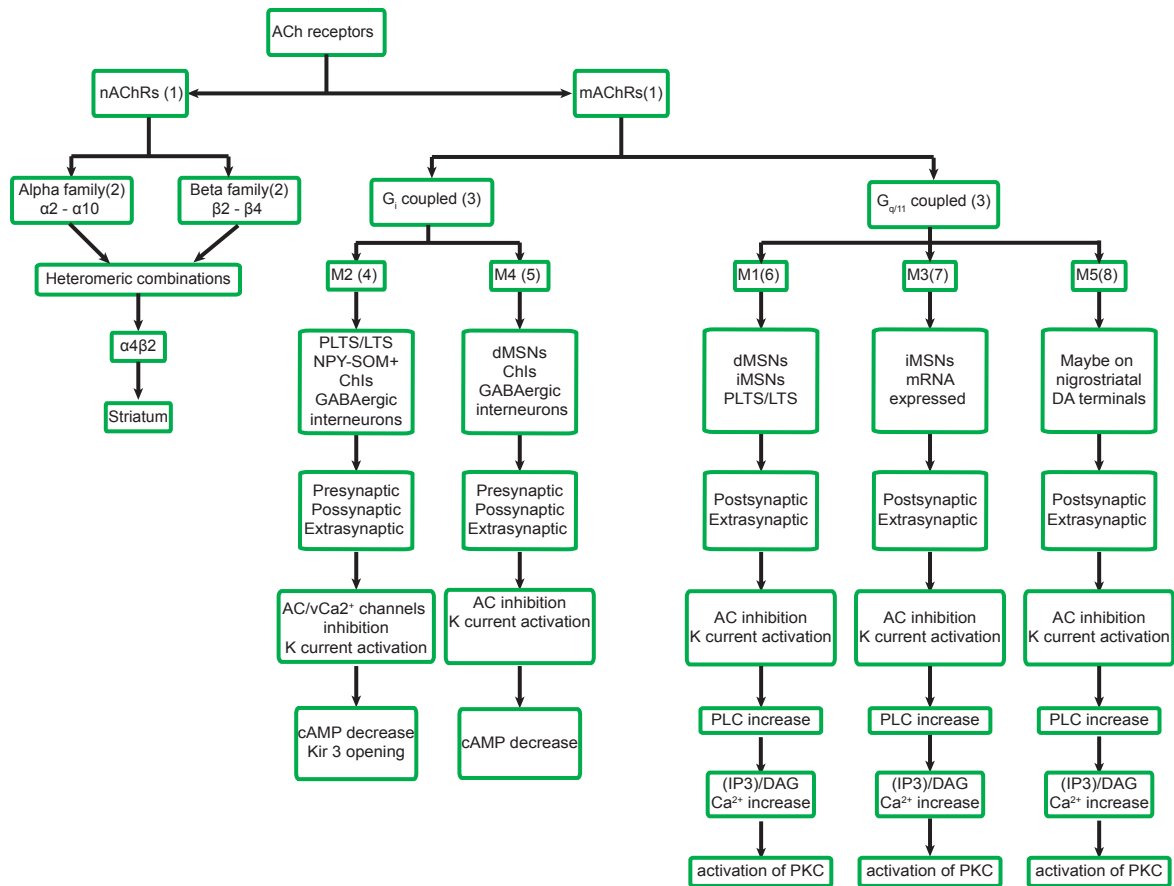


**Figure 1.5 ACh receptor subtypes distinct expression on striatal neurons and signal transduction pathways.**

**Table 1. 2 Full list of systematic articles included for ACh receptor subtypes**

	Related references
1	Hulme <i>et al.</i> (1990)
2	Hurst <i>et al.</i> (2013)
3	Eglen (2006); Ishii and Kurachi (2006)

4	Peralta <i>et al.</i> (1987); Hulme <i>et al.</i> (1990); Bernard <i>et al.</i> (1992); Hersch <i>et al.</i> (1994); Bernard <i>et al.</i> (1998); Eglen (2006); Eskow Jaunaraajs <i>et al.</i> (2015)
5	Hulme <i>et al.</i> (1990); Bernard <i>et al.</i> (1992); Bernard <i>et al.</i> (1998); Bernard <i>et al.</i> (1999); Yan <i>et al.</i> (2001); Eglen (2006); Pancani <i>et al.</i> (2014); Eskow Jaunaraajs <i>et al.</i> (2015)
6	Shapiro <i>et al.</i> (1988); Hulme <i>et al.</i> (1990); Bernard <i>et al.</i> (1992); Hersch <i>et al.</i> (1994); Alcantara <i>et al.</i> (2001); Yan <i>et al.</i> (2001); Eglen (2006); Qin <i>et al.</i> (2011); Eskow Jaunaraajs <i>et al.</i> (2015)
7	Akiba <i>et al.</i> (1988); Hulme <i>et al.</i> (1990); Hersch <i>et al.</i> (1994); Niittykoski <i>et al.</i> (1999); Yan <i>et al.</i> (2001); Zhang <i>et al.</i> (2002); Eglen (2006); Qin <i>et al.</i> (2011); Eskow Jaunaraajs <i>et al.</i> (2015)
8	Bonner <i>et al.</i> (1988); Liao <i>et al.</i> (1989); Hulme <i>et al.</i> (1990); Hersch <i>et al.</i> (1994); Yan <i>et al.</i> (2001); Eglen (2006); Qin <i>et al.</i> (2011); Foster <i>et al.</i> (2014); Eskow Jaunaraajs <i>et al.</i> (2015)

## 1.5 Striatal microcircuits

The striatum is a subcortical brain region with little visible anatomical sub-structure (**Figure 1.2**). Paired recordings from different cell types made it possible to measure the strength of connection between different cell types (**Figure 1.4**). Increasingly the initial divisions into direct output pathway for GO signals and indirect pathway to stop has not been supported by experiment (Albin *et al.*, 1989; Cui *et al.*, 2013). Instead we have the notion that this internally inhibitory network works by selecting assemblies of neurons dynamically to control animal behavior (Jaidar *et al.*, 2019). The exact role of the ChIs in this is not clear but they are in an excellent position to control both the intensity of firing among MSNs and also, because of the extent of their axonal arbors, to choose groups of cells to be included in assemblies.

Early work by a pioneer in the field of striatal assemblies (Carrillo-Reid *et al.* 2009) suggested that the presence of ACh in striatal slices made the assemblies align in ‘sentences’ of longer sequences. The arrangement allowed for the recognition of groups of striatal neurons in the slice to fire as dynamic assemblies and the sequences of their recruitment became more complex in the presence of cholinergic agonists. This thesis explores some of the anatomical

and behavioral consequences of damage to the ChIs in DLS, in the expectation that the changes in circuit dynamics would have some obvious consequences for the functions of the area. The thesis describes the time course of the damage to the striatal cholinergic system and the behavioral results of the damage.

## 1.6 Striosomes and matrix

Almost 40 years ago Graybiel and Ragsdale (1978) reported two distinct densities or compartments in the distribution of AChE in the striatum of primates and cats. These two topographically heterogeneous compartments are called striosomes or patches, and the matrix that constitutes around 80% of striatum volume. Striosomes and matrix are chemically and functionally distinct units that develop at different stages (Graybiel & Ragsdale, 1978; Johnston *et al.*, 1990). The patch and matrix are identified by neuro-chemicals and enzymes. Patch and matrix have different input and output synaptic connections. An early tracing study by injecting anterograde axonal tracer Phaseolus Vulgaris leucoagglutinin into different cortical areas and cortical layers found that deep layer V and VI cortical neurons project to striatal patches which are zones for enkephalin (EnK), AChE and other neuronal markers (Gerfen, 1989). Moreover, he observed that the projection to the matrix compartment originated from layer V, II, and III. Striosomes receive DA afferents from SNc and glutamatergic afferents from medial prefrontal, anterior cingulate, orbitofrontal and anterior insular cortices whereas matrix receives inputs from sensorimotor cortex (Kawaguchi *et al.*, 1989; Benarroch, 2016; Abudukeyoumu *et al.*, 2018).

Patch GABAergic MSNs project to GPi, GPe, SNr (in squirrel monkeys), D1MSNs of striosome project to SNc (Fujiyama *et al.*, 2011; Watabe-Uchida *et al.*, 2012; Crittenden *et al.*, 2016). Similarly, matrix MSNs project to GPi, GPe and SNr (Fujiyama *et al.*, 2011). Interestingly, both striosome and matrix mosaic compartments include direct and indirect pathway GABAergic neurons (Gimenez-Amaya & Graybiel, 1991; Fujiyama *et al.*, 2011). Furthermore, matrix GABAergic projection neuron targets are thought to be different, which means that matrix indirectly regulates the afferent-efferent of striatal microcircuit especially the output of striatum (Kawaguchi *et al.*, 1990; Fujiyama *et al.*, 2011; Watabe-Uchida *et al.*, 2012; Crittenden *et al.*, 2016). To sum up, even though both patch and matrix have both types

of MSNs (direct and indirect pathway), the neurochemical and connectional heterogeneity suggest different functions.

Stereological analysis in humans has revealed a differential distribution of ChIs with most of them located in the periphery of the striosomes (Bernacer *et al.*, 2007). Similarly in rodents, ChIs are found in the border of striosomes (Kubota & Kawaguchi, 1993) with extended processes into both compartments (Kubota *et al.*, 1993). In recent reviews, ChIs and their dendrites are described as preferentially located in the matrix, whereas their axons are abundant in both compartments (Crittenden & Graybiel, 2011; Crittenden *et al.*, 2017). Using new tools, attempts to exclusively stimulate one compartment in vitro are clarifying the location of ChIs. Whole-cell patch recordings of ChIs with a posterior identification of their compartment location, revealed that GABAergic currents mediated by nAChRs are more frequently observed in the matrix than the striosome (Inoue *et al.*, 2016). Also, photoactivation of the matrix compartment with a matrix specific adeno associated virus serotype 10 (AAVrh10) and patch-clamp recordings revealed lack of direct synaptic connectivity between matrix and striosome MSNs (Lopez-Huerta *et al.*, 2016). The presence of ChIs in the areas high in calbindin-D28K and ChAT (Prensa *et al.*, 1999) referred to as the “peristriosomal boundary”, reaffirm the location of ChIs between, as well as within, matrix and striosome compartments (Brimblecombe & Cragg, 2017; Abudukeyoumu *et al.*, 2018).

A separation between matrix and striosomes has been established in rats by their different thalamic afferents. Unzai *et al.* (2017) reported that striatum and nucleus accumbens receive afferents to the striosome compartment mostly from thalamic midline nuclei, whereas the intralaminar nuclei innervate the matrix compartment (Fujiyama *et al.*, 2011; Dautan *et al.*, 2014; Unzai *et al.*, 2017). Moreover, whereas most terminal fields form en passant boutons, clusters or plexus containing many boutons are observed in terminal fields of the pf. From the functional point of view, information from these two thalamic areas support the function previously inferred (Vertes *et al.*, 2015): limbic (emotional) control for the striosomes and sensorimotor associative for the matrix (White & Hiroi, 1998; Crittenden & Graybiel, 2011; Buot & Yelnik, 2012; Abudukeyoumu *et al.*, 2018).

## **1.7 Movement disorders related to cholinergic interneurons**

Impairment of striatal ChIs is central in the production of movement disorders and variable patterns of pathology (Pisani *et al.*, 2007). Altered cholinergic signalling is seen in a diverse class of syndromes that include Parkinson's disease (PD) (Brichta *et al.*, 2013; Kalia *et al.*, 2013; Ztaou *et al.*, 2016), dystonia (Peterson *et al.*, 2010; Eskow Jaunarajs *et al.*, 2015; Scarduzio *et al.*, 2017), Tourette's syndrome (Xu *et al.*, 2015; Albin *et al.*, 2017) and Huntington's disease (Di Filippo *et al.*, 2007; Abudukeyoumu *et al.*, 2018).

**PD** is a common neurological disorder characterized by a decreased DA level in the brain. Early clinical and experimental studies suggested that PD was also characterized by increased striatal extracellular levels of ACh (Barbeau, 1962; Cachope & Cheer, 2014). The main symptoms of PD include: resting tremor, slowness, shuffling gait, flexed posture, festination, falls, soft speech, dysphagia, "saliva trickling from the mouth", disturbed sleep, "torpid bowels" and dementia (Kempster *et al.*, 2007). Indeed, the earliest pharmacological treatment of PD consisted of administration of anti-cholinergic agents: diethazine (diparcol), solanaceous plant alkaloids, ethopropazine (parsidol), antimuscarinic agents, benztropine mesylate (cogentin), trihexyphenidyl (artane), cycrimine (pagitane), phenothiazine derivatives, ayurvedic herbs (e.g., weak antimuscarinic diphenylhydramine, benztropine, orphenadrine) procyclidine (kemadrin), biperiden (akinton) (Duvoisin, 1967; Manyam, 1990; Fahn, 2014). However, the cumulative effect of anticholinergic medication 'anticholinergic burden' (peripheral side effects), and the "anticholinergic risk" (risk of heart attack) was associated with a decrease in the use of anticholinergic in old hospitalized patients. In a study of databases reporting side effects of anticholinergics, Salahudeen *et al.* (2015) compiled a list of those anticholinergics frequently prescribed and indicated that medicated patients suffer more frequent falls and hip fractures, increased dyskinesias and suffer from hallucinations, blurry vision and memory impairment more than non-medicated patients. An elevation of cholinergic signalling in PD has been hypothetically related to alterations in ChI spiking (Tanimura *et al.*, 2017; Abudukeyoumu *et al.*, 2018).

As described before, M<sub>4</sub> autoreceptors in ChIs slow firing rate and ACh release (Zhang *et al.*, 2002). In the rodent model of PD, DA depletion induces an upregulation of RGS4-dependent processes that result in decreased M<sub>4</sub> signalling in ChI (Ding *et al.*, 2006). Thus, regulators of G protein signalling (RGS) modulation of ACh release might aid future treatment of patients. Experiments using the same animal model of PD, report that halorhodopsin photoinhibition of ChIs in mice, reduces akinesia, bradykinesia and sensory motor neglect;

whereas in wild type mice the specific striatal blockade of M<sub>1</sub> and M<sub>4</sub> receptors has a similar effect (Ztaou *et al.*, 2016). These results agree with the electrophysiological studies of muscarinic and dopaminergic interactions described by Hernandez-Flores *et al.* (2015); (Abudukeyoumu *et al.*, 2018).

Recently Burbulla *et al.* (2017), using long-term cultures of human induced pluripotent stem cell-derived DA neurons, have demonstrated a toxic cascade triggered by dysfunctional mitochondria that can induce neuronal pathological changes and the cellular dysfunctions observed in PD (Dagani *et al.*, 1992; Greenamyre, 2018; Singh *et al.*, 2019). Now research is centered on whether the same toxic mitochondrial intracellular cascade is present in the genetic and idiopathic forms of the disease and other hypotheses are also being tested. More work may eventually demonstrate the primary cause of SNc DA neuron death (Burbulla *et al.*, 2017; Abudukeyoumu *et al.*, 2018).

**Dystonia** involves intermittent or sustained abnormal involuntary muscle contractions that produce twisting postures in the absence of other neurological signs. Repetitive movement and uncontrolled muscle contractions can start early in childhood (Valente *et al.*, 1998; Klein & Fahn, 2013). Early onset of dystonia is a genetically determined mutation in the gene, TOR1A (Sciamanna *et al.*, 2012). As in PD, the reciprocal modulation between DA and ACh is at the center of dystonia. For instance, high-doses of anticholinergics (trihexyphenidyl, orphenadrine and biperiden) are used in the treatment of this disease (Burke *et al.*, 1986). Electrophysiological experiments in ChIs of mice overexpressing mutant torsin A, show that the sensitivity of a D<sub>2</sub> agonist-mediated inhibition of Ca<sub>v</sub>2.2 N-type current is increased. Following D<sub>2</sub> agonists a reduction in mAHP and threshold for action potentials is expected (Sciamanna *et al.*, 2011). In mice with a conditional knockout of the dystonia 1 protein, activation of thalamostriatal inputs induces a short pause and increased rebound activity in ChIs, that could result from a postsynaptic increase and a presynaptic decrease in M<sub>1</sub> and M<sub>2</sub>-dependent currents (Sciamanna *et al.*, 2012; Abudukeyoumu *et al.*, 2018).

**Gilles de la Tourettes syndrome**, is a neurodevelopmental disorder characterized by motor (blink eyes, head jerking, foot stamping, neck stretching, body twisting, bending, self-harming behavior like lip or cheek biting and head banging), vocal and phonic (often clearing throat over and over again, cough, sniff, grunt, yelp, bark or shout) tics, usually measured by the Yale Global Tic Severity Scale (Leckman *et al.*, 1989a). The symptoms vary a lot from



mild to severe, tic types and in different genders. In general, vocal or phonic tics appear in the earliest stage of TS onset and males have higher chance than females. In the last few years several advances have been achieved towards the understanding of the neuropathology of this syndrome (Abudukeyoumu *et al.*, 2018).

The participation of ChIs in Tourette's syndrome is supported by post-mortem findings of a significant 49% loss of cholinergic and 42% loss of parvalbumin-positive FS interneurons with no significant change in DARPP-32 expression in MSNs (Kataoka *et al.*, 2010), targeted lesion of ChIs in the DLS of adult mice show abnormal stereotypies (Xu *et al.*, 2015). Moreover, the radiotracer [<sup>18</sup>F] fluoroethoxy-benzovesamicol that is successfully used to image over-expressed vAChT marker in mice (Janickova *et al.*, 2017), failed to detect changes in the number of ChIs in Tourette's syndrome patients because this method does not provide enough resolution to count cells (Albin *et al.*, 2017), perhaps obscured by the pedunculopontine cholinergic afferents (Abudukeyoumu *et al.*, 2018).

Stereotypy is regarded as a predominant aspect of this syndrome. Using cocaine-induced stereotyped behaviours to test the function of ChIs, it is observed that a lesion of ChIs or blockade of mAChR (scopolamine) prolongs the time course of the stereotypy, whereas blockade of DA D<sub>2</sub> receptors (raclopride) stops the stereotypy presumably by increasing the extracellular ACh concentration (Aliane *et al.*, 2011). These results suggest that a restoration of cholinergic transmission may have important consequences in the arrest of stereotypy. This is supported by a decrease in stereotyped behaviors in children following administration of a cholinesterase inhibitor (donepezil) (Cubo *et al.*, 2008; Abudukeyoumu *et al.*, 2018). However, mice with increased ACh release also show increased stereotypy in response to amphetamine or cocaine, suggesting that it might be the overall balance rather than absolute levels of ACh that predicts pose to stereotypy (Crittenden *et al.*, 2014; Janickova *et al.*, 2017).

Pharmacological animal models of the syndrome have been produced following blockade of striatal GABA<sub>A</sub> receptors. In rats, mice and monkeys intrastriatal administration of specific GABA<sub>A</sub> antagonists (picrotoxin or bicuculine) induce increased activity in striatum and its outputs (i.e., STN and thalamus) and motor abnormalities similar to tics (McCairn *et al.*, 2009; Bronfeld *et al.*, 2013) for review see Yael *et al.* (2015); (Abudukeyoumu *et al.*, 2018).

**Huntington's disease (HD)** is a progressive late-onset neurodegeneration in the brain characterized by variable pathological pattern which includes psychiatric episodes, motor symptoms (rapid, irregular, and involuntary movement, chorea, dystonia at later stage) and cognitive deficit (mood swing, depression, irritability, aggression, anxiety, obsessive behavior, cognitive deficits). HD is caused by a CAG trinucleotide repeat expansion within the gene coding site that was identified in 1993. The resulting mutant huntingtin accumulates forming inclusion bodies with other proteins, initially in neurons of striatal and cortical motor and prefrontal areas (Shepherd, 2013). In post-mortem human tissue and rodent models of the disease, there is striatal pre- and postsynaptic loss of GABA, glutamate, and mAChRs (Penney & Young, 1982; Dure *et al.*, 1991) and a preferential degeneration of MSNs (Reiner *et al.*, 1988) with a faster loss of iMSNs (Cha *et al.*, 1998; Deng *et al.*, 2004; Starr *et al.*, 2008). Although the number of ChIs is relatively normal (Ferrante *et al.*, 1987) these interneurons have decreased levels of vAChT and ChAT (Smith *et al.*, 2006). The loss of various cells types and neuronal markers contributes to the dramatic reduction of striatum volume that can be observed at different stages of HD. The gradient of degeneration observed in human brain was reported as follows: from tail to head direction in caudate nucleus, from caudal to rostral in putamen, and more degeneration in dorsolateral than ventral region of striatum in coronal axis (Vonsattel & DiFiglia, 1998). There is 21-29% neuronal loss in cerebral cortex and a 57% neuronal loss in caudate nucleus that contributes to a total brain weight decrease to 20-30% (from about 1350g to 1067g on average). The source of variability in symptom subtype is not clear (de la Monte *et al.*, 1988; Abudukeyoumu *et al.*, 2018). However, the recent study showed that the degeneration of neurons in striosomes of striatum significantly associated with mood dysfunction in Huntington's disease patients (Tippett *et al.*, 2007).

In an animal model of the disease (Q140 Huntington-like mice), Deng and Reiner (2016) studied the specific vGLUT2 thalamic inputs to ChIs. They observed a reduction in the extension of the ChIs dendritic trees, with a subsequent loss of synapses, as also reported before (Deng *et al.*, 2013). The authors propose that a reduced cortical input to dMSNs could be responsible for an initial observed hypokinesia in mice. Then deficiency of thalamic excitatory input drive onto ChIs could lead to a subsequent loss of input on iMSNs that would be predicted to contribute to the early hyperkinesia in this animal model (Abudukeyoumu *et al.*, 2018).

## Chapter 2 Partial lesion of cholinergic interneurons from dorsolateral striatum and its progression

### 2.1 Introduction

The striatum (neostriatum) is the biggest portion and the main entrance of the BG circuits, which form a cortico-striato-thalamo-cortical loop that modulates motor control, motivation, learning and memory which ultimately contribute to survival of animals (Alexander & Crutcher, 1990; Graybiel, 1995; Wichmann & DeLong, 1996; McFarland & Haber, 2002).

ChIs are the subpopulation of striatal local circuit neurons that constitute less than 1 % of total cell number and are identified by the expression of ChAT in the cell body (Bolam *et al.*, 1984b; Kawaguchi, 1993; Lim *et al.*, 2014). The sparsely distributed giant ChIs are the main source of ACh in the striatum via cholinergic innervation (McGeer *et al.*, 1971; Lynch *et al.*, 1972; Zhou *et al.*, 2002). Given the preponderance of cholinergic innervation, ChIs interact with a heterogeneously mixed group of cell types endowed with other neurotransmitter's various receptors (Kawaguchi, 1993; Kawaguchi *et al.*, 1995). ChIs form strong synaptic connections to and from MSNs and other interneurons by mechanisms that modulate the excitability of cells through cholinergic receptors (nAChRs or mAChRs) and indirectly participating in the modulation of neurotransmitter (DA and GABA) release by volume transmission in the striatal pool (Cachope *et al.*, 2012; Threlfell *et al.*, 2012; Nelson *et al.*, 2014).

Many human pathological conditions are associated with altered cholinergic signaling and disorders in striatal circuits including Parkinson's disease (Brichta *et al.*, 2013; Kalia *et al.*, 2013; Ztaou *et al.*, 2016), Huntington's disease (Penney & Young, 1982; Smith *et al.*, 2006), dystonia (Burke *et al.*, 1986; Peterson *et al.*, 2010; Sciamanna *et al.*, 2011; Sciamanna *et al.*, 2012; Eskow Jaunarajs *et al.*, 2015; Scarduzio *et al.*, 2017), Gilles de la Tourette's syndrome (Leckman *et al.*, 1989b; Taylor *et al.*, 2002), and drug addiction (Albin *et al.*, 1989; Koob, 1992; Chudasama & Robbins, 2006; Cepeda *et al.*, 2007). These diseases are linked to altered ACh balance but ChIs overall functions in the pathological states are hard to study. In addition,

quantitative measurement of how changes cholinergic in synaptic action give rise to different diseases has not been documented at the cellular level or network level.

The death of ChIs in DLS and cholinergic deficit in ventral striatum is associated with Tourette's syndrome and schizophrenia respectively (Holt *et al.*, 1999; Kataoka *et al.*, 2010; Lenington *et al.*, 2016). Interestingly, ChIs are not homogeneously distributed in the striatum, which may contribute to the diverse functional properties of the DLS, medial striatum and ventral striatum (Alexander *et al.*, 1986; Yin & Knowlton, 2006; Threlfell & Cragg, 2011). The DLS is suggested to be responsible for stimulus-driven habits or sensorimotor habits (Yin & Knowlton, 2006).

The earliest non-specific lesion study of striatum identified the origin of ACh in the local circuit, morphology, and distribution of cells. However, the study did not reveal or estimate the total number of ChIs in the striatum (Lynch *et al.*, 1972). In addition, the previous cell-specific lesion study showed that the saporin toxin linked to rat nerve growth factor (NGF) receptors (192 IgG) to selectively destroy cholinergic neurons without damaging other cell types (Wiley *et al.*, 1991; Book *et al.*, 1992) successfully destroyed basal forebrain cholinergic cells. However, the NGF linked saporin toxin was ineffective for ChIs in the striatum because NGF receptors are not seen in adult ChIs due to expression being dramatically decreased in postnatal development stages. Interestingly, NGF receptors can be recovered when there is damage in adult tissue (Gage *et al.*, 1989). The advance in recent studies confirmed that saporin toxin linked to choline acetyltransferase (ChAT-sap) can specifically destroy striatal ChIs in rat striatum (Stirpe *et al.*, 1983; Laplante *et al.*, 2011; Aoki *et al.*, 2015). In the present study we sought to investigate the anatomical changes and the specificity of lesion after selective ablation of ChIs induced by targeted cell-specific elimination with immunotoxin in *mice*. In the present research DLS was targeted, an area associated with the motor control of the forepaws. A better understanding and quantification of ChIs number, functions and anatomy in this subcortical brain region will provide an opportunity to comprehend the participation of ChIs in diseases and perhaps open up new possible pharmacotherapies.

## **2.2 Materials and methods**

### 2.2.1 Animals and groups

**Table 2. 1 The ChAT-sap toxin treated group**

Number of brain sections studied (13 sections in each animal)						
ChAT-sap toxin treated group						
Survival time	2 weeks/p35		4 weeks/p49		6 weeks/p63	
Animals	n=10		n=11		n=10	
Hemisphere	Right	left	Right	left	Right	left
Sections	n=130	n=130	n=143	n=143	n=130	n=130
Counted	ChIs	ChIs	ChIs	ChIs	ChIs	ChIs
	vAChT	vAChT	vAChT	vAChT	vAChT	vAChT
Total sections analyzed for ChIs			n=806			
Total sections analyzed for vAChT			n=806			
Total animals			n=31			

**Table 2. 2 The Control group**

Number of brain sections studied (13 sections in each animal)						
Control group						
Survival time	2 weeks/p35		4 weeks/p49		6 weeks/p63	
Animals	n=6		n=5		n=5	
Hemisphere	Right	left	Right	left	Right	left
Sections	n=78	n=78	n=65	n=65	n=65	n=65
Counted	ChIs	ChIs	ChIs	ChIs	ChIs	ChIs
	vAChT	vAChT	vAChT	vAChT	vAChT	vAChT
Total sections analyzed for ChIs			n=416			
Total sections analyzed for vAChT			n=416			
Total animals			n=16			

**Table 2. 3 The Sham group**

Number of brain sections studied (13 sections in each animal)						
Control group						
Survival time	2 weeks/p35		4 weeks/p49		6 weeks/p63	

Animals	n=4		n=4		n=5	
Hemisphere	Right	left	Right	left	Right	left
Sections	n=52	n=52	n=52	N=52	n=65	n=65
Counted	ChIs	ChIs	ChIs	ChIs	ChIs	ChIs
	vAChT	vAChT	vAChT	vAChT	vAChT	vAChT
Total sections analyzed for ChIs			n=338			
Total sections analyzed for vAChT			n=338			
Total animals			n=13			

Sixty virgin, male wild-type *C57BL/6J* mice (21-24 days old) weighing 10-15g were used in a series of experimental groups in the present study. These mice had been delivered from the Japan Clea at age 21 days old. Mice were group housed in plastic cages with bedding, and all animals were provided with food and water ad libitum and housed under standard conditions (12 h light/dark cycle with lights on at 7 a.m, at 23°C) until stereotaxic surgery experiments. Thereafter animals were placed back to standard conditions and group housed. Three groups of animals were compared: intact control (**Table 2. 2**), sham (saline injections, **Table 2. 3**), and DLS lesion with ChAT-sap toxin (**Table 2. 1**). In addition, three different post treatment times were analyzed at 2, 4 and 6 weeks.

D1/D2 eGFP transgenic mice (MSNs had been labeled with green fluorescent protein) (21-24 days old, n=10) weighing 10-15g were used in a series of experiment to determine whether ChIs lesion with ChAT-sap toxin could be specific for only ChIs cells in mice striatum.

### 2.2.2 Stereotaxic Surgery

To selectively lesion ChIs, animals were anesthetized by continuous isoflurane inhalation, USP (IsoFlo, Abbott Laboratories, IL, 1.0%–1.5% in medical O<sub>2</sub>). The respiratory rate, heart rate, and hindpaw withdrawal reflexes were monitored throughout the procedure to maintain an adequate anesthetic level as stably as possible. Animals were fixed with atraumatic ear-bars, the cornea protected with myochlorin ointment 2% and the skin rubbed with anesthetic gel (10% ketoprofen and lidocaine). Then animals received stereotaxic injections of the saporin ribosome-inactivating-immunotoxin that targets choline acetyltransferase (ChAT-sap toxin) 0.3µl (at concentration of 0.5µg/µl) into the left hemisphere according to the mouse

brain atlas (Franklin & Paxinos, 2008) (**Figure 2. 1. A**). The toxin targeting ChIs was injected into the DLS on left hemisphere (bregma: AP, 0.98mm; L, -1.89mm; -3.45mm) (for estimated spread of toxin see **Chapter 3.3.12**). Injections were carried out at a constant flow rate of 0.1 $\mu$ l/min with a PHD ULTRA™ Programmable syringe pump. During surgery, the body temperature was kept at normal physiological conditions using a disposable heating pad. After completion of injections, the needle was left in place for additional 10 mins to allow diffusion of the toxin before retraction and kept mice were kept warm until they came out of anesthesia (<15 min). During the first 72 hours after surgery, post-operative care was administered to control hypothermia, and dehydration with a can of diet gel with carprofen (e.g., MediGel CPF, Portland, ME, USA).

For sham treated animals, 0.3ul saline was injected into the DLS on left hemisphere (bregma: AP, 0.98mm; L, -1.89mm; -3.45mm) and other experimental procedures are same with toxin treated group.

To selectively lesion ChIs in D/D2 eGFP transgenic mice, 0.3 $\mu$ l ChAT-sap toxin was injected into the DLS on left hemisphere (bregma: AP, 0.98mm; L, -1.89mm; -3.45mm) and other experimental procedures are the same as described above.

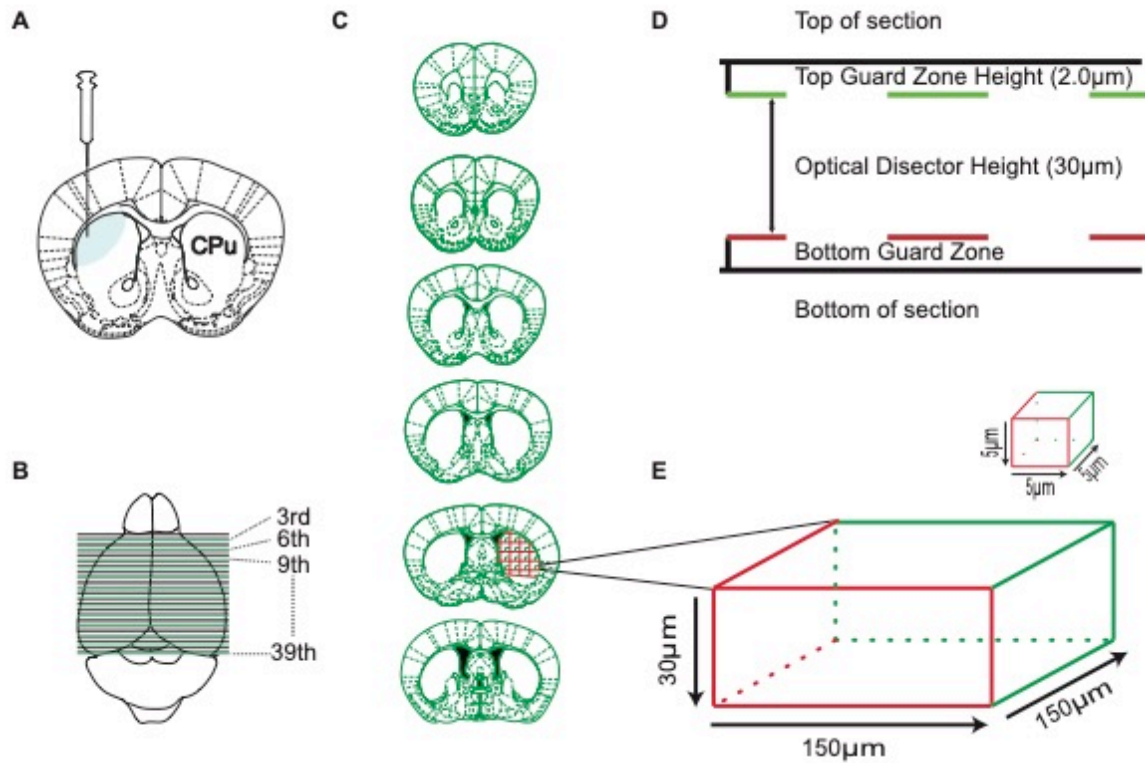


**Figure 2. 1 A schematic diagram for tissue preparation process for stereological systematic random sampling.**

*A*, stereotaxic injection of ChAT-sap toxin into DLS. *B*, every third section was collected for stereological sampling from a brain (in total 13 striatal sections were used for analysis). *C*, a diagrammatic coronal brain sections modified from brain atlas (Franklin & Paxinos, 2008); we kept the order of sections during the process. *D*, a diagrammatic illustration showing the ChIs sampling in a thick section. This figure depicts a section view from the lateral edge of a  $60\mu\text{m}$  thick section. To avoid bias, a section guard is employed at the upper and lower surfaces of the section. *E*, a diagrammatic sampling frame created a 3D virtual wall ( $30\times 150\times 150\mu\text{m}$  for ChIs,  $5\times 5\times 5\mu\text{m}$  for vAChT), shown in the form of lines, the red lines representing forbidden lines and green lines representing including lines. Any cells or boutons superimposed over the red line are excluded from counting, while particles totally inside the disector volume or superimposed over a green line are included as disector particles.

The incision on the scalp was sutured using surgical silk. After surgery, at least two weeks were allowed before anatomical confirmation of cell loss was performed by immunohistochemistry. The injection procedure was followed by histology procedure as described below.

### 2.2.3 Perfusion



For stereological investigation, the mice were deeply anesthetized via isoflurane, then transcardially perfused with phosphate buffer 0.1 M (pH 7.4) followed by phosphate buffer containing 4 % paraformaldehyde and final concentration on 14 % saturated solution of picric acid. The brain was removed after decapitation (*Figure 2. 1. B*), postfixed in the same solution for 24hrs at 8°C and then cryoprotected in a 50/50 mixture of fixative (phosphate buffer containing 4 % paraformaldehyde and 14 % picric acid) and 20 % sucrose in 0.1 M phosphate buffered saline (PBS) for at least 24h or until the brain sank to the bottom of the vial.

#### **2.2.4 Sectioning**

Each brain was serially sectioned in the coronal plane, on a sliding microtome with a freezing stage (Yamato electrofreeze, MC-802A) at an instrument setting of 60 µm. Total sections were divided into three sets of consecutive sections A, B and C (*Figure 2. 1. B*). A set (in total 13 section in which contained striatal formations) was processed for immunocytochemistry to visualize ChIs and vAChT and was used for stereological systematic random sampling (*Figure 2. 1. C*). The remaining B and C sets of sections were held in reserve and stored in an anti-freeze (ethylene glycol) cryoprotectant solution at -30°C.

#### **2.2.5 Histology**

Sections were incubated for 4h at room temperature in 10% normal donkey serum (NDS) or 20% normal goat serum (NGS) diluted in Stockholm PBS (to one liter 1.15g Na<sub>2</sub>HPO<sub>4</sub>, 0.26g NaH<sub>2</sub>PO<sub>4</sub>.H<sub>2</sub>O, 8g NaCl, and 0.2g KCl added). They were then incubated in ChAT primary antibody against ChIs (Millipore, California USA, goat polyclonal antibody, 1:100 dilution) in antibody diluent (Triton0.3%, NaN<sub>3</sub> Azide0.05%, PBS) in dark room for at least 24h at 4°C on shaker, washed in PBS (4×5min) and then incubated with vAChT primary antibody (Synaptic systems, Gottingen, Germany, rabbit polyclonal, 1: 1000 dilution) washed with PBS (4×5min). Following this procedure, sections were incubated with secondary antibodies separately in dark room 12h at 4°C on shaker (dilution 1:200). For vAChT and ChIs double staining, the secondary antibodies used were Alexa fluor 488-donkey anti-rabbit (Life technologies, Eugene, OR, USA; 1:200) and Alexa fluor 350-donkey anti-goat (Life Technologies, Eugene, OR, USA; 1:200), respectively. For ChIs single staining, the secondary antibody used was Alexa fluor 488-donkey anti-goat (life technologies, Eugene, OR, USA;

1:200). Sections were again washed in PBS (4×5min) and mounted. The subsequent immunostained slices were visualized using a spinning disc confocal microscope (Olympus BX-DSU) and confocal microscope (Carl Zeiss LSM780). Pictures were taken using ZEN software or Neurolucida software and a Hamamatsu (EM-CCD C91) camera under high magnification (40 ×/0.90 or 100 ×/1.40 oil immersion lens).

### **2.2.6 Estimation of the total number of ChIs and vAChT boutons using the optical fractionator**

We counted ChIs and vAChT boutons in ChAT-sap toxin injected animals 2, 4 and 6 weeks after the injection of toxin. All of the mice were injected at the same stereotaxic parameters, toxin concentration, perfusion, fixation, sectioning, staining, and mounting procedures as described above in order to avoid biased cell counting (West, 2012). Stereo Investigator version 11, Neurolucida software and Hamamatsu (EM-CCD C91) camera were used to image and count ChIs stained for ChAT and boutons stained for vAChT from coronal sections. In each of the sections sampled, the number of ChIs and vAChT bouton number were counted and total estimates in the striatum were obtained using the optical fractionator technique [see (Gundersen, 1977; Gundersen & Jensen, 1987; West *et al.*, 1991; Olesen *et al.*, 2017) for detailed description of the optical fractionator].

ChIs and vAChT positive boutons were directly counted in a selected set of sections at predetermined uniform intervals of one-third of total sections obtained from a brain. The first section was randomly determined according to the shape of the striatum and the brain section which contained striatal formation was traced at low magnification (4×/0.16 Hamamatsu) for striatal volume estimation. A grid with a total frame size of 400×400µm was placed over the striatal region to be traced and the software placed equally spaced counting frames at random. ChIs were counted under high magnification (20 ×/0.75 objective lens). The size of the counting frames was X=150µm and Y=150µm (**Figure 2. 1. E**). The number of counting sites per section depended on the size of striatum in each section. Size varied from section to section throughout the brain. The top guard zone height was 2µm after manually focusing on the surface of the section and the dissector height was set at 30µm (**Figure 2. 1. D**). The striatal ChIs that fell within the borders of the counting frames and did not touch the red exclusion borders were included in the analysis. Data from lesioned (left hemisphere) and non-lesioned

(right hemisphere) sites were analyzed separately. In total, 13 striatal sections were analyzed from each brain. As each section was double-stained to identify ChIs and vAChT boutons, we used the same sections for both counts. Similarly, with a grid of 800×800µm and at 100X magnification counted vAChT boutons in 5µm square frames (**Figure 2. 1. E**).

The number of counted neurons in the subdivision (N) is estimated as:

$$N = \Sigma Q \cdot \frac{t}{h} \cdot \frac{1}{asf} \cdot \frac{1}{ssf}$$

$asf$  = counting frame size /counting grid size.

$ssf$  = the interval of sections sampled through an object

Where  $\Sigma Q$  is the total number of neurons actually counted,  $t$  is thickness of the sections,  $h$  is the height of the disector,  $asf$  is fraction of area of section sampled,  $ssf$  is the section sampling fraction. In our study:

$asf = 22500$  (the counting frame is 150× 150µm)/160000 (the sampling grid is 400×400µm)

$$ssf = 1/3$$

Estimation of the total number:

$$N_{\text{total}} = N \times k$$

Where N is sum counts, k is the interval of sections sampled through an object, the  $ssf$  and k is same.

NOTE: We conducted a pilot study including a few animals from each experimental group to determine the optimal sampling parameters, such as the number of the sections to be analyzed, the thickness of the tissue, grid size, counting frame size, lower magnification to delineate the area of interest and high magnification to count. From the pilot study we obtained initial results for cell numbers, CV (coefficient of variation) and CE (coefficient of error) and then optimized the parameters described above to obtain a satisfactory precision of estimates (CE≤10%). The tissue thickness was measured in each sampling area within the region of interest.

### 2.2.7 Statistical analysis

Numerical values systematically counted for ChIs and vAChT number are reported as the per group mean ± SEM. Significance of differences between group data was determined by one-way ANOVA followed by Tukey's multiple-comparisons test, and for comparison of

lesioned and all control groups tested by Kolmogorov-Smirnow test. Differences were considered to be significant if  $p$  values were  $< 0.05$ .

## 2.3 Results

### 2.3.1 The confirmation of lesion with dual immunolabelling: ChIs and vAChT

In the fluorescent microscope, ChIs and boutons of the striatum were identified by the ChAT labeled ChIs and vAChT labeled boutons/terminals in the unilateral ChAT-sap toxin injected DLS of wild-type C57BL/6J mice (**Figure 2. 2. A, B**). Two weeks after the injection, there was a significant depletion of ChIs at the injection site and there was a widespread bilateral expression of the vAChT as shown in (**Figure 2. 2. A, B**). The cholinergic lesion with immunotoxin as shown in (**Figure 2. 2. A**) in mice is consistent with previous rat studies using the same immunotoxin (Laplante *et al.*, 2011; Aoki *et al.*, 2015). The DLS that received the ChAT-sap toxin displayed no immunolabeling for ChAT at the injection site. At the injection site, most ChIs were destroyed and recovery or regrowth of ChIs was not observed at post-lesion times of 2 weeks, 4 weeks and 6 weeks in our study.

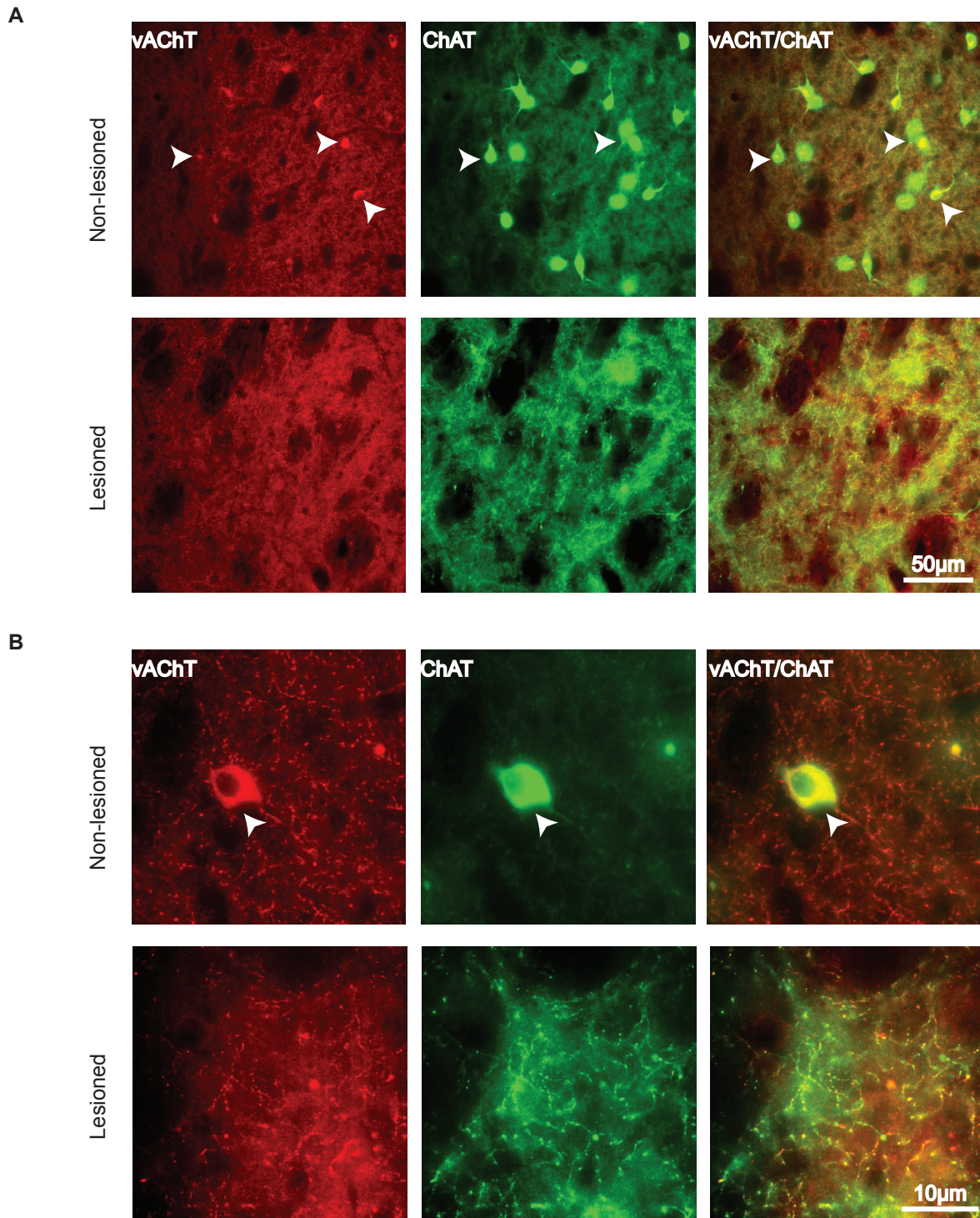


**Figure 2. 2** Histological verification of specific lesion of cholinergic interneurons in the striatum.

*A*, Photomicrographs of confocal microscope images of cholinergic double-immunostained sections of control and ChAT-sap toxin injected striatum following survival of 2 weeks. Top pictures striatal tissue taken from the control hemisphere of striatum, pictures underneath are taken from the toxin-injected side. *B*, Images were captured at 100X magnification are from *A*, images on the

top are tissue at 20X magnification and 100X taken from the control hemisphere of striatum, pictures underneath are taken from the toxin-injected side, the arrows indicate ChIs soma.

### 2.3.2 ChIs decrease in ChAT- sap immunotoxin injected striatum

Three experimental groups (ChAT-sap toxin, saline, and intact control) with three post lesion times (2 weeks, 4 weeks and 6 weeks) were included in quantitative stereological cell counting to compare two hemispheres individually in each group. ChAT-sap toxin selectively lesioned ChIs and no damage to ChIs was observed in sham groups as described previously (Laplante *et al.*, 2011; Laplante *et al.*, 2012; Aoki *et al.*, 2015). For each experimental group of animals after lesion time, coronal sections of striatum were cut and double stained for ChAT and vAChT terminals. We analyzed the effect of post-treatment time on the alteration of ChIs numbers in the different experimental groups (**Figure 2. 3. A, B, C**).

To quantify the ChIs number at 2 weeks post lesion time (**Figure 2. 3. A, A'**), we compared lesioned group to control group hemispheres (right hemisphere is contralateral side, left hemisphere is ipsilateral side in both groups) which includes four hemispheres: control group (C-contra, C-ipsil) and lesioned group (L-contra, L-ipsil) respectively. There were no statistical differences between intact control and sham groups in both hemisphere with ChIs number, therefore intact control and sham animals were collectively considered as the control group in this study. We found a significant depletion of ChIs in lesion group hemisphere compared to the three control conditions (C-contra, C-ipsil and L-contra) ( $7940 \pm 778.4$ , n=9 for L-ipsil vs  $10728 \pm 433.7$ , n=10 for C-contra,  $\rho < 0.0187$ ; L-contra:  $10529 \pm 844.9$ , n=9,  $\rho < 0.0409$ ; one-way ANOVA followed by Tukey's multiple-comparisons test). Within control groups, we didn't observe any statistical differences (C-contra vs C-ipsil  $\rho > 0.9999$ , C-contra vs L-contra  $\rho > 0.9999$ , C-ipsil vs L-contra  $\rho > 0.9999$ ; one-way ANOVA) which indicates that the toxin treatment into one hemisphere does not affect the ChIs number in the other hemisphere of the same animal (**Figure 2. 3. A**).

In addition, ChIs showed a significant depletion at post-treatment time 4 weeks (**Figure 2. 3. B, B'**) compared to control hemispheres ( $6108 \pm 630.4$ , n=11 for L-ipsil vs  $10403 \pm 378.8$ , n=10 for C-contra,  $\rho < 0.0007$ ; C-ipsil:  $10962 \pm 313.2$ , n=11,  $\rho < 0.0001$ ; L-contra:  $9220 \pm 1099$ , n=11,  $\rho < 0.0169$ ; one-way ANOVA followed by Tukey's multiple-

comparisons test). These group data indicate that ChIs continue to die with ChAT-sap injection because at 4 weeks more ChIs are lost than at 2 weeks.

Subsequently, we counted ChIs number at 6 weeks after ChAT-sap toxin administration (**Figure 2. 3. C, C'**), we found a consistent loss with former two results in which ChIs depletion further remains and significantly fewer than in control hemispheres ( $7769 \pm 541.5$ ,  $n=10$  for L-ipsil vs  $10187 \pm 530.2$ ,  $n=9$  for C-contra,  $\rho < 0.0201$ ; C-ipsil:  $10800 \pm 633.2$ ,  $n=10$ ,  $\rho < 0.0016$ ; L-contra:  $9698 \pm 409.4$ ,  $n=10$ ,  $\rho < 0.0319$ ; one-way ANOVA followed by Tukey's multiple-comparisons test). Those ChIs counting data, confirm that spontaneously active striatal ChIs, exhibit statistically significant reduction following the application of ChAT-sap immunotoxin at post-lesion times of 2 weeks, 4 weeks and 6 weeks. There was the most significant depletion observed at 4 weeks post-lesion timesds, however, we didn't observe continued depletion with extended survival times. Furthermore, the recovery or reappearance of ChIs at the lesion side was not observed in our present study.

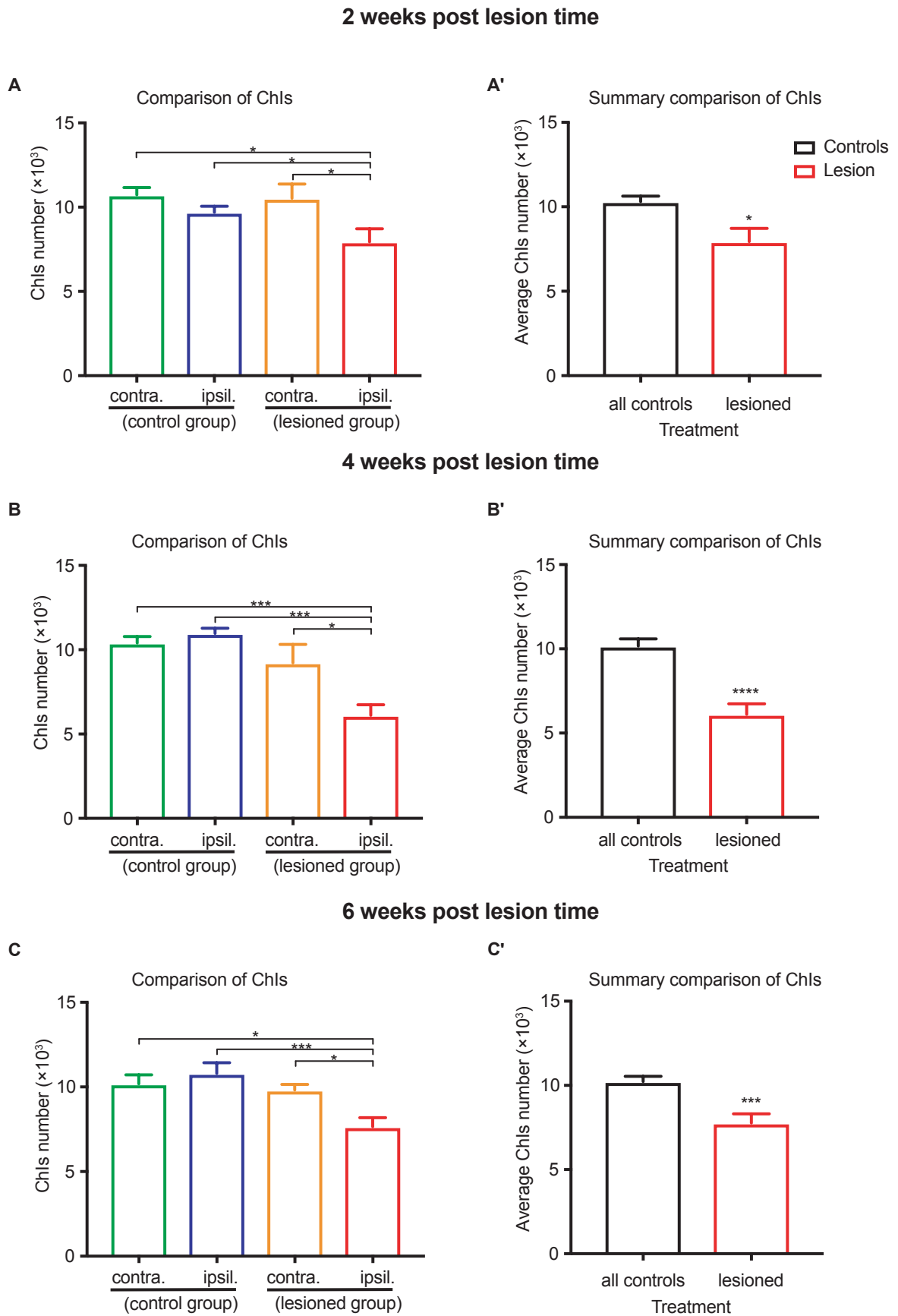


**Figure 2. 3 The ablation of ChIs in the striatum.**



The number of ChIs counted in both hemispheres of control animals (C-contra, C-ipsil), and ChAT-sap toxin treated animals both hemisphere (L-contra, L-ipsil) after toxin administration. **A and A'**, to allow the toxic effect to take place, mice were housed for two weeks before anatomical confirmation was performed by (postnatal age p35 and number of animals n=9 for lesioned group, n=10 for control groups respectively) ChIs sampling from both hemispheres for comparison. **B and B'**, The ChIs number counted at post treatment (postnatal age p49 and number of animals n=11 for lesioned group, n=10 for control groups respectively). **C and C'**, The ChIs number counted at post treatment (postnatal age p63 and number of animals n=10 for lesioned group, n=10 for control groups respectively). Data are shown as means  $\pm$  SEM. \* $p < 0.05$ , \*\* $p < 0.01$ , and \*\*\* $p < 0.001$ .

### 2.3.3 vAChT positive sprouts in ChAT-sap immunotoxin injected striatum

To further analyze the effect of ChAT-sap on striatal microcircuits we counted the number of vAChT positive terminals and varicosities in double-stained sections. The numbers of such sites are an indirect representation of ACh levels in the striatum. The systematic stereological counting of vAChT puncta allowed us to analyze the alteration of cholinergic synapses in control and lesioned striatum. The result revealed that in contrast to depleted ChI numbers in the lesioned group, the number of vAChT puncta was elevated on the lesioned side of ChAT-sap toxin treated animals. At post-lesion time 2 weeks (**Figure 2. 4. A, A'**), we compared the vAChT number from the lesioned group to control group. We found significant increase of vAChT in lesion group compared to other three control hemispheres ( $766280974 \pm 86786841$ , n=9 for L-ipsil vs  $509765667 \pm 40874446$ , n=10 for C-contra,  $\rho < 0.0172$ ; C-ipsil:  $519247158 \pm 40489736$ , n=10,  $\rho < 0.0229$ ; L-contra:  $538544818 \pm 56512024$ , n=9,  $\rho < 0.0475$ ; one-way ANOVA followed by Tukey's multiple-comparisons test). Within control groups, we didn't observe any statistical differences which indicates that the toxin treatment into one hemisphere increases the vAChT at the lesion site of ChAT-sap treated animals.

Interestingly, the vAChT number showed a gradually decreasing pattern from post-treatment time of 4 weeks (**Figure 2. 4. B, B'**) compared to control groups ( $606197350 \pm 48199786$ , n=11 for L-ipsil vs  $393977907 \pm 30086173$ , n=10 for C-contra,  $\rho < 0.0019$ ; C-ipsil:  $422741091 \pm 41573929$ , n=10,  $\rho < 0.0088$ ; one-way ANOVA followed by Tukey's multiple-comparisons test).

Furthermore, we counted vAChT terminal number at 6 weeks after ChAT-sap administration (*Figure 2. 4. C, C'*), however, the elevated vAChT number returned to the normal level in spite of the reduction in the cells that were their source. The biggest upregulation of vAChT was observed at 2 weeks post-lesion. However, we didn't observe continued increase with time, our results indicated a recovery of cholinergic synapse number by 6 weeks in spite of continuing loss of cells.

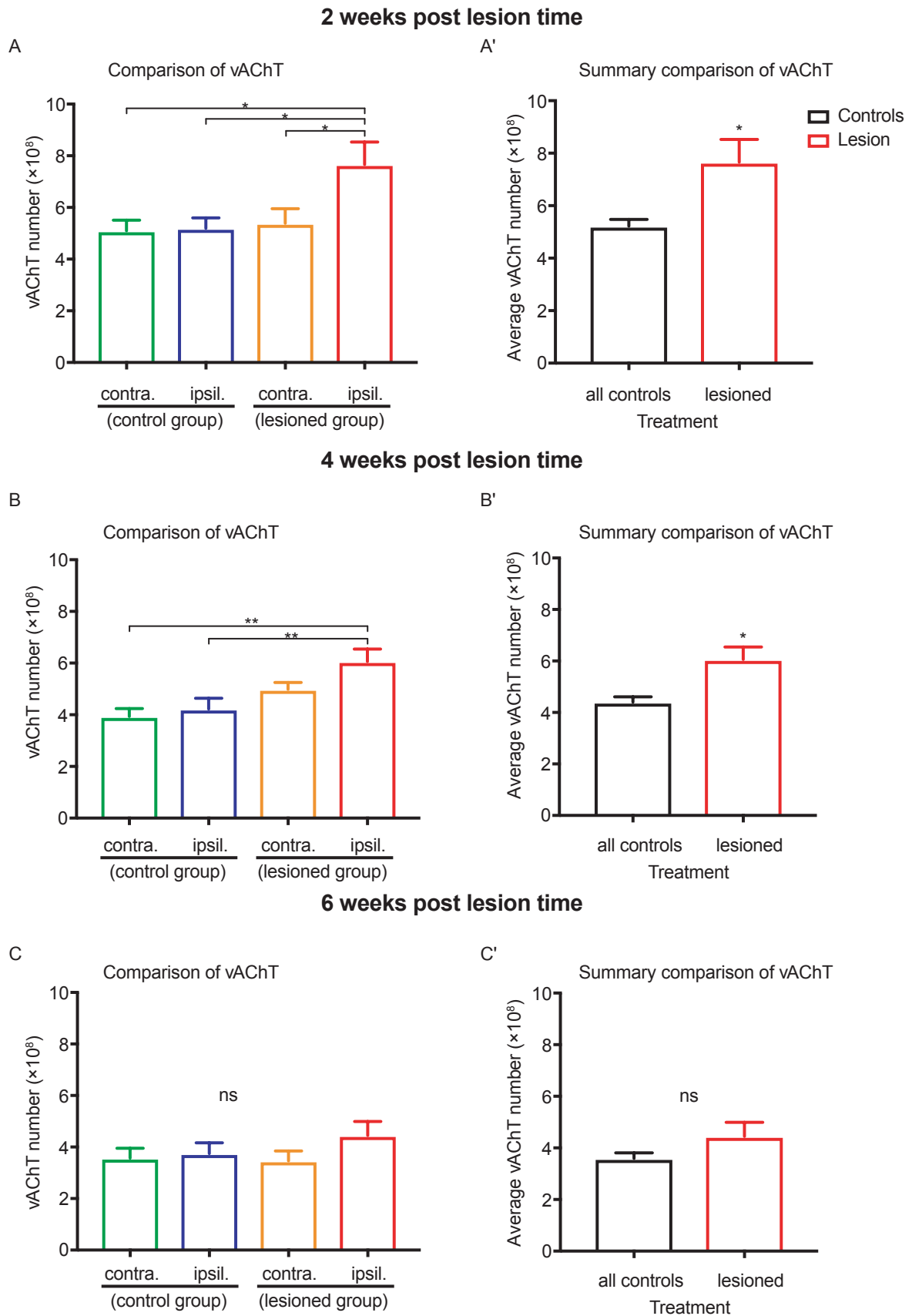


**Figure 2. 4 vAChT positive puncta in the striatum show transient increase after ChAT-sap treatment.**

The number of vAChT counted in both hemispheres of control animals (C-contra, C-ipsil), and toxin treated animals both hemisphere (L-contra, L-ipsil) after toxin administration. **A and A'**, vAChT numbers counted 2 weeks post lesion time (postnatal age p35 and number of animals n=9 for lesioned group, n=10 for control groups respectively) in both hemispheres for comparison. **B and B'**, The vAChT number counted at 4 weeks post treatment (postnatal age p49 and number of animals n=11 for lesioned group, n=10 for control groups respectively). **C and C'**, The vAChT number counted at 6 weeks post treatment (postnatal age p63 and number of animals n=10 for lesioned group, n=10 for control groups respectively). Data are shown as means  $\pm$  SEM. \*p < 0.05, \*\*p < 0.01, and \*\*\*p < 0.001.

### 2.3.4 The observation of ChIs lesion in eGFP transgenic mice

To determine whether ChIs lesion with ChAT-sap toxin could be specific for only ChIs cells in mice striatum, the ChAT-sap toxin was injected unilaterally into the DLS of eGFP D1/D2 transgenic mice whose MSNs had been labeled with green fluorescent protein. This procedure only targeted striatal ChIs, no evidence of damage to MSNs was observed.

Previous septum cholinergic cells lesion studies revealed that the remaining cholinergic neurons were enlarged. Similarly, DA lesion studies showed that TH neurons soma size alters after lesion (Gage *et al.*, 1989; Hagg *et al.*, 1989; Betarbet *et al.*, 1997; Meredith *et al.*, 1999; Huot & Parent, 2007). However, we were unable to see the alteration in soma size and the MSNs seemed also not to have been harmed by the toxin, as shown a typical example of striatum (**Figure 2. 5**). In addition, in our D2-eGPF transgenic animals GFP is not expressed in ChIs in the striatum, so we didn't observe any double stained ChIs in control group animals.

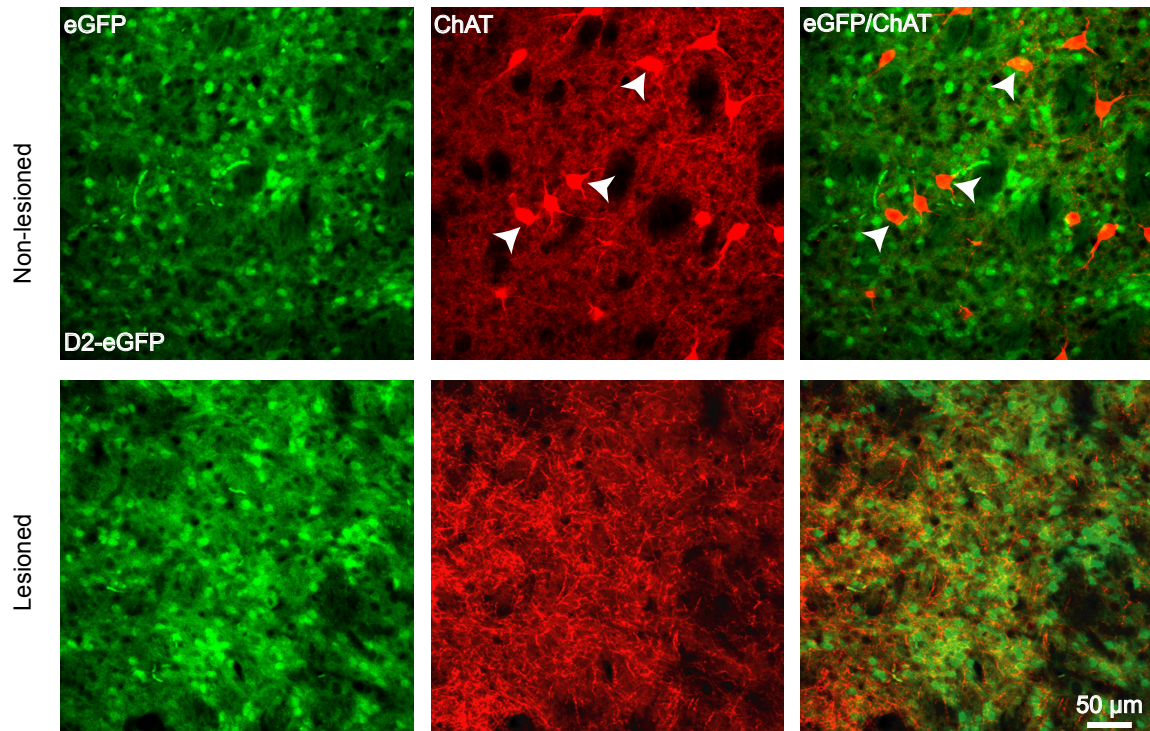


**Figure 2. 5 Histological verification of specific lesion of ChIs in transgenic mice striatum.**

Confocal microscope images of ChAT immunostained sections of control and ChAT-sap toxin injected striatum following a survival time of 2 weeks. Top pictures striatal tissue taken from the control hemisphere of striatum, pictures underneath are taken from the ChAT-sap toxin injected side (n=10). In our sections no ChIs were positive for D2 receptors.

### 2.3.5 The examination of PPN cholinergic neurons

Next, we attempted to determine whether ChIs lesion of the DLS could damage PPN cholinergic neurons which project from midbrain. The ChAT-sap unilaterally injected brains (n=10) were stained for ChIs. In previous studies, the PPN and LDT has been considered the main external cholinergic innervation of striatum which sends projection into various part of the striatum (Dautan *et al.*, 2014; Mena-Segovia & Bolam, 2017). We compared the PPN cholinergic cells in toxin-treated group to control group PPN (**Figure 2. 6**) at 2 weeks, 4 weeks, and 6 weeks after the lesion into the striatum. Based on anatomical data, there was a similar degree of axonal arborization, extended dendrites and soma size compared to control groups. The cell numbers in the three conditions were similar and difficult to find sharp contrast or significant decrease. Although we observed many sections of PPN, none of the ChAT-sap treated mice PPN cholinergic neurons showed any change in the cells there. In addition, the injection of retrograde tracer cholera toxin B subunit into the same coordinate used for ChAT-sap toxin did not reveal any cells filled with tracer in PPN, perhaps because the major innervation is to medial areas or because innervation from PPN is very sparse.

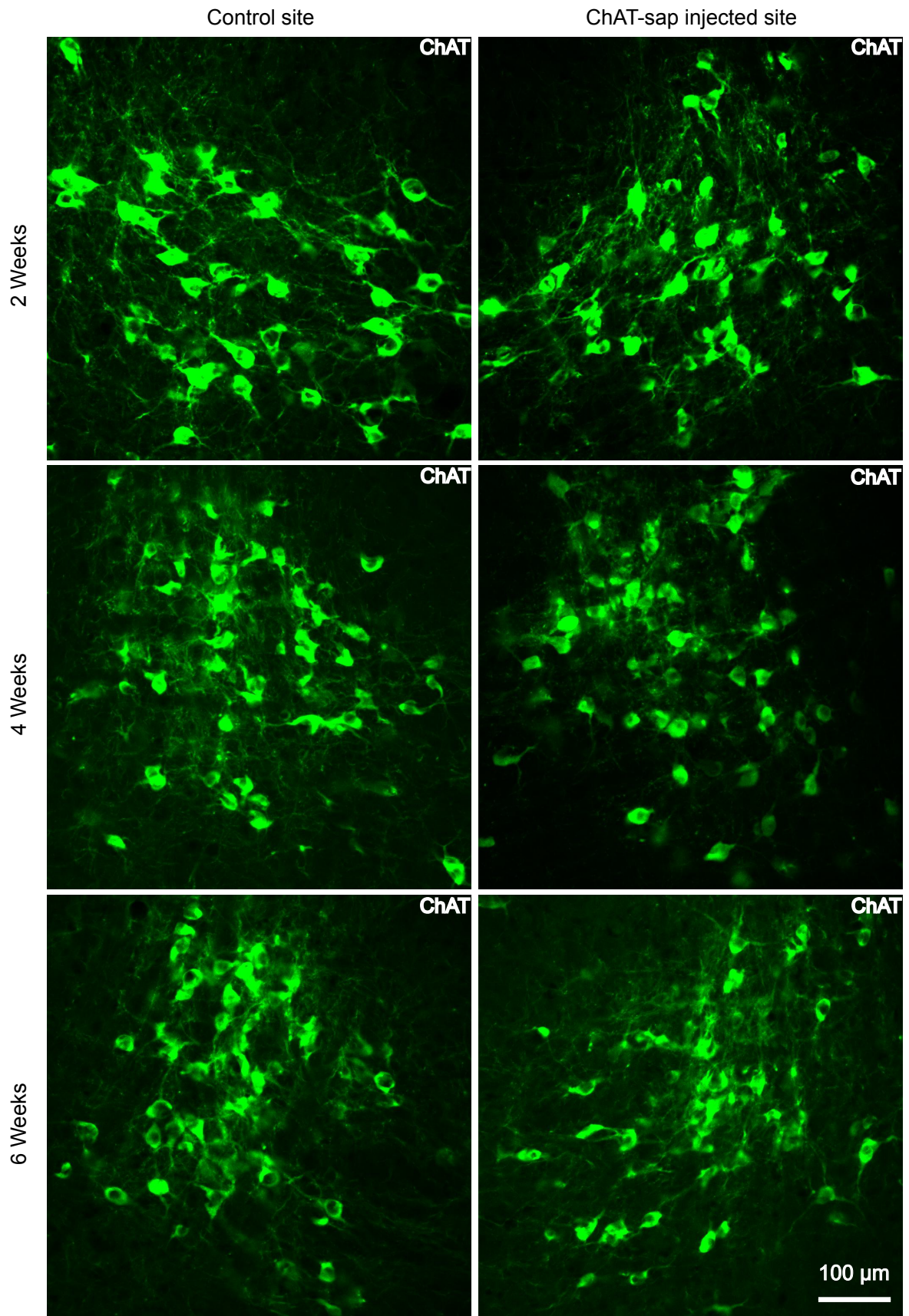


**Figure 2. 6 Histological verification of cholinergic neurons in PPN.**

Confocal microscope images of PPN cholinergic neurons immunostained sections of control and ChAT-sap toxin injected brain following post-lesion of 2, 4, 6 weeks. Pictures on the left is PPN tissue taken from the control site, pictures on the right site are taken from the toxin-injected site.

### 2.3.6 Striatal volume loss in ChAT-sap lesioned group as measured by stereology during cell counting.

To determine whether lesion with ChAT-sap toxin could affect the volume of striatum, we decided to conduct statistical analysis of striatal volume which has measured and collected based on contour drawn during cell and boutons counting by stereological method. At two weeks post lesion time, the mean total striatal volume for normal control subject (contra, ipsil) and the lesioned group (contra, ipsil) were  $7.5 \pm 0.13 \text{ mm}^3$ ,  $7.5 \pm 0.19$ ,  $7.7 \pm 0.11$ , and  $7.2 \pm 0.11 \text{ mm}^3$  (mean  $\pm$  SEM,  $p > 0.9999$ ,  $p > 0.9096$ ,  $p > 0.8383$ ,  $p > 0.9999$ ) respectively (**Figure 2. 7. A**). The volume changes in the two groups were unvaried and statistically insignificant. However, there was a trend for reduced volume in lesioned striatum.

Furthermore, we measured volume changes at 4 weeks post-lesion in control (contra, ipsil) and ChAT-sap (contra, ipsil) groups which were  $7.8 \pm 0.21$ ,  $7.9 \pm 0.11$ ,  $7.4 \pm 0.20$ , and  $6.9 \pm 0.2 \text{ mm}^3$  (C-contra vs L-ipsil:  $p < 0.0259$ ; C-ipsil vs L-ipsil  $p < 0.0057$ ) respectively (**Figure 2. 7. B**). At this time, the lesioned group ipsilateral hemisphere (toxin injected side) volume decreased significantly compared to control groups (contra, ipsil) but remains the same as the contralateral hemisphere (intact hemisphere) of lesioned group which means that the lesioned group both hemispheres were perhaps affected by unilateral lesion.

Finally, we measured volume at 6 weeks in control group (contra, ipsil) and ChAT-sap (contra, ipsil) groups which were  $7.8 \pm 0.18$ ,  $8.2 \pm 0.11$ ,  $7.6 \pm 0.14$ , and  $7.1 \pm 0.16 \text{ mm}^3$  (C-contra vs L-ipsil:  $p < 0.0148$ ; C-ipsil vs L-ipsil:  $p < 0.0001$ ) respectively (**Figure 2. 7. C**) in which ChAT-sap ipsilateral side declined remarkably compared to controls. The mean total striatal volume loss in subject with ChAT-sap at 4 weeks and 6 weeks were 10.4 % and 9.7% respectively. These results indicating unchanged volume at 2 weeks post-lesion might be related to vAChT the bouton number increase at 2 weeks post lesion time, even though ChIs depletion were significant compared to controls. Other factors involved with unchanged volume includes: the number of cells loss is less, macrophages reducing debris and astrocyte expansion.



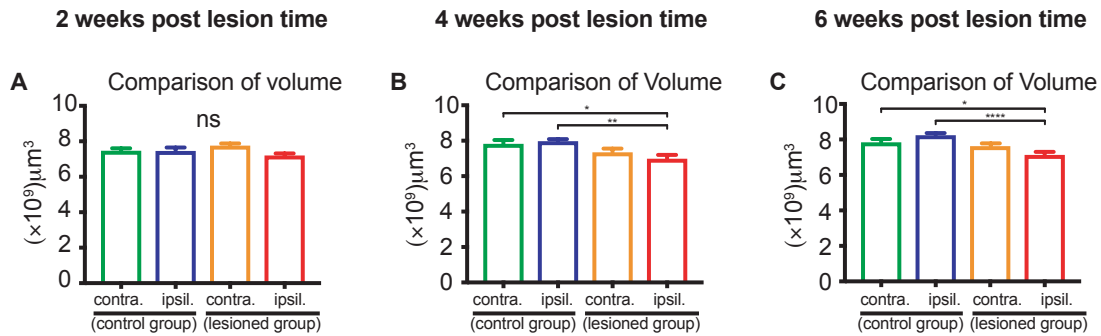


**Figure 2. 7 Striatal volume comparison in control and ChAT-sap treated groups.**

The volume for both hemisphere of control condition (C-contra, C-ipsil), and toxin treated animals both hemisphere (L-contra, L-ipsil). **A**, volume measured at 2 weeks post lesion time (postnatal age p35 and number of animals  $n=9$  for lesioned group,  $n=10$  for control groups respectively). **B**, the volume at 4 weeks post lesion time (postnatal age p49 and number of animals  $n=11$  for lesioned group,  $n=10$  for control groups respectively). **C**, the volume at 6 weeks post lesion time (postnatal age p63 and number of animals  $n=10$  for lesioned group,  $n=10$  for control groups respectively). Data are shown as means  $\pm$  SEM. \* $p < 0.05$ , \*\* $p < 0.01$ , and \*\*\* $p < 0.001$ .

Interestingly, the striatal asymmetry reported in previous human studies (Peterson *et al.*, 1993; Rosas *et al.*, 2001) with the smaller right hemisphere data were consistent with our current study and the differences of hemisphere were more obvious with increase of age as shown in (**Figure 2. 8**) (p35:  $7.5 \pm 0.13 \text{ mm}^3$ ,  $7.5 \pm 0.19$ ; p49:  $7.8 \pm 0.21$ ,  $7.9 \pm 0.11$ ; p63:  $7.8 \pm 0.18$ ,  $8.2 \pm 0.11$ ; 2 weeks C-contra. vs 6 weeks C-ipsil:  $p < 0.0157$ ; 2 weeks C-ipsil vs 6 weeks C-ipsil:  $p < 0.0140$ ).

In contrast, ChIs lesioned left hemispheres were smaller than controls at post lesion time 4 weeks and 6 weeks. Although, lesioned group was small, there were a significant difference between left and right hemisphere among p35 and p63 control groups. In this study, we were unable to test for a sex correlation with striatal left and right hemisphere volume at different age since we only used males.

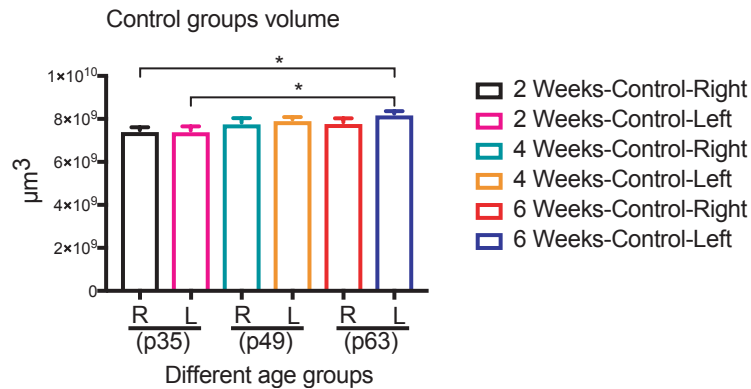


**Figure 2. 8 Control groups volume.**

The control groups volume at age p35, p49 and p63 measured and statistically analyzed. Color code represent different hemisphere at different age.

### 2.3.7 Evaluation of ChIs counting accuracy with two different CEs

To evaluate the precision and reproducibility of design-based stereological systematic cell counting from biological materials, coefficient errors (CE) is commonly employed.

$$\text{CE} = \text{standard deviation/mean of the number of events per probe}$$

The optical fractionator method generates CE during cell counting, and the commonly practiced CE were Gundersen CE and Schmitz-Hof CE second estimate with ~10% per individual (Gundersen & Jensen, 1987; Gundersen *et al.*, 1999; Schmitz & Hof, 2000; Herculano-Houzel *et al.*, 2015). In the current study, we used Gundersen CE and Schmitz-Hof CE second estimates to evaluate the accuracy of terminal and cell counting.

At two weeks post lesion time, the mean total Gundersen CE for normal control subject (contra, ipsil) and the lesioned group (contra, ipsil) during ChIs counting were  $0.058 \pm 0.001$ ,  $0.058 \pm 0.001$ ,  $0.062 \pm 0.002$ ,  $0.07 \pm 0.003$  (C-contra vs L-ipsil:  $p < 0.0092$ , C-ipsil vs L-ipsil:  $p < 0.0092$ ) respectively as shown in (**Figure 2. 9. A**). The Schmitz-Hof CE for normal control subject (contra, ipsil) and the lesioned group (contra, ipsil) during ChIs counting were  $0.06 \pm 0.001$ ,  $0.059 \pm 0.001$ ,  $0.06 \pm 0.002$ ,  $0.07 \pm 0.003$  (C-ipsil vs L-ipsil:  $p < 0.011$ , L-contra vs L-ipsil:  $p < 0.016$ ) respectively as shown in (**Figure 2. 9. A**). The CE for lesioned group ChAT-

sap injected hemisphere (L-ipsil) cell counting fluctuates more often compare to other groups and was statistically significant.

At four weeks post lesion time, the mean total Gundersen CE for normal control subjects (contra, ipsil) and the lesioned group (contra, ipsil) during ChIs counting were  $0.056 \pm 0.002$ ,  $0.055 \pm 0.002$ ,  $0.069 \pm 0.006$ ,  $0.08 \pm 0.005$  (C-contra vs L-ipsil:  $p < 0.0025$ , C-ipsil vs L-ipsil:  $p < 0.0016$ ) respectively as shown in (**Figure 2. 9. B**). The Schmitz-Hof CE for normal control subjects (contra, ipsil) and the lesioned group (contra, ipsil) during ChIs counting were  $0.056 \pm 0.002$ ,  $0.055 \pm 0.001$ ,  $0.069 \pm 0.006$ ,  $0.08 \pm 0.005$  (C-contra vs L-ipsil:  $p < 0.0294$ , C-contra vs L-ipsil:  $p < 0.0003$ ) respectively as shown in (**Figure 2. 9. B**). The both types of CEs variation in each group very similar but lesioned group cell counting CE still fluctuates and statistically significant.

At six weeks post lesion time, the mean total Gundersen CE for normal control subject (contra, ipsil) and the lesioned group (contra, ipsil) during ChIs counting were  $0.059 \pm 0.003$ ,  $0.054 \pm 0.001$ ,  $0.062 \pm 0.002$ ,  $0.069 \pm 0.002$  (C-contra vs L-ipsil:  $p < 0.00281$ , C-ipsil vs L-ipsil:  $p < 0.0004$ ) respectively as shown in (**Figure 2. 9. C**). The Schmitz-Hof CE for normal control subject (contra, ipsil) and the lesioned group (contra, ipsil) during ChIs counting were  $0.059 \pm 0.002$ ,  $0.054 \pm 0.001$ ,  $0.06 \pm 0.001$ ,  $0.06 \pm 0.002$  (C-contra vs L-ipsil:  $p < 0.0294$ , C-contra vs L-ipsil:  $p < 0.0003$ ) respectively as shown in (**Figure 2. 9. C**). The both CEs variation in each group very similar but lesioned group cell counting CE still fluctuates and statistically significant compared to other control groups.

To sum up, either type of CE measurement was less than 10%, which fulfills the requirement for accuracy of cell counting in all three groups. However, the lesioned group CEs were higher at the lesioned side, maybe because the number of depleted cells were different in each individual.

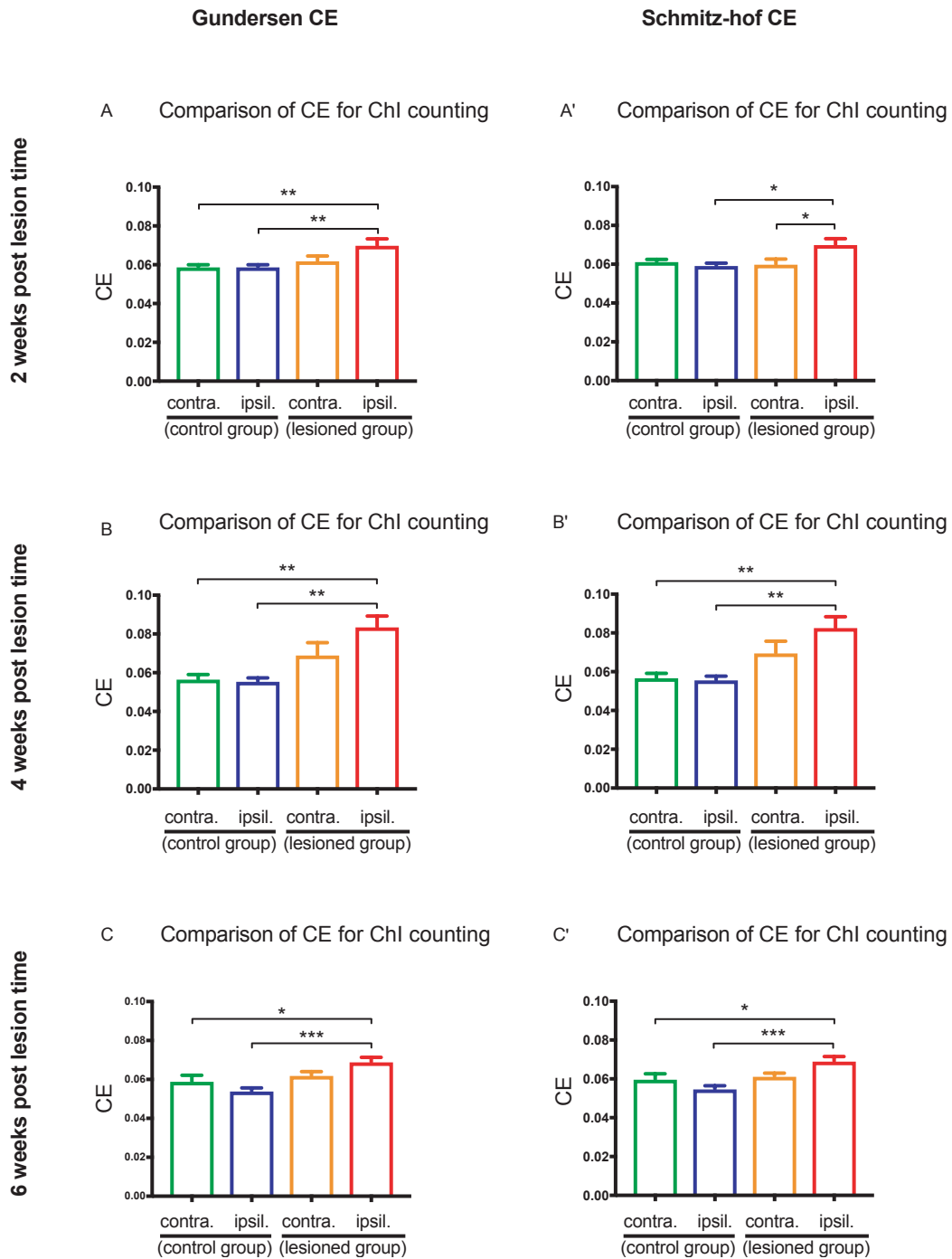


**Figure 2. 9 CE for ChIs counting.**

Bar graph of the two kinds of CE generated during cell counting for both hemispheres of control group (C-contra, C-ipsil), and toxin treated animals (L-contra, L-ipsil). **A**, CE measured at 2 weeks post lesion time (postnatal age p35 and number of animals n=9 for lesioned group, n=10 for control groups respectively). **B**, the CE at 4 weeks post lesion time (postnatal age p49 and the number of animals n=11 for lesioned group, n=10 for control groups respectively). **C**, the CE at 6 weeks post lesion time (postnatal age p63 and number of animals n=10 for lesioned group, n=10 for control groups

respectively). Data are shown as means  $\pm$  SEM. \* $p < 0.05$ , \*\* $p < 0.01$ , and \*\*\* $p < 0.001$ .

### 2.3.8 Evaluation of vAChT counting accuracy with two different CEs

To analyze the precision and reproducibility of vAChT bouton counting we used the same CEs estimation methods.

In short, the Schmitz-hof CE estimated that the CE was smaller in lesioned group at post lesion time two and four weeks (*Figure 2. 10. A', B'*) which reflects that more vAChT bouton were counted and that is consistent with our increased number of vAChT bouton count per individual. However, at 6 weeks post lesion time (*Figure 2. 10. C, C'*) there was no statistically significant difference in CE observed as vAChT bouton numbers were no longer elevated.

In conclusion, both CEs comply with a criterion of less than 10%. Although at two weeks post lesion time there were many individual differences in each group of vAChT counting CEs, it was not statistically significant with Gundersen CE estimate. The Schmitz-hof CE second estimate was more sensitive compared to Gundersen CE to detect the changes in each individual.

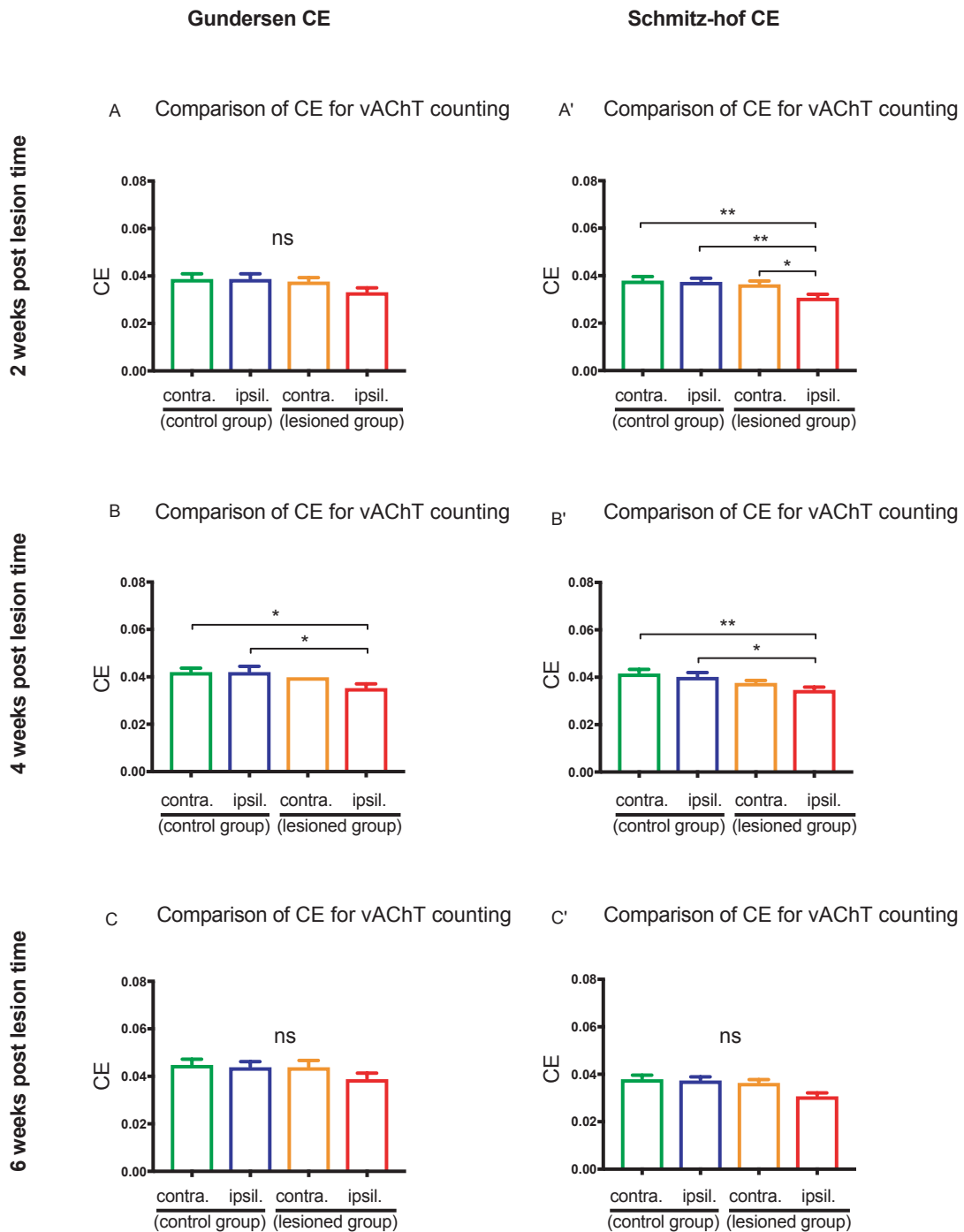


**Figure 2.10 CE for terminal counting.**

The two kinds of CE were generated during terminal counting for both hemispheres of control group (C-contra, C-ipsil), and toxin treated animals (L-contra, L-ipsil). **A**, CE measured at 2 weeks post lesion time (postnatal age p35 and number of animals n=9 for lesioned group, n=10 for control groups respectively). **B**, the CE at 4 weeks post lesion time (postnatal age p49 and the number of animals n=11 for lesioned group, n=10 for control groups respectively). **C**, the CE at 6 weeks post lesion time (postnatal age p63 and number of animals n=10 for lesioned group, n=10 for control groups

respectively). Data are shown as means  $\pm$  SEM, \* $p < 0.05$ , \*\* $p < 0.01$ , and \*\*\* $p < 0.001$ , one-way ANOVA followed by Tukey's multiple-comparisons test was applied.

## 2.4 Discussion

The current experiment combined specific ChIs manipulation with immunotoxin in DLS and unbiased cell counting. We demonstrate fundamental alterations in the number of ChAT and vAChT stained structures across three different post-lesion times. Although the lesions were not intended to denude the whole striatum, we counted stereologically in the whole striatal volume for both markers. This method allows us to estimate the total numbers of each target in the whole striatum. We counted numbers of axon terminals, varicosities and cell bodies in the striatum of wildtype *C57BL/6J* mice. We counted in both lesioned animals and in mice given injections of the same amount of saline into the same area and in untreated mice.

The stereological estimation of average number of ChIs total number in the mice striatum was compared at 35, 49 and 63 days of postnatal age. We did not find any age-related alterations of ChIs number in control groups. The variation in total number of ChIs in striatum may include: the antibody binding probabilities differences in each set even though we strongly controlled the experimental procedure, the depth of penetration of the antibodies, storage condition before counting starts, variation in perfusion efficiency between animals as well as normal biological variation between individuals. Our preliminary procedures assured us that the antibodies did not interfere with the numbers seen in naïve animals and that the counting efficiency was adequate to the task.

Based on the stereological random sampling method we show that lesions of ChIs in DLS are permanent and significantly eliminated neurons already after 2 weeks of post-injection time. There was an ongoing decrease in cell number that reached maximum at post-lesion time 4 weeks. The loss of the ChIs remained stable between 4- and 6- weeks post-injection. Thus, the number of ChIs was reduced and the significant removal of ChIs was stable between 4- and 6-weeks post-lesion.

Our research study can be summarized in the following two points: (a) this is the first study to compare the effects of the toxin at three post-lesion times; (b) the systematic random sampling method implementation enables quantitative estimation of the effect of the toxin at three post-lesion times. Our study looked not only at cell body losses, but also at the effect of the toxin on synaptic localization of vAChT and so we conclude that the loss of ACh action may not have been reduced in proportion with the cell damage.

Furthermore, we assume that the specific lesion of ChIs in the DLS is a partial lesion that could make significant changes at cellular and molecular level in striatal microcircuits. The ChIs specific lesion and consequent changes in vAChT number may play an important role in striatal function since the lack of the soma will change the input and hence the control of the release of ACh at these remaining synapses. No effect on the animals' behavior would imply that as long as ACh is available in the striatum detailed control of its release is unimportant. In these experiments, we have developed a test system that may let us understand how the specific local control of ACh release in DLS might be important for the life of the animal.

ChAT-sap toxin injected into the DLS of BAC EGFP-D1 and D2 transgenic mice showed that toxin injected lesioned side was significantly depleted of ChIs (**Figure 2. 5**). The ChIs depletion with ChAT-sap toxin seemed to be permanent for both mice as well as rats as reported previously (Aoki *et al.*, 2015).

In addition, we found toxin specific ablation of ChIs in DLS region results in sprouting of vAChT terminals locally in the striatum. We found that vAChT stained varicosities in the lesioned hemisphere were increased relative to control animals and non-lesioned hemisphere. This sprouting was largest at the shortest post-lesion time of 2 weeks. Interestingly, the increased number of vAChT terminals slowly returned to normal levels compared to control, sham and non-lesioned hemisphere over the 6 weeks of the study, in spite of the reduced number of ChAT positive cells.

A previous study in which there were multiple injections of di-isopropyl fluorophosphate (DFP) into striatum demonstrate that AChE staining in the local lesioned area decreases at 4h, 10h and 15h post-injection but the staining recovered at longer time periods



(Lynch *et al.*, 1972), suggesting that even less specific lesions lead to some recovery of ACh availability.

It has been a puzzle for a long time whether the elimination of ChIs is an important cause of behavioral modifications. Our results suggest that careful timing of the behavioral studies need to be taken into account in their interpretation.

Because most lesioning methods take time to develop, we measured the effect of the toxin at several times after the original injection. There are already several studies using the toxin in the striatum but the quantitative anatomical properties of the lesion have not been studied. Because we believed that the important effect of the ChAT-sap was likely to be upon the synaptic connections of the ChIs we also stained for the terminal vesicles using the protein responsible for uptake into vesicles: the vAChT. Double immunofluorescent labeling experiments were conducted with the antibodies to ChAT for cell bodies, and to vAChT for boutons (putative synaptic terminals).

At present, we have no direct evidence about the source of these extra terminals – they are still increased when the cell bodies are depleted, based on ChAT immunolabeling, at 6 weeks after the injection of toxin. Some preliminary experiments showed no visible change in the PPN. We consider the simplest interpretation to be that the elevated boutons from ChIs in the lesioned hemisphere are developed by the surviving ChIs in the rest of the undamaged striatum.

Our lesion study results proved further complexity of anatomical and morphological properties of ChIs in striatal circuits and extensive resilience and recovery of structure with time. The existence of sprouting or recovering of cholinergic neurons has been reported in multiple brain regions such as medial septum, dorsal vagal nucleus, hypoglossal nucleus and cortex in rat studies (Wenk & Olson, 1984; Lams *et al.*, 1988; Hagg *et al.*, 1989). An axotomized medial septum lesion study revealed that highest recovery rate of cholinergic neurons was achieved with nerve growth factor (NGF) infusion within a week after lesion, but with longer delayed post-lesion time between the lesion and NGF treatment decreased the possibility of full recovery. In addition, the axotomised cholinergic neurons showed signs of hypertrophy but the lesion results in the loss of ChAT staining but not actual neurons (Gage *et al.*, 1988; Hagg *et al.*, 1989). Similarly, the early histochemical changes of the dorsal vagal and

hypoglossal nucleus, which were loss of both transmitter associated enzymes (ChAT & AChE) after axotomy tested by counter staining with Nissl and True blue, indicate that the neurons are not dead and showed the presence of functioning cell membrane (Lams *et al.*, 1988). These findings from previous studies suggest that neurotransmitter associated enzymes may not be a reliable source of indicator in terms of testing whether neurons are alive or not. Because, these enzymes production experienced alteration in response to external lesion or insult (Lewis *et al.*, 1972; Lams *et al.*, 1988). Although we could not do equivalent experiments in our system, the loss of striatal volume on the lesioned side suggests a real loss of cells might be involved here.

In the next chapter we look at the time course of functional recovery in animal behavior and at the losses in behavioral repertoire after the lesions.

## Chapter 3 Impaired reach-to-grasp responses in mice depleted of striatal cholinergic interneurons

### 3.1 Introduction

Basal ganglia (BG) are highly organized subcortical brain structures that play critical roles in learning habits, motor skills (Hikosaka *et al.*, 2002; Kawai *et al.*, 2015) and modulation of motor behaviors at the neuronal and regional level. In parallel, the biggest portion of BG structure is the striatum that is involved in learning and motor functions with participation of extrastriatal brain areas (Hikosaka *et al.*, 2002; Diekelmann *et al.*, 2009). A wealth of excitatory glutamatergic inputs from cortical regions (Fonnum, 1984; Gerfen, 1984; Niciu *et al.*, 2012), internal/external cholinergic modulations (Dautan *et al.*, 2014; Mena-Segovia & Bolam, 2017), and dopaminergic inputs (Surmeier *et al.*, 1993; Berridge & Robinson, 1998; Haber *et al.*, 2000; Gerfen & Surmeier, 2011) from midbrain region are essential for subcortical motor circuits that underlie learning and motor functions of striatum. These functions, stored in striatal microcircuits, are enriched by a diverse and complex collection of different types of striatal neurons (Lynch *et al.*, 1972; Fonnum *et al.*, 1978; Graveland & DiFiglia, 1985; Kawaguchi, 1993; Kawaguchi *et al.*, 1995; Kreitzer, 2009).

The main input nucleus of the BG is the striatum, which is subdivided into three regions based on the functions and the distinct inputs they receive: they are the dorsolateral striatum (DLS), dorsomedial striatum (DMS) and nucleus accumbens (NAc/NAcc) as shown in (**Figure 3. 1**) (Kelley *et al.*, 1982; Gerfen, 1984; Malach & Graybiel, 1986; Voorn *et al.*, 2004; Pan *et al.*, 2010; Bosch-Bouju *et al.*, 2013). Much evidence points to the fact that DLS receives inputs from multiple cortical regions (sensory cortex, motor cortex, insular cortex, orbitofrontal cortex, dorsolateral prefrontal cortex) and the interconnected local neurons form microcircuits that are dedicated to achieve success in limb-movement related learning, or other learning processes (Lemon, 1993; Reiner *et al.*, 1998; Floresco *et al.*, 2008; Hilario & Costa, 2008). Notably, DLS functions to shape faster and efficient ongoing skilled activity such as sequential reach-to grasp behavior (Lopez-Huerta *et al.*, 2016).

Reach-to-grasp task formation is a process by which a grasping behavior through regular repetition becomes automatic or habitual (Tucci *et al.*, 2007; Chen *et al.*, 2014; Lopez-

Huerta *et al.*, 2016). The habit formation process of the grasping task depends on the cue, the behavior and the reward. The skill of the grasping task can be increased and refined with repetitions and by multiple days of training (Donoghue *et al.*, 1992; Girgis *et al.*, 2007; Li *et al.*, 2017). In addition, each individual has a unique approach to form the reach-to grasp skill in terms of speed, trial, angle of paws in 3D workspace and preferences of paws, even though the reward pellets are placed into the same position during the whole acquisition process (McKiernan *et al.*, 1998; Chen *et al.*, 2014; Li *et al.*, 2017).

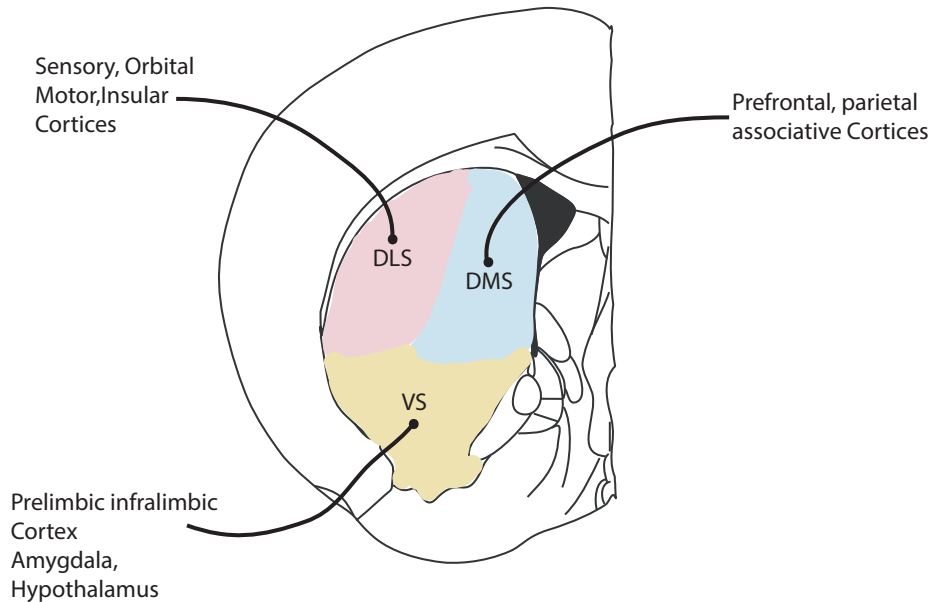


**Figure 3. 1 Gradients of function and the subdivision of the striatum.**

Schematic depicting the striatal regions with different extrastriata inputs and correspondent functions; modified from (Hilario & Costa, 2008; Tops *et al.*, 2014; Fuccillo, 2016).

How is reach-to-grasp behavior chosen so that the result is optimal and the animal achieves maximum reward? The highest success rate or optimal success in reach-to-grasp task can be defined in a variety of ways based on the different stages of training. However, there are two factors that are particularly relevant for reach-to grasp task. Firstly, optimal success rate can be driven by the outcome of achieving a single chocolate pellet and eating the pellet. For example, rats or mice will increase the speed of reach to grasp task movements to maximize the number of rewarded chocolate pellets in each 20-pellet session. Secondly, high success rate can be achieved when reaching and grasping behaviours are combined, and animals learn to find the shortest distance, angle or speed to minimize the cost for the reward (Gholamrezaei &

Whishaw, 2009; Marques & Olsson, 2010; Klein & Dunnett, 2012). Those approaches in food deprived animals can optimize the success rate through reducing the energy spent on the reach.

A fundamental question is what role does local cholinergic modulation in BG nuclei have in particular in new behavior formation and elimination. In this chapter, we focused on specific lesion of local ChIs population in the reach to grasp task already studied in human and many mammals (Farr & Whishaw, 2002; Marques & Olsson, 2010; Lopez-Huerta *et al.*, 2016). We examined the acquisition of a reach-to-grasp task and maintenance of the sequential motor skill in mice with a partially lesioned striatum, missing ChIs in the DLS area known to be involved in the task.

## 3.2 Methods

### 3.2.1 Animals and groups

72 virgin, male wild-type *C57BL/6J* mice (21-24 days old) weighing 10-15g were used in a series of experimental groups in the present study. These mice had been delivered from the Japan Clea at age 21 days old. Mice were group housed in plastic cages with bedding, and all animals were provided with food and water *ad libitum* and housed under standard controlled environment (temperature:  $21 \pm 1$  °C; humidity 55 %; light schedule 12/12 h with lights off at 7 p.m.) until stereotaxic surgery experiments. Thereafter animals were placed back to standard animal house. All mice were housed in groups of 3–4, according to the test group. To balance for potential litter effects, mice from the same litter were randomly assigned to a test group, so that each test group included mice of all litters. Standard rodent pellets and water were provided *ad libitum* except during the test period, when food restriction was introduced (week 4-postnatal day 28).

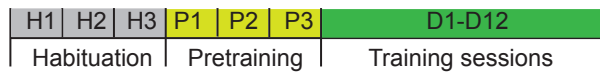
Seven groups of animals were trained for behavior experiments including: control group (**Figure 3. 2. A**), sham group (**Figure 3. 2. B**), ChAT-sap treated group (**Figure 3. 2. C**), control + lesion (15 days) group (**Figure 3. 2. D**), control + control (15 days) group (**Figure 3. 2. E**), control + lesioned (7 days) group (**Figure 3. 2. F**), control + control (7 days) group (**Figure 3. 2. G**).

### 3.2.2 Behavioral habituation and training

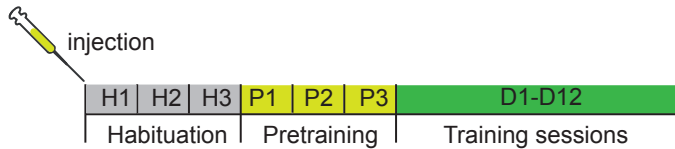
We used a training box of the same dimensions and followed procedures established in earlier publications by Marques and Olsson (2010); Lopez-Huerta *et al.* (2016). Briefly, food restriction schedule provided enough food to maintain approximately 85% of body weight (1.4 g of food/animal/day) for week 4. The daily amount of food was provided after completion of that day's training and testing, in pieces scattered on the bottom of the cage, so that all mice could eat. 20 mg dustless precision pellets with chocolate flavor (Bio-Serv, USA) were used as reward during training and testing. Three days prior to the beginning of the test, mice were habituated to the reward pellets and the training box, pellets scattered on the bottom of the cage once daily (0.2 g/animal/day). During the testing week, 20 pellets were provided as reward for each daily session after which the daily amount of food was provided. All tests were performed between 7 p.m -12 a.m. Testing order was kept the same on each day, so that each animal was tested always at the same hour. Mice were observed from the front of the cage. Shaping/pretraining of grasping response (from pellet retrieval with the tongue to use of a preferred paw) was performed on 10-min sessions for 2-3 days. The preferred paw was determined on the first 10 attempts to reach. If a mouse used both paws, the preferred paw was considered the one used more frequently (out of 10 reaches). Grasp response was made easier by gradually moving the pellet towards the indentation contralateral to the preferred paw (Miklyeva *et al.*, 1994). We recorded all sessions with EthoVision software for further analysis. Performance was analyzed according to the quantitative measures established by Marques and Olsson (2010); Lopez-Huerta *et al.* (2016).

Note: each habituation and pretraining sessions are 10min/day.

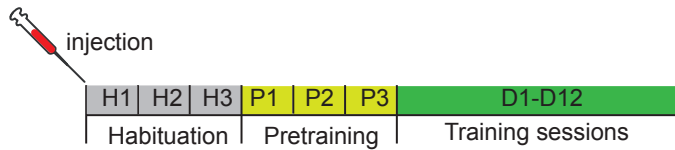
## A Control group



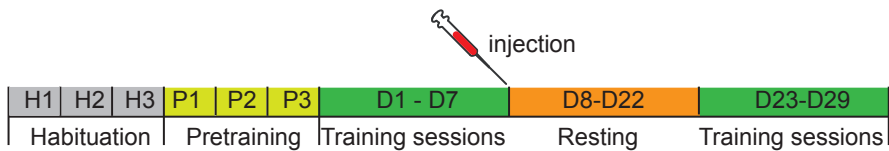
## B Sham group



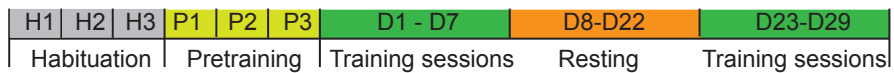
## C ChAT-sap lesioned group



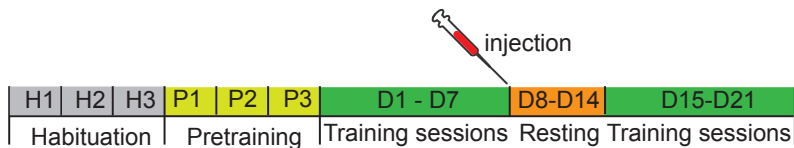
## D Control + lesion(15 days)



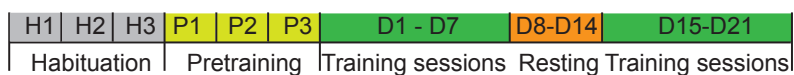
## E Control + Control(15 days)



## F Control + lesion (7 days)



## G Control + Control (7 days)

**Figure 3. 2 Experimental time line.**

A, Control group: experiments began after 3 days (D) of habituation (H) and 3 days of pretraining (P). B, Sham group:  $0.3\mu\text{l}$  saline was injected into DLS, followed by 3 days of habituation and 3 days of pretraining, and then experiments began. C, ChAT-sap lesioned group:  $0.3\mu\text{l}$  ChAT-sap toxin was injected into DLS, and followed by 3 days of habituation and 3 days of pretraining, and then experiments began. D, after 3 days of habituation and 3

days of pretraining animals were trained for 7 consecutive days (from day 1 to day 7). On day 8, 0.3 $\mu$ l ChAT-sap toxin was injected into DLS then animals rested for 2 weeks (from day 8 to day 22). Animals again trained for 7 days (from day 23-29). E, after 3 days of habituation and 3 days of pretraining animals trained for 7 consecutive days (from day 1 to day 7). From day 8 to day 22 animals rested for 2 weeks and then animals were again trained for 7 days (from day 23-29). F, after 3 days of habituation and 3 days of pretraining animals were trained for 7 consecutive days (from day 1 to day 7). On day 8, 0.3 $\mu$ l ChAT-sap toxin was injected into DLS then animals rested for a week (from day 8 to day 14). Animals were again trained for 7 days (from day 15-21). G, after 3 days of habituation and 3 days of pretraining animals were trained for 7 consecutive days (from day 1 to day 7). From day 8 to day 14 animals rested for a week and then animals were again trained for 7 days (from day 15-21).

### 3.2.3 Stereotaxic Surgery

To selectively lesion ChIs, animals were anesthetized by continuous isoflurane inhalation, USP (IsoFlo, Abbott Laboratories, IL, 1.0%–1.5% in medical O<sub>2</sub>). The respiratory rate, heart rate, and hind paw withdrawal reflexes were monitored throughout the procedure to maintain an adequate anesthetic level as stably as possible. Animals were fixed with atraumatic ear-bars, the cornea protected with mycochlorin ointment 2% and the skin rubbed with anesthetic gel (10% ketoprofen and lidocaine). Then animals received stereotaxic injections of the saporin ribosome-inactivating-immunotoxin that targets choline acetyltransferase (ChAT-sap toxin) 0.3 $\mu$ l (at concentration of 0.5 $\mu$ g/ $\mu$ l) into the contralateral hemisphere (in group D & F) of preferred paw, or injected into the DLS (in group B & C) on the left hemisphere according to the mouse brain atlas (Franklin & Paxinos, 2008) (**Figure 3. 3. A**). The toxin targeting ChIs was injected into the dorsal lateral striatum (DLS) on left hemisphere (bregma: AP, 0.98mm; L, -1.89mm; -3.45mm). Injections were carried out at a constant flow rate of 0.1 $\mu$ l/min with a PHD ULTRA™ Programmable syringe pump. During surgery, the body temperature was kept at normal physiological conditions using a disposable heating pad. After completion of injections, the needle was left in place for additional 10 mins to allow diffusion of the toxin before retraction and kept mice warm until they came out of anesthesia (<15 min). During the first 72 hours after surgery, post-operative care administered to control hypothermia, dehydration with a can of diet gel with carprofen (e.g., MediGel CPF, Portland, ME, USA). For sham treated animals, 0.3 $\mu$ l saline was injected into the DLS (bregma: AP, 0.98mm; L, -1.89mm; -3.45mm) and other experimental procedures are the same with toxin treated group. After surgery, at least a week was allowed before starting behavioral training. The injection



procedure was followed by behavioral training based on each group and then histology procedure as described below (**Figure 3. 3. A**).

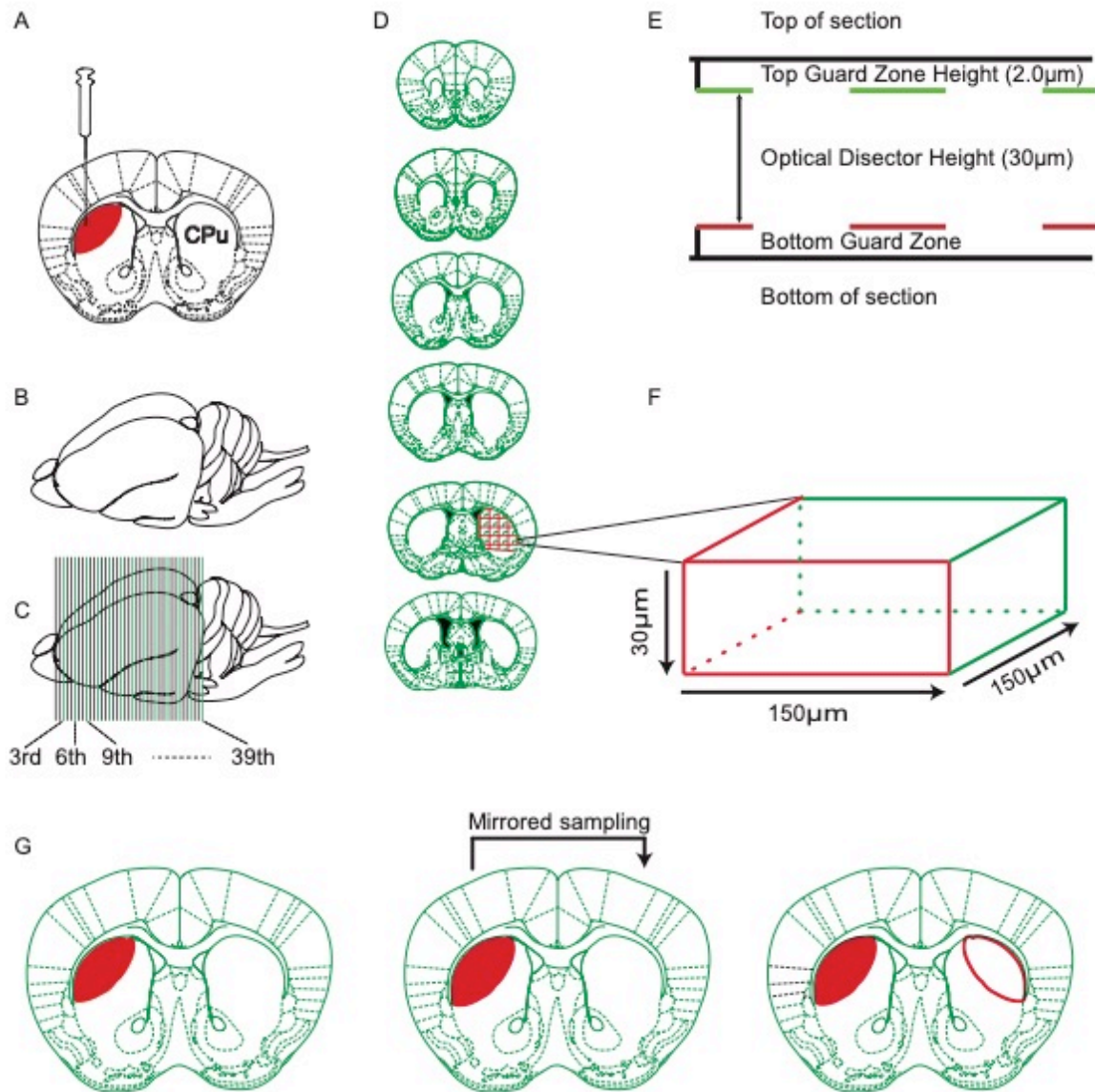


**Figure 3. 3 Schematic diagram for tissue preparation process for stereological systematic random sampling.**

**A**, stereotaxic injection of ChAT-sap toxin. **B**, the mouse whole brain after decapitation. **C**, every third section through the striatum was collected for stereological sampling. From each brain a total of 13 sections were used for analysis. **D**, a diagrammatic coronal brain sections modified from (Franklin & Paxinos, 2008) brain atlas, shown we kept the order of each sections during the process. **E**, a diagrammatic illustration showing the ChIs sampling in a thick section. This figure depicts a section view from the lateral edge of a 60µm thick section. To avoid biases, a section guard is employed at the upper and lower surfaces of the section. **F**, a diagrammatic sampling frame created a 3D virtual wall ( $30 \times 150 \times 150 \mu\text{m}$  for ChIs,  $5 \times 5 \times 5 \mu\text{m}$  for vAChT), shown in the form of lines, the red lines representing forbidden lines and green lines representing including lines. Any cells superimposed over the red line are excluded from counting, while particles totally inside the dissector volume or superimposed over a green line are included as dissector particles. **G**, Mirrored sampling, conducted by only drawing contour for lesioned region and reflecting the exact

same contour to intact hemisphere and then comparing the counted cells from both hemispheres of coronal sections.

### 3.2.4 Perfusion

After the behavioral training, to conduct stereological and anatomical investigation, the mice were deeply anesthetized with isoflurane, then transcardially perfused with phosphate buffer 0.1 M (pH 7.4) followed by phosphate buffer containing 4 % paraformaldehyde and 14 % saturated picric acid. The brain was removed after decapitation, postfixed in the same solution for 24hrs at 8°C and then cryoprotected in a 50/50 mixture of fixative and 20 % sucrose in 0.1 M phosphate buffered saline (PBS) for at least 24h or until the brain sank to the bottom of the vial (**Figure 3. 3. B**).

### 3.2.5 Sectioning

Each brain was serially sectioned in the coronal plane, on a sliding microtome with a freezing stage (Yamato electrofreeze, MC-802A) at an instrument setting of 60  $\mu\text{m}$ . Total sections were divided into three sets of consecutive sections A, B and C. A set sections were processed for immunocytochemistry to visualize choline acetyltransferase (ChAT) to identify ChIs, glial fibrillary acidic protein (GFAP) to identify astrocytic response to damage, and DAPI fluorescent stain that binds strongly to DNA to identify the cell nucleus. Sections that contained the striatal formation were used for stereological systematic random sampling (13 sections). The remaining B and C sets of sections were held in reserve and stored in an anti-freeze (ethylene glycol) cryoprotectant solution at  $-30^{\circ}\text{C}$  (**Figure 3. 3. C**).

### 3.2.6 Histology

Sections were incubated for 4h at room temperature in 10% normal donkey serum (NDS) or 20% normal goat serum (NGS) diluted in PBS. They were then incubated in ChAT primary antibody (Millipore, California USA, goat polyclonal antibody, 1:100 dilution) in antibody diluent (Triton0.3%,  $\text{NaN}_3$  Azide0.05%, PBS) in the dark room for at least 24h at 4°C on a shaker, washed in PBS (4×5min) and then incubated GFAP primary antibody (Biosensis, Thebarton, South Australia, rabbit antibody, 1: 1000 dilution) washed with PBS (4×5min).

Following this procedure, sections were incubated with secondary antibodies separately in the dark room for 12h at 4°C on a shaker (dilution 1:200). For GFAP and ChAT double staining, the secondary antibodies used were Alexa fluor 594-donkey anti-rabbit (Life Technologies, Eugene, OR, USA; 1:200) and Alexa fluor 488-donkey anti-goat (Life Technologies, Eugene, OR, USA; 1:200), respectively. For ChAT single staining, the secondary antibody used was Alexa fluor 488-donkey anti-goat (Life Technologies, Eugene, OR, USA; 1:200). Sections were again washed in PBS (4×5min) and mounted. The subsequent immunostained slices were visualized using a spinning disc confocal microscope (Olympus BX-DSU) and (Carl Zeiss LSM780) confocal microscope. Pictures were taken using ZEN software or NeuroLucida software and a Hamamatsu (EM-CCD C91) camera.

### **3.2.7 Estimation of the total number of ChIs in ChAT-SAP injected and behaviorally trained animals using the optical fractionator**

The post-lesion time for ChAT-SAP toxin injected animals were 7 days and 14 days in different groups as described above (section 3.2.1 Animals and groups) which were used for ChIs counting after training was completed. All of the mice were injected at the same stereotaxic co-ordinates, toxin concentration, perfusion, fixation, sectioning, staining, and mounting procedures as described above in order to avoid biased cell counting (West, 2012). Stereo Investigator version 11, NeuroLucida software and Hamamatsu (EM-CCD C91) camera were used to image and count ChIs stained for ChAT from coronal sections. In each of the sections to be sampled, the total ChIs number counted and estimated in the striatum were obtained using the optical fractionator technique [see (West *et al.*, 1991; Olesen *et al.*, 2017) for detailed description of the optical fractionator].

ChIs were directly counted in a selected set of sections at predetermined uniform intervals of one-third of total sections obtained from a brain. The first section was randomly determined according to shape of striatum and brain section was traced at low magnification 4×/0.16 Hamamatsu for striatal volume estimation. A grid with a total frame size of 400×400µm was placed over the striatal region to be traced and the software placed equally spaced counting frames at random. ChIs were counted under high magnification 20×/0.75NA objective lens. The size of the counting frames was X=150µm and Y=150µm (**Figure 3. 3. F**). The number of counting sites per section depended on the size of striatum in each section. Size

varied from section to section throughout the brain. The top guard zone height was 2 $\mu$ m after manually focusing on the surface of the section and the dissector height was set at 30 $\mu$ m (**Figure 3. 3. E**). The striatal ChIs that fell within the borders of the counting frames and did not touch the red exclusion borders were included in the analysis. Data from lesion (left hemisphere) and non-lesion (right hemisphere) sites were analyzed separately. In total, 13 striatal sections were analyzed from each brain. As each section was double-stained to identify ChIs and GFAP, we used the same sections for both counting and anatomical study.

The number of counted neurons in the subdivision (N) is estimated as:

$$N = \Sigma Q \cdot \frac{t}{h} \cdot \frac{1}{asf} \cdot \frac{1}{ssf}$$

$asf$  = counting frame size /counting grid size.

$ssf$  = the interval of sections sampled through an object

Where  $\Sigma Q$  is the total number of neurons actually counted,  $t$  is thickness of the sections,  $h$  is the height of the dissector,  $asf$  is fraction of area of section sampled,  $ssf$  is the section sampling fraction. In our study:

$asf = 22500$  (the counting frame is 150 $\times$  150 $\mu$ m)/160000 (the sampling grid is 400 $\times$ 4000 $\mu$ m)

$$ssf = 1/3$$

Estimation of the total number:

$$N_{total} = N \times k$$

Where N is sum counts, k is the interval of sections sampled through an object, the  $ssf$  and k is same.

NOTE: We conducted a pilot study including a few animals from each experimental group to determine the optimal sampling parameters, such as the number of the sections to be analyzed, the thickness of the tissue, grid size, counting frame size, lower magnification for delineate the area interest and high magnification to count. From the pilot study, we obtained initial result for cell numbers, CV (coefficient of variation) and CE (coefficient of error) then determined the parameters as described above to obtain a satisfactory precision of estimates. The tissue thickness was measured in each sampling area within the region of interest.

### 3.2.8 Quantitative analysis of performance

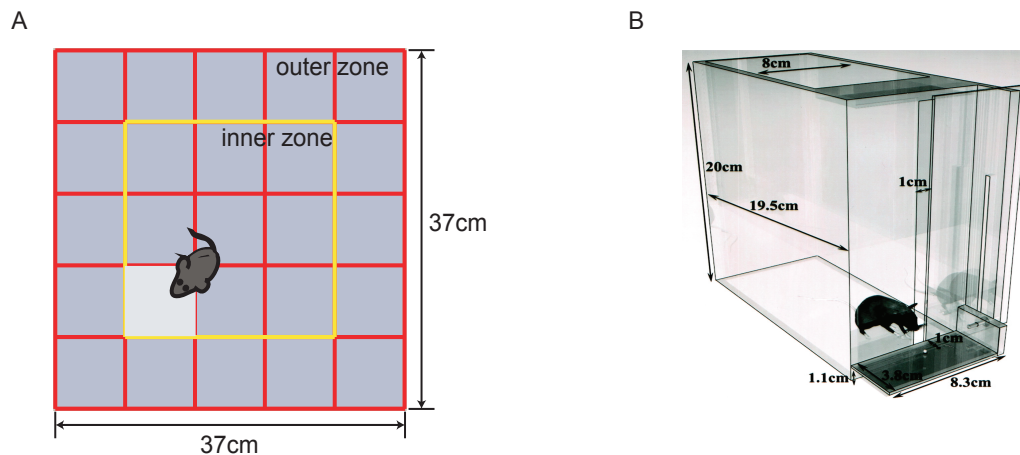


**Figure 3. 4 Two behavior tests used for animals**

**A.** Open field test (OFT) chamber  $37 \times 37 \times 28$  (length  $\times$  width  $\times$  height)  $\text{cm}^3$  with O'HARA multi-chamber software analysis package used to evaluate subjects' tracks. In addition to general behavior analysis, with the addition of sensors, the subject's vertical activity also can be measured (the hardware detects beams broken by the animal so that the software can determine the location of the mice within the cage). **B.** The single pellet reach-to-grasp task apparatus. The **B** image taken from (Farr & Whishaw, 2002).

#### 3.2.8.1 Placement of pellet

In each daily session, there were 20 trials with 1 pellet/trial. A pellet was placed contralateral to the preferred paw into indentations on the front tray of the training box (**Figure 3. 4. B**). Which indentation to place the pellet was determined based on paw preference of mice determined during pre-training.

#### 3.2.8.2 1<sup>st</sup> attempt

Each time, pellet was placed into indentation after mice walked away from the front part of the training box. Once mice come back to the front and used their preferred paw to grasp the pellet, we considered this as the first attempt for each new pellet.

#### 3.2.8.3 Successful retrieval on the first reach-to-grasp

The pellet is obtained with one single reach to grasp action and placed directly into the mouth. On an analysis sheet a success is marked with ‘1’ and number of grasps counted as one.

#### **3.2.8.4 Success or fail**

A successful reach-to-grasp was defined as the ability to reach and grasp the pellet, then pull the limb back through the slit and place the pellet directly into the mouth. This is true regardless of how many attempts were made to get the pellet. A failed reach-to-grasp is defined when the pellet is batted out of reach or successfully reached and grasped but dropped on the floor before eaten, even if the mice eat the dropped pellets afterwards. On video analysis sheet a success is marked with ‘1’ and a fail is marked with ‘0’.

#### **3.2.8.5 Grasp count**

Each reach-to-grasp attempt made with preferred paw is scored when a pellet is present in indentation within reaching distance. However, a reach-to-grasp attempt made with the preferred paw (without a pellet present) is excluded from grasp count analysis.

#### **3.2.8.6 Failed reaches**

A failed reach was defined when the pellet has been batted too far away and the ability to obtain a pellet is impossible.

#### **3.2.8.7 Criteria for learning curve within intact control animals**

The criteria were as follows:

Normal learner: compared to the first day, if the animals increase success rates around 10-20% in the following days (from day 2 to day 4), they were considered as normal learners.

Slow learner: compared to the first day, if the animal’s success rate did not improve through training sessions by 10-20%, they were considered as slow learners.

Fast learner: from the first day on, if the animals' success rate was above 50% they were considered as fast learners.

### 3.2.9 Statistical analysis

Numerical values systematically measured for the performance of the mice were analyzed using two-way ANOVA with repeated measures with days as the within subject factor and treatment groups and days as between subject factors followed by Tukey's multiple-comparisons test. Differences were considered to be significant if  $p$  values were  $< 0.05$ . All statistical analyses were performed using Prism software for Mac.

### 3.2.10 Ethical approval

All our experimental procedures complied with guiding policies and principles for experimental procedures endorsed by the government of Japan and supervised by the local Animal Care and Use Committee. Wild-type C57BL/6J male mice ( $n=71$ ) of age postnatal day P 21 were purchased from Japan Clea and delivered to Okinawa Institute of science and Technology (OIST). Mice were housed at the OIST animal facility until the experiments were finished and brains collected.

## 3.3 Results

### 3.3.1 Immunostaining for ChAT shows loss of cholinergic interneurons after ChAT-sap toxin administration.

All animals treated with ChAT-sap toxin were processed for anatomical confirmation of ChIs lesion in striatum (**Figure 3. 5. A, B**). The triple labeling immunohistochemistry with DAPI staining confirmed that ChAT-sap toxin injected animals show significant depletion of ChIs around the injection site and dense expression of GFAP, a marker for active glial fibrillary acidic protein (**Figure 3. 5. A, B** red color).



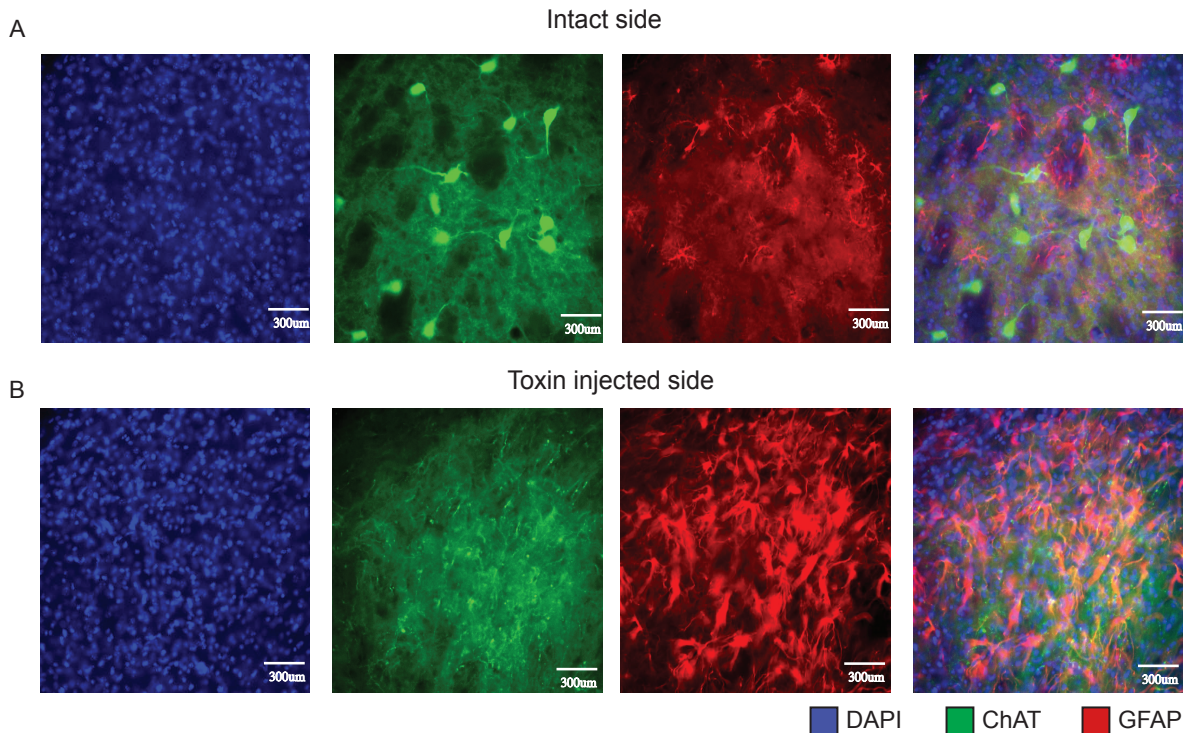


**Figure 3. 5 The confirmation of ChIs depletion in ChAT- sap injected animals after behavioral training.**

**A.** Low-magnification images of a coronal triple contained striatal section triple-labeled for ChAT, GFAP and DAPI showing that the striatal ChIs were depleted with ChAT-sap toxin treatment. **B.** Images of a triple-stained intact hemisphere of ChAT- sap injected animals.

### 3.3.2 The quantitative analysis of reach to grasp task performance in different groups

In continued training paradigm (**Figure 3. 2. A**), mice were trained for 12 consecutive days with a single pellet reach to grasp task to evaluate skilled motor performance after selective lesioning of ChIs in DLS. Three experimental groups were as follows: intact control, sham, and ChAT-sap toxin injected ( $n=25$ ,  $n=9$ ,  $n=13$ ) mice respectively (**Figure 3. 6. A**). The two-way ANOVA of success rates revealed a significant group variability [ $F(2,664) = 101.1$ ,  $p < 0.0001$ ], indicating that the mice in intact and sham group were statistically different from the ChIs lesioned group (ChAT-sap toxin injected) (control vs ChAT-sap:  $p \leq 0.0001$ , sham vs ChAT-sap:  $p \leq 0.0001$ ). Intact control and sham achieved higher success rate on average ( $53.09 \pm 1.4$ ,  $48.29 \pm 1.2$ ,  $27.15 \pm 1.1$  respectively intact control, sham, ChAT-sap injected). However, there was no significant variability of days [ $F(11,664) = 0.58$ ,  $p \leq 0.84$ ], but the interaction by groups was significant [ $F(2,664) = 101.1$ ,  $p \leq 0.0001$ ]. In addition, the learning curves of the intact control and sham groups were similar throughout daily sessions,

statistically there were no significant differences (control vs sham:  $p \geq 0.7461$ ), in intact and sham group suggested that the stereotaxic surgery has no impact unless there is specific lesion on ChIs. Although the animals treated with ChAT-sap, the learning curve displayed a trend toward improving (higher success rate) after training day 5, the success rate was not high enough to reach control/sham groups performance.

Furthermore, to study the ChIs lesion impact on reach-to-grasp task performance in mice, we compared success rate of two groups which were control+lesioned (15 days) and control+control (15 days) (**Figure 3. 6. B**) (for detailed behavioral paradigm see from (**Figure 3. 2. D, E**)). The two-way ANOVA on success rate revealed a statistically significant difference between before (D1-7) and after (D23-29) ChAT-sap toxin lesion with 15 days resting sessions [F (3,140) =19.98,  $p \leq 0.0001$ ]. Within intact control group, the mice on average learned better after 15 days resting period compared to former 7 days session (D1-7:  $57.38 \pm 4.5$  vs D23-29:  $69.52 \pm 3.6$ ,  $p \leq 0.0001$ , Mean  $\pm$  SEM, %). The success rates of lesioned group were statistically significant before and after 15 days (D1-7:  $62.50 \pm 3.3$  vs D23-29:  $51.54 \pm 5.3$ ,  $p \leq 0.0001$ , Mean  $\pm$  SEM, %). In general, lesioned group achieved lower success rates compared to intact control group after 15 days of resting period (lesioned group's D23-29:  $51.54 \pm 5.3$  vs control group's D23-29:  $69.52 \pm 3.6$ ,  $p \leq 0.0001$ , Mean  $\pm$  SEM, %) (see **Figure 3. 6. B**).

Finally, we compared success rate of two groups which were control+lesioned (7 days) and control+control (7 days) (**Figure 3. 6. C**) (for detailed behavioral paradigm see (**Figure 3. 2. F, G**)). The two-way ANOVA on success rates showed a significant group variability [F (3,125) =28.53,  $p \leq 0.0001$ ] and day to group interaction variability [F (18,125) =2.74,  $p = 0.0005$ ]. D1-7 control training session compared with control group's retraining session D15-21 and lesioned group's retraining session D15-21 after 7 days resting period. Control groups achieved higher success rate after 7 days resting period (D1-7:  $56.8 \pm 4.4$  vs D15-21:  $66.1 \pm 3.73$ ,  $p \leq 0.0175$ , Mean  $\pm$  SEM, %). However, the lesioned group success rate dropped after 7 days of treatment (D1-7:  $62.14 \pm 6.15$  vs D15-21:  $38.28 \pm 8.8$ ,  $p \leq 0.0001$ , Mean  $\pm$  SEM, %). Lesioned group achieved lower success rates compared to intact control group after 7 days of resting period (lesioned group's D15-21:  $38.28 \pm 8.8$  vs control group's D15-21:  $66.1 \pm 3.73$ ,  $p \leq 0.0001$ , Mean  $\pm$  SEM, %). This result implies that DLS ChIs depletion has a significant impact on reach-to-grasp success rate of mice with a week of toxin infusion time.

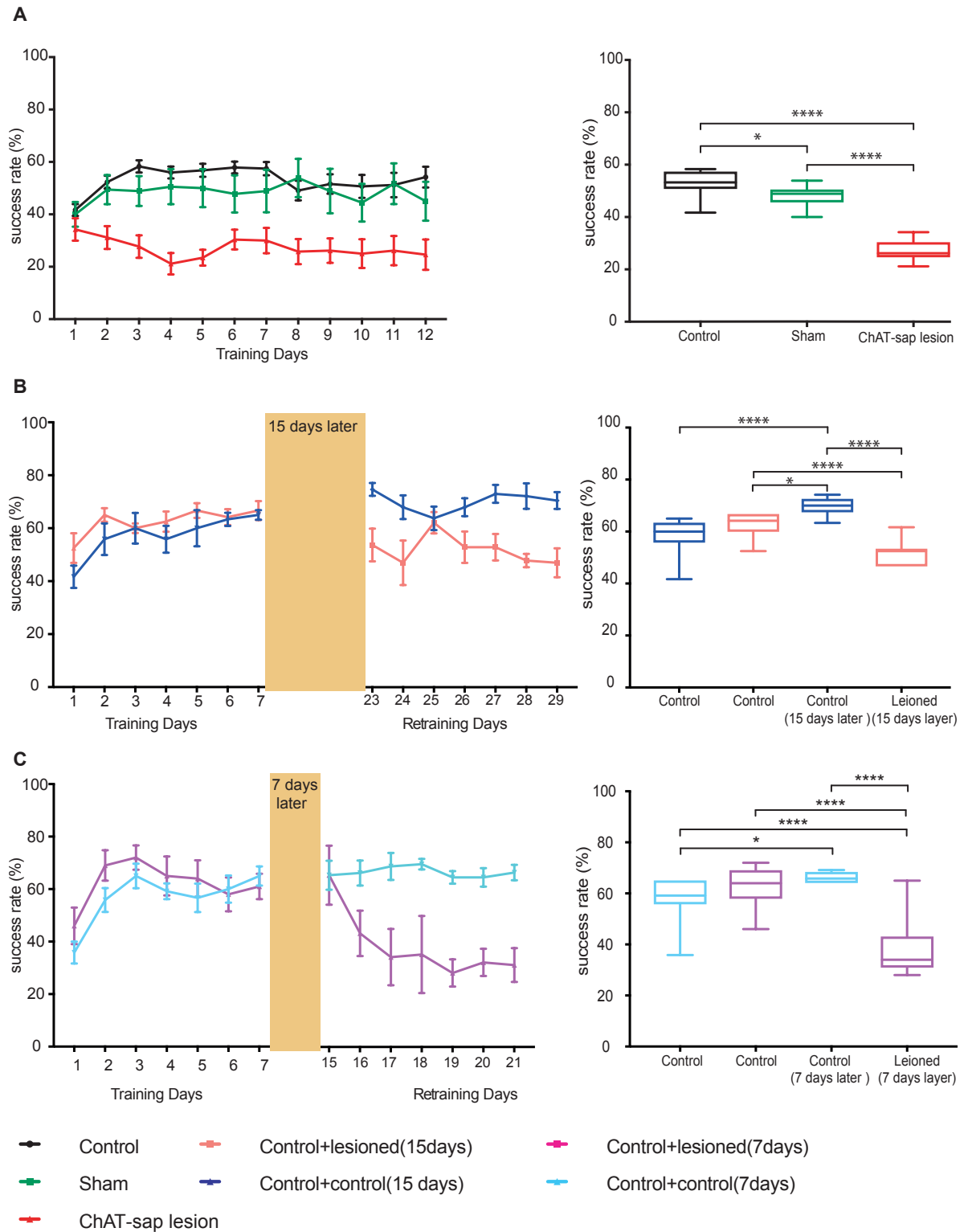


**Figure 3. 6 The reach to grasp task performance.**

**A.** Intact control, sham, and ChAT-sap lesioned groups (black, green, and red respectively) tested for 12 consecutive days training. **B.** Comparison of success rate before and after the toxin lesion with 15 days resting period. **C.** Comparison of success rate before and after the toxin lesion with 7 days resting period. The success rate of each group drawn with different colors. All data shown in the figure is (Mean±SEM). The number mice used were n=25, n=9, n=13, n=6, n=6, n=6, n=5 respectively for intact control, sham, ChAT-sap lesioned,

control+control (15days), control+lesioned (15days), control+control (7days), control+lesioned (7days). The box plots on the right are summary data from left, the whiskers (Min to Max) (\*  $P \leq 0.05$ ; \*\*  $P < 0.01$ ; \*\*\*  $P < 0.001$ ; \*\*\*\*  $P < 0.0001$ ). The box always extends from the 25th to 75th percentiles. The line in the middle of the box is plotted at the median.

### 3.3.3 Paw preferences of mice in different groups

The hand preference in human or paw preference in non-primates mammals are complicated traits of different species which are a reflection of hemispheric organization and interaction with environment. The earliest studies showed that 90% of the human population is right handed and only about 10% left handed. On the other hand, there are an equal number of left/right pawed non-primate mammals (dog, cats and mice). The right hand/paw is controlled by left hemisphere and the left hand/paw is controlled by right hemisphere (Tan, 1987; Tan *et al.*, 1990; Bulman-Fleming *et al.*, 1997).

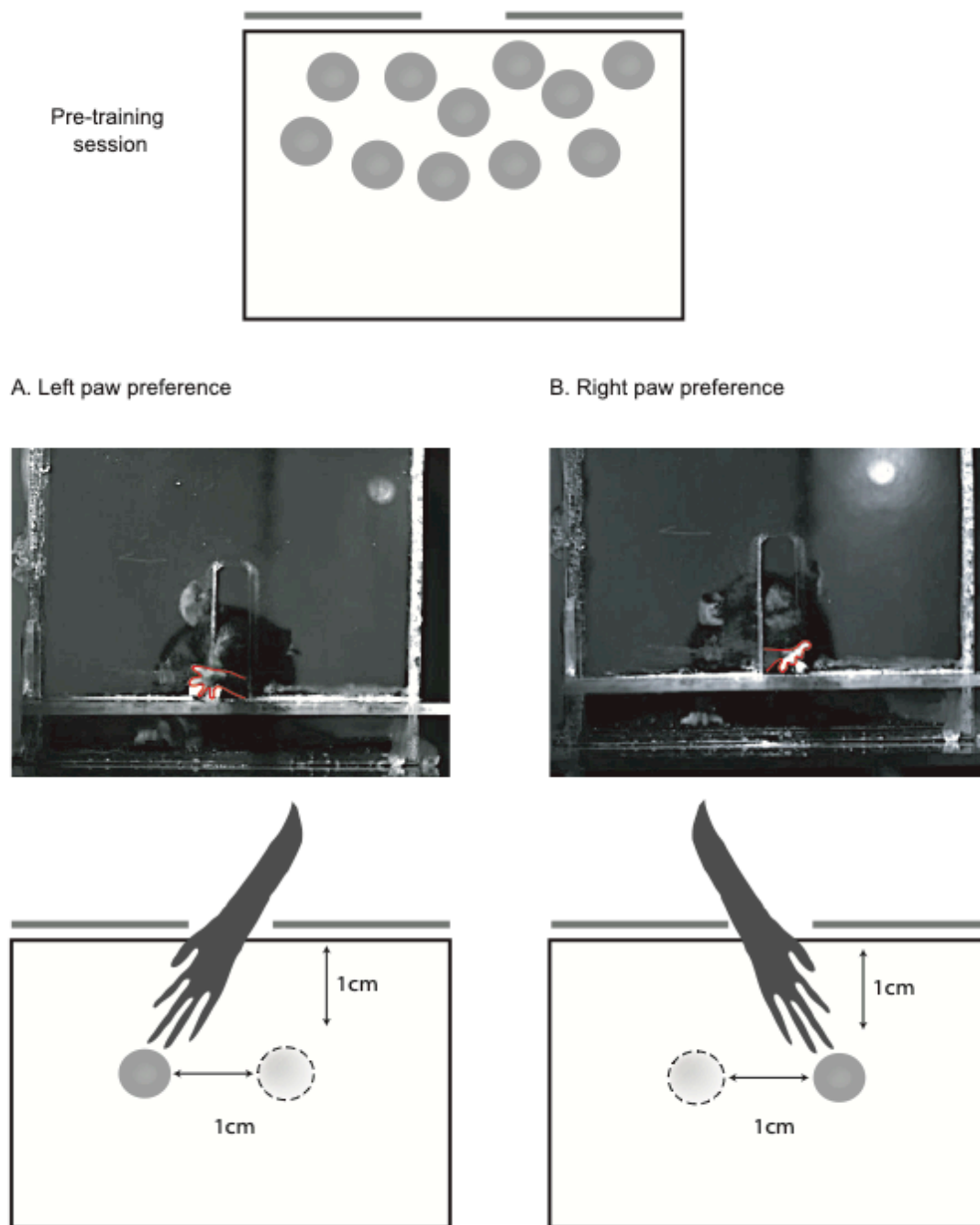


**Figure 3. 7 Shaping paw preference.**

**A.** The mice preferred to use left paw. **B.** The mice preferred to use right paw (the diagrams underneath are the observation from top, the empty depression is depicted with dashed line, the depression with pellet is grey color).

During the pretraining session of reach-to-grasp task, mice were observed from the front of the cage (**Figure 3. 7**). Shaping/pretraining of grasping response was performed on 10-min sessions for 2-3 days. The preferred paw was determined on the first 10 attempts to reach.

If a mouse used right/left paws, the preferred paw was considered the one used more frequently (out of 10 reaches).

We analyzed the dynamics of paw preferences in unbiased symmetrical reach-to-grasp task training box where mice, wild-type *C57BL/6J*, could freely choose which paw to use during reach to grasp task in all groups (see **Figure 3. 2**). Seven groups exhibited almost equal paw preference within and between training sessions which were 15 days and 7 days apart from second session of training (see **Figure 3. 8. A, B, C**).

During the continued training sessions (see **Figure 3. 8. A, B, C**) with the intact control group, half of the mice used their left paw, the half used their right paw (n=25). In the sham group, 55.55% animals used their right paw (n=5, total n=9) which is very similar to an earlier research report (Bulman-Fleming *et al.*, 1997; Lopez-Huerta *et al.*, 2016). But in the ChAT-sap injected group, 69% animals used their left paw (n=9, total n=13). The sham and ChAT-sap injected groups were slightly different from the intact control. However, we didn't observe any polarized distribution of paw preference among these three groups during training. The sample size differences in each group could be the main reason for the deviation from the control group. In general, the paw preference remained the same throughout the whole training sessions.

Interestingly, the mice didn't change paw preferences in control+lesioned (15 days) and control+lesioned (7days) before and after the lesion with ChAT-sap toxin injection (see **Figure 3. 8. D, E**). The paw preference in control+control (15 days) and control+lesioned (15 days) is the same in both directions (right and left respectively 66.67% and 33.33%). By contrast, in control+control (7days) and control+lesioned (7days) the paw preferences were largely varied (**Figure 3. 8. E**).

Next, we analyzed the possible tendency of ChIs lesioned groups paw preference (see **Figure 3. 8. F**). The ChAT-sap injected groups (ChAT-sap, control+lesioned (15 days), control+lesioned (7days)), 58.33% used left and 41.66% used the right paw. In addition, in the control groups with different training paradigm (control, sham, contro+control (15 days) and control+control (7days)), around 43.47% used left and 56.525% used right paw.

Furthermore, we analyzed the right/left paw preference of all mice used for reach-to grasp single pellet task without considering the group differences. There are 51.42% right paw and 48.58% left paw preferred mice.

Overall, these results confirmed again that the mice paw preferences are evenly distributed (**Figure 3. 8. G**).

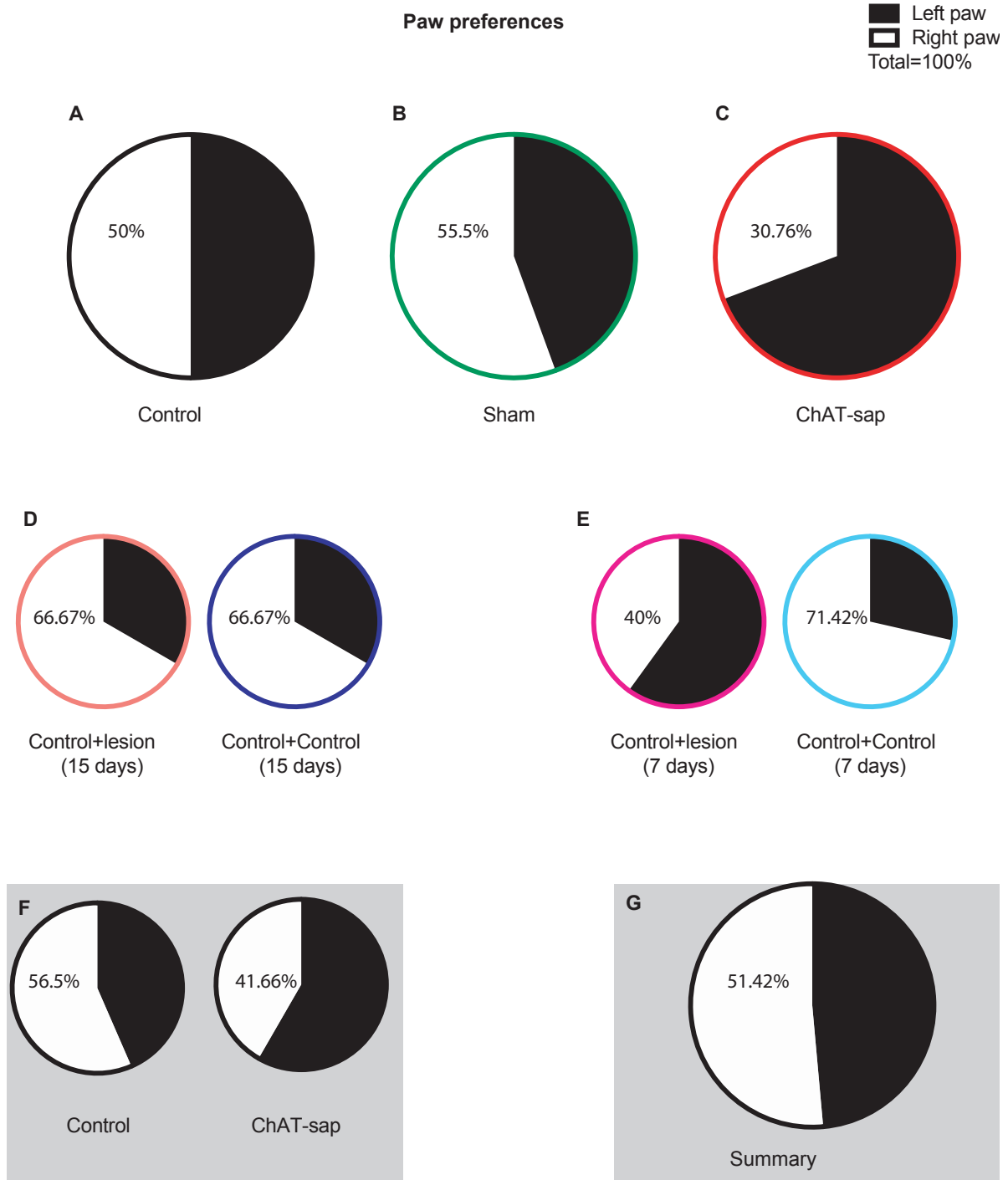


**Figure 3. 8 Percentage of paw preferences of mice assessed by reach-to-grasp task.**

**A.** Control group paw preferences. **B.** Sham group paw preferences (saline injection in left striatum). **C.** ChAT-sap lesioned group paw preferences (lesion in left striatum). **D.** Control+lesioned (15 days) and control+control (15 days) groups paw preferences (lesion in striatum contralateral to preferred paw). **E.** Control+lesioned (7days) and control+control (7days) groups paw preferences (lesion in striatum contralateral to preferred paw). **F.** Summary of paw preferences in percentage from all control conditions and all ChAT-sap injected animals. **G.** Summary of paw preferences in all of animals used in reach-to-



grasp task. (**black color**-left paw and **white color**-right paw which are depicted in pie chart. The different color around pie chart used to distinguish the different treatment groups).

Last, but not the least, among 72 animals trained for reach-to grasp task, only 2.8% (n=2) animals changed paw preferences during the training sessions. In addition, the animals changed paw preferences were not from ChAT-sap but from non-ChAT-sap injected groups (sham, control+control (15 days)), which means that, mice paw preference changes during the reach-to-grasp task is irrelevant with ChIs lesion into DLS in the present study (**Figure 3. 9**).

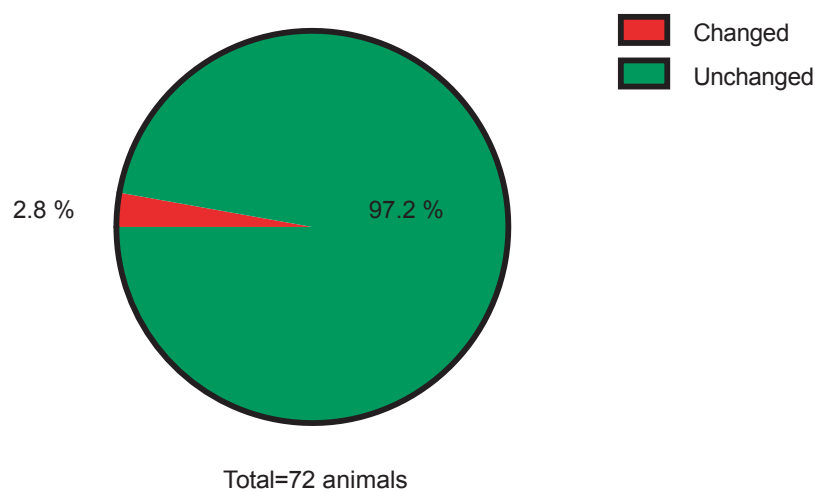
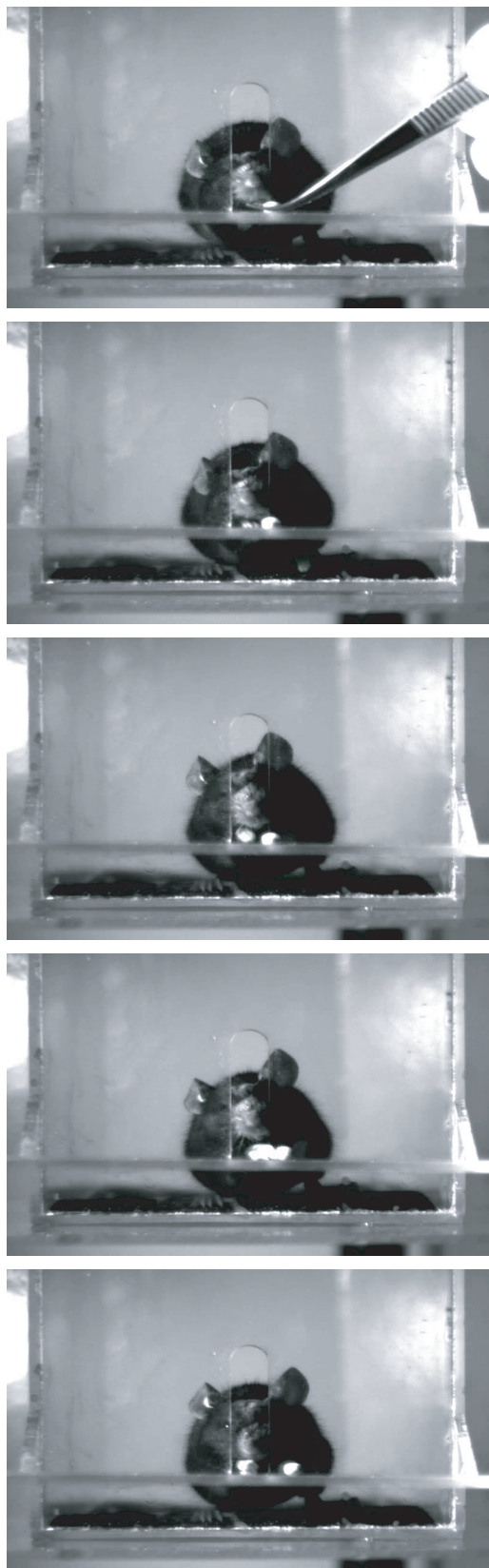


**Figure 3. 9 Paw preferences changes during the training sessions.**

### 3.3.4 The variability of reaching-approaches in lesioned and non-lesioned group

The lesioned and non-lesioned animals' success rates were different as discussed in former section (3.3.2). The video recordings from each training session showed that the reaching approaches in ChAT-sap lesioned and control groups were different (**Figure 3. 10. A, B**). As shown in the example in the figure (**Figure 3. 10. A**), the lesioned group failed to grasp the chocolate pellet. Instead the mice were able to reach the pellet but their fingers flexion and extension movements were occurred at an incorrect distance and pushed the pellet away.

A. ChAT-sap injected group



B. Control group

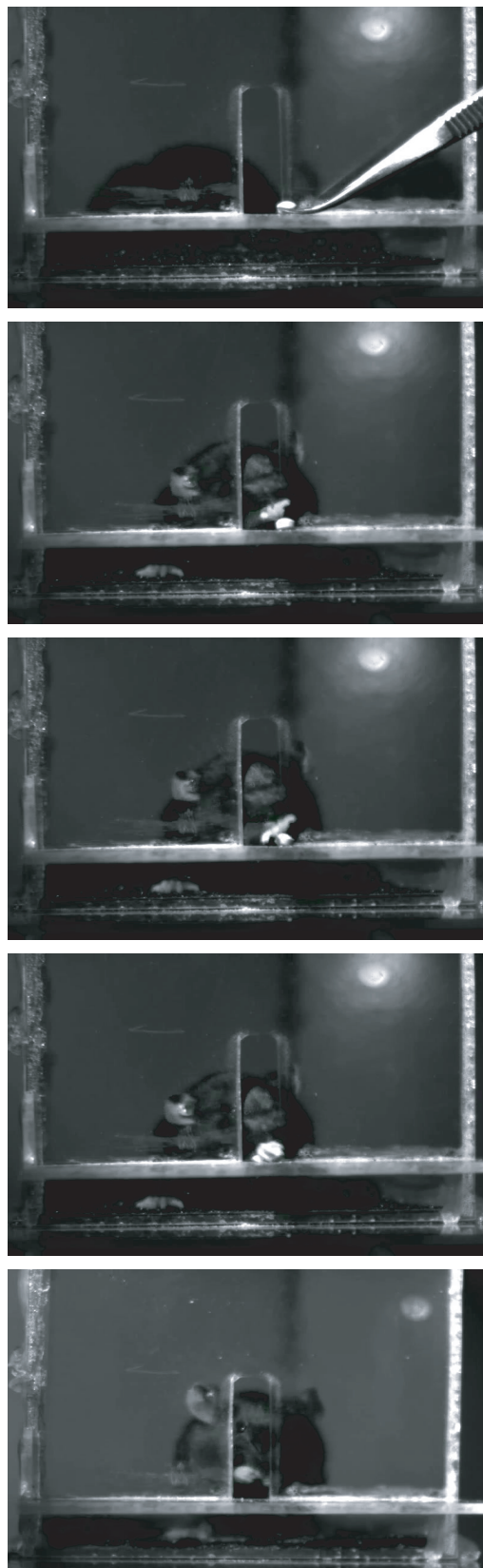


**Figure 3. 10 The distinct reach to grasp task approach in lesioned and control group.**

**A.** The ChAT-sap toxin injected (ChIs lesioned) mouse performing a failed reach-to-grasp task. (The mice in the image use right paw to reach a chocolate pellet placed in front of training box,). **B.** The intact control mouse performing a successful reach-to-grasp- task. (The mice in the image use right paw to reach a chocolate pellet placed in front of training box and successfully eats pellet). (These are sequential images taken from mice during the task performance).

The ChAT-sap lesioned animals incorrect reaching approaches were observed repeatedly compared to intact control and sham treated animals. In many cases, even though the pellet was placed on the designated location, the mouse often missed the pellet. Generally, the ChAT-sap lesioned mice stretched their paw high above, twisted to one direction, and too short to reach the pellet (**Figure 3. 11**). These are probably the main reasons that ChIs lesioned animals in most of the training days were not able to reach the highest success rate as control or sham groups, instead only able to achieve 31.15% success rate (around 6 out of 20 pellets) in the continued training paradigm (**Figure 3. 6. A, red color**).



**Figure 3. 11** The various reaching approaches of ChIs lesioned mice.

Photographs of a mouse treated with ChAT-sap toxin performing reach-to-grasp task, in which the mouse used incorrect approaches to achieve success. The mouse was unable to achieve success.

### 3.3.5 The different levels of performance within intact control group

Different levels of learners (normal, slow, and fast) were found in the intact control group which were trained in different training paradigms. The learning curve established from day 1 to day 7, and then from day 7 on the performance of mice was stable within control groups. To confirm whether the learning ability was different within each group, the learning curve criteria (see section 3.2.8.7) were established and we performed statistical tests for data from day1 to day7.

Significant interactions were found between the day of training and the different levels of learners (interactions:  $F(12,309) = 2.798, p \leq 0.0012$ ; Days:  $F(6,309) = 3.434, p \leq 0.0027$ ; different levels of learners  $F(2,309) = 152, p \leq 0.0001$ ), suggesting that all learners performed differently (**Figure 3. 12. A**). Both slow and fast learners' performance (success rate) did not improve throughout the days of training. In addition, all learner (normal, slow, fast) performance was statistically different from each other (normal vs slow:  $p \leq 0.0001$ ; normal vs fast:  $p \leq 0.0002$ ; slow vs fast:  $p \leq 0.0001$ ) (**Figure 3. 12. B**).

The different levels of learners by proportion of intact control group population are 54.17% normal learners, 12.5% slow learners, and 33.33% fast learners as seen in (**Figure 3. 12. C**). The different levels of learners reflected the huge variation of performance not only throughout training days, but also among individual mice.

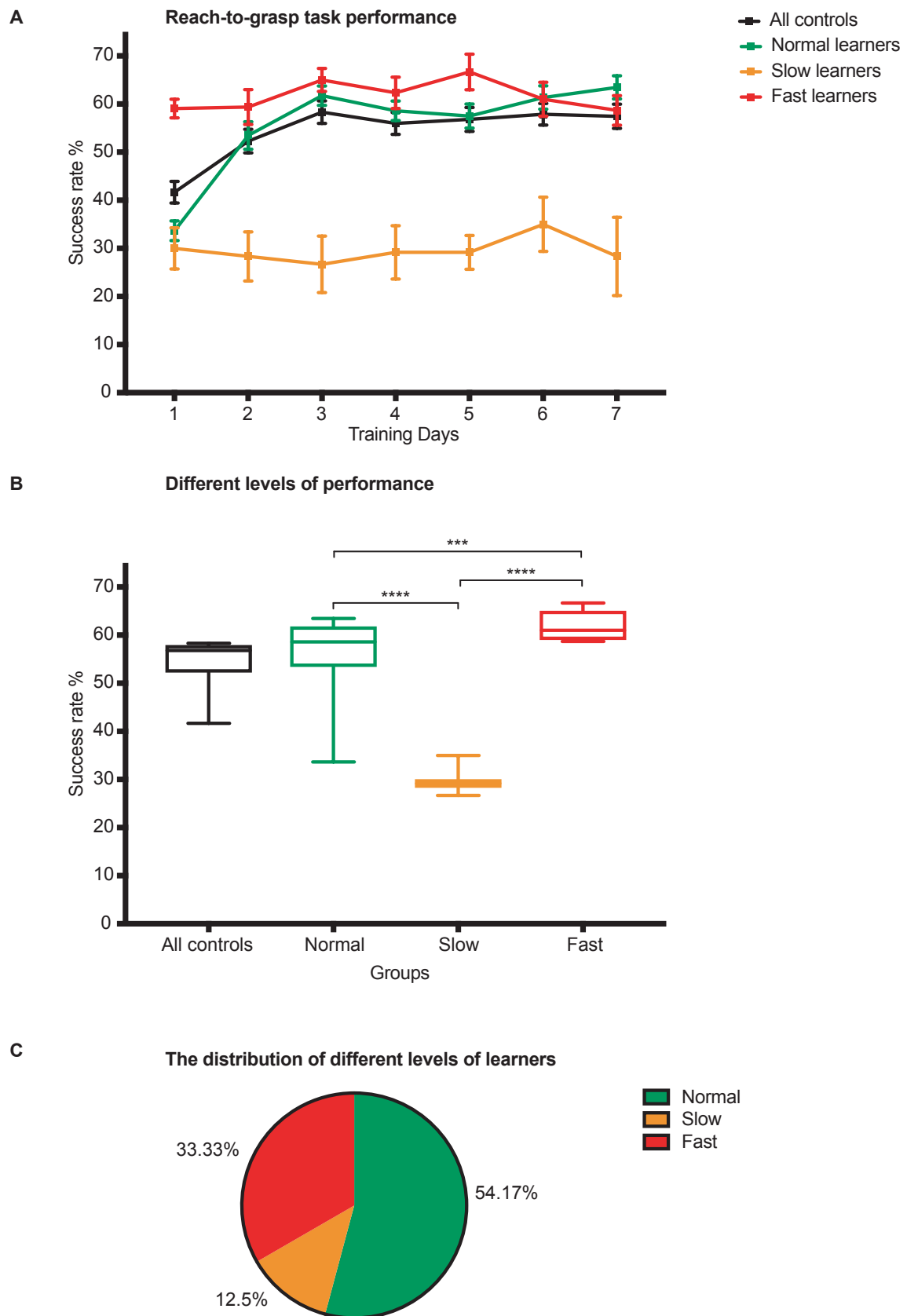


**Figure 3. 12 Different levels of learners within intact control group.**

A. The subdivision of reaching performance of intact control group from day 1 to day 7, with the intact control group divided into normal learners (n=16), slow

learners (n=6), fast learners (n=16) (green, orange, red color respectively). B. The average performance of different levels of learners. C. The different levels of learners by proportion of intact control group population. The whiskers of box plot is (Min to Max) (\*  $P \leq 0.05$ ; \*\*  $P < 0.01$ ; \*\*\*  $P < 0.001$ ; \*\*\*\*  $P < 0.0001$ ). The box always extends from the 25th to 75th percentiles. The line in the middle of the box is plotted at the median. Two-way ANOVA followed by Tukey's multiple-comparisons test was applied.

### 3.3.6 The latency to retrieve 5 pellets

It has long been reported that the reaching accuracy improves by daily sessions (see section 3.3.2 for seven different groups learning curve) and decreases the task time which has been measured by the latency to retrieve 5 pellets (Marques & Olsson, 2010).

In the continued training paradigm (**Figure 3. 2. A**), we used three groups which were intact control, sham, and ChAT-sap toxin injected (n=25, n=9, n=13 respectively). We measured the latency to retrieve 5 pellets for 12 consecutive days (**Figure 3. 13. A**), with a single pellet reach to grasp tasks to evaluate improved skilled motor performance after selective lesioning of ChIs in DLS. The two-way ANOVA of latency to retrieve 5 pellets revealed a significant group variability [ $F(2,603) = 28.74, p \leq 0.0001$ ], indicating that the mice (in intact and sham) are statistically different from ChIs lesioned group (ChAT-sap toxin injected) (control vs ChAT-sap:  $p \leq 0.0001$ , sham vs ChAT-sap:  $p \leq 0.0001$ ). Three groups decreased task time from  $470.8 \pm 62.96$ ,  $471.2 \pm 92.01$ ,  $537.2 \pm 104.2$  to  $159.7 \pm 18.48$ ,  $180 \pm 28.21$ ,  $191.1 \pm 23.45$  respectively in intact control, sham, ChAT-sap injected groups (mean  $\pm$  SEM, time unit is second (s)). The intact control and sham latency to retrieve 5 pellets curve was similar throughout daily sessions, there was no significant difference (control vs sham:  $p \leq 0.6360$ ), but there was a significant impact of days [ $F(11,603) = 15.65, p \leq 0.0001$ ]. The mice treated with ChAT-sap spent longer time, but improved throughout daily sessions (**Figure 3. 13. A**).

Furthermore, the same analyses were conducted on two groups, control+lesioned (15 days) and control+control (15 days) (**Figure 3. 13. B**). The control period (D1-7) was statistically different from retraining period D23-29 (control vs lesioned  $p \leq 0.002$ , control vs control  $p \leq 0.0001$ ). However, for the control and lesioned group of mice at retraining period D23-29 the latency to retrieve 5 pellets was similar and statistically not significant.

Finally, for control+lesioned (7 days) and control+control (7 days) groups the latency to retrieve 5 pellets was analyzed (**Figure 3. 13. C**). The control period (D1-7) was statistically different from the retraining period (D15-21) of control ( $p \leq 0.0012$ ) but not with lesioned group ( $p \leq 0.9$ ). At retraining period D15-21, the lesioned group still spent more time than control group which is statistically significant ( $p \leq 0.0133$ ).

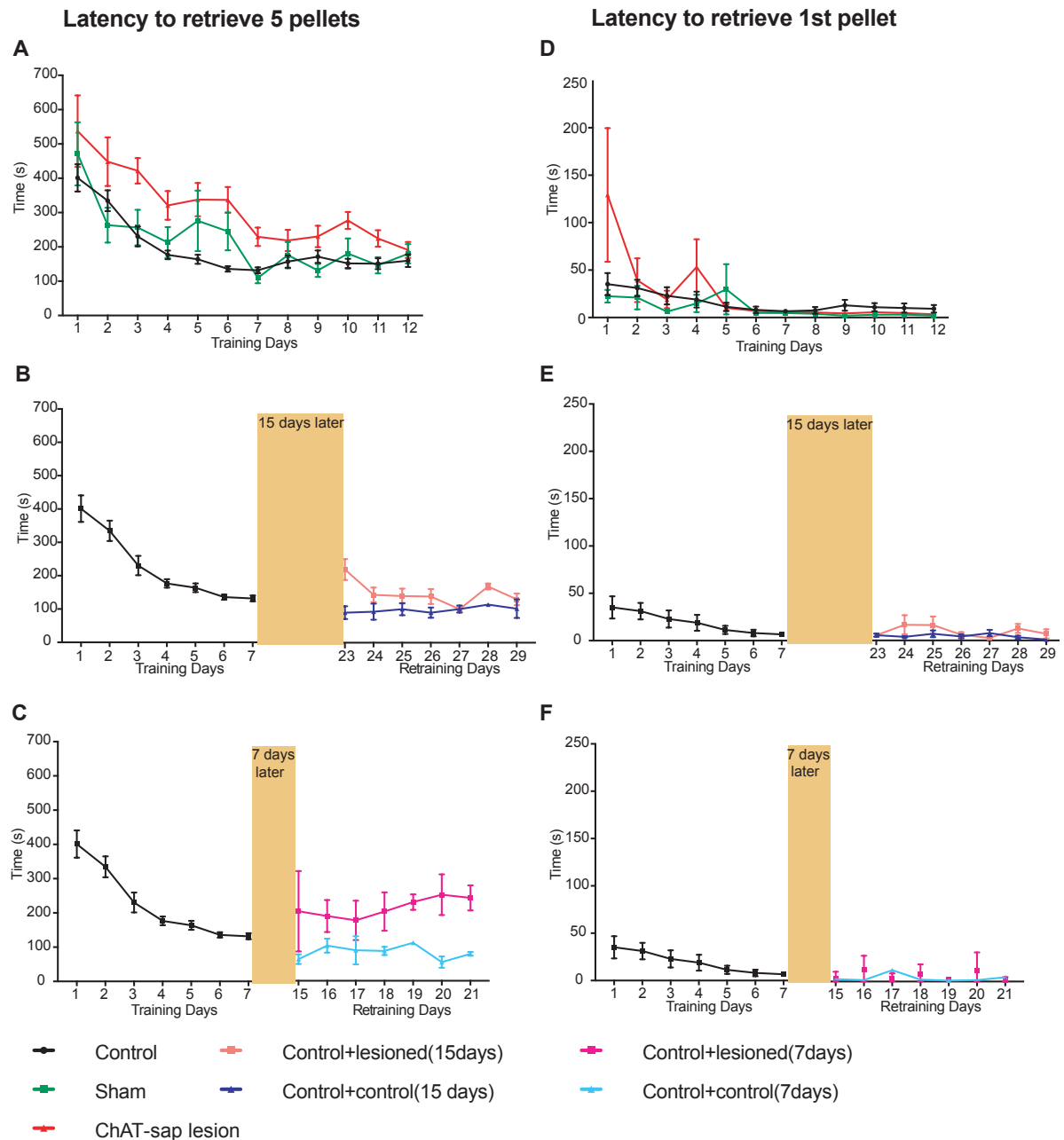


**Figure 3.13 Latency to retrieve pellets**

A. Intact control, sham, and ChAT-sap lesioned groups latency to retrieve 5 successful pellets (black, green, and red respectively) tested for 12 consecutive days training. B. Comparison of latency to retrieve 5 successful pellets before and after the toxin lesion with 15 days resting period. C. Comparison of latency to retrieve 5 successful pellets before and after the toxin lesion with 7 days resting period. D. Latency to retrieve the 1<sup>st</sup> pellet in intact control, sham, ChAT-sap group. E. Latency to retrieve 1<sup>st</sup> pellet before and after the toxin lesion with 15 days resting period. F. Latency to retrieve 1<sup>st</sup> pellet before and after the toxin lesion with 7 days resting period. The latency of each group drawn with different colors. All data shown in the figure is (Mean $\pm$ SEM),time(s).



### 3.3.7 The latency to retrieve first pellet

Following up the latency to retrieve 5 pellets, we analyzed the latency to retrieve the 1<sup>st</sup> pellet which also reportedly decreases throughout the daily sessions (Lopez-Huerta *et al.*, 2016).

The latency to retrieve the 1<sup>st</sup> pellet for 12 consecutive days (**Figure 3. 13. D**) with a single pellet reach-to-grasp task, decreases throughout the daily sessions [ $F(11,624) = 4.16$ ,  $p \leq 0.0001$ ]. The ChAT-sap lesioned group from day1-day5 spent longer time compared to intact control and sham. However, from training day 5, all three groups' latency to retrieve the pellet was almost the same and no statistical significance was found ( $p \leq 0.0524$ ).

Furthermore, the same analyses were conducted on two groups, control+lesioned (15 days) and control+control (15 days) (**Figure 3. 13. E**). The control period (D1-7) was statistically not different from the retraining period D23-29 even though the three groups decreased the latency by daily sessions.

Finally, control+lesioned (7 days) and control+control (7 days) groups latency to retrieve 1st pellet was analyzed (**Figure 3. 13. F**). The control period (D1-7) and retraining period (D15-21) was not statistically different. In addition, there is no differences among the groups.

### 3.3.8 The number of reach-to-grasp attempts

The number of reach to grasp attempts is a key feature of the reach-to-grasp single pellet task. The improved learning skills can be explained with decreased number of reach-to-grasp and increased success rate throughout the daily sessions. In the optimal condition, if each reach-to-grasp brings a successful pellet retrieval, 20 reaches would be predicted for 20 pellets in each daily session in the current research design. To test the hypothesis, the total number of reaches was counted for each group.

The reach-to-grasp attempts in 12 consecutive days sessions (**Figure 3. 14. A**) with a single pellet reach-to-grasp task decreases throughout the daily sessions. The variation in groups, days, and interaction variability statistically was significant [F (2,610) =26,  $p \leq 0.0001$ ], [F (11,610) =3.13,  $p \leq 0.0004$ ], and [F (22,610) =1.73,  $p \leq 0.021$ ] respectively. The ChAT-sap injected group reaches statistical difference from intact control and sham (ChAT vs Control:  $p \leq 0.0001$ , ChAT vs Sham:  $p \leq 0.0001$ ) in which the number of reaches in ChAT-sap lesioned group was higher than control and sham.

Next, the same analyses were conducted on two groups which were control+lesioned (15 days) and control+control (15 days) (**Figure 3. 14. B**). During the retraining session (D23-29) the number of reaches compared to former control training period (D1-7) for both control and lesioned groups. The control group is statistically different from lesioned group ( $p \leq 0.0001$ ).

Finally, for control+lesioned (7 days) and control+control (7 days) groups, the number of reach-to-grasp attempts were analyzed (**Figure 3. 14. C**). The control period (D1-7) was not statistically different from the retraining period D15-21 due to the fact that there was a huge fluctuation in retraining period.

The number of reach-to-grasp attempts

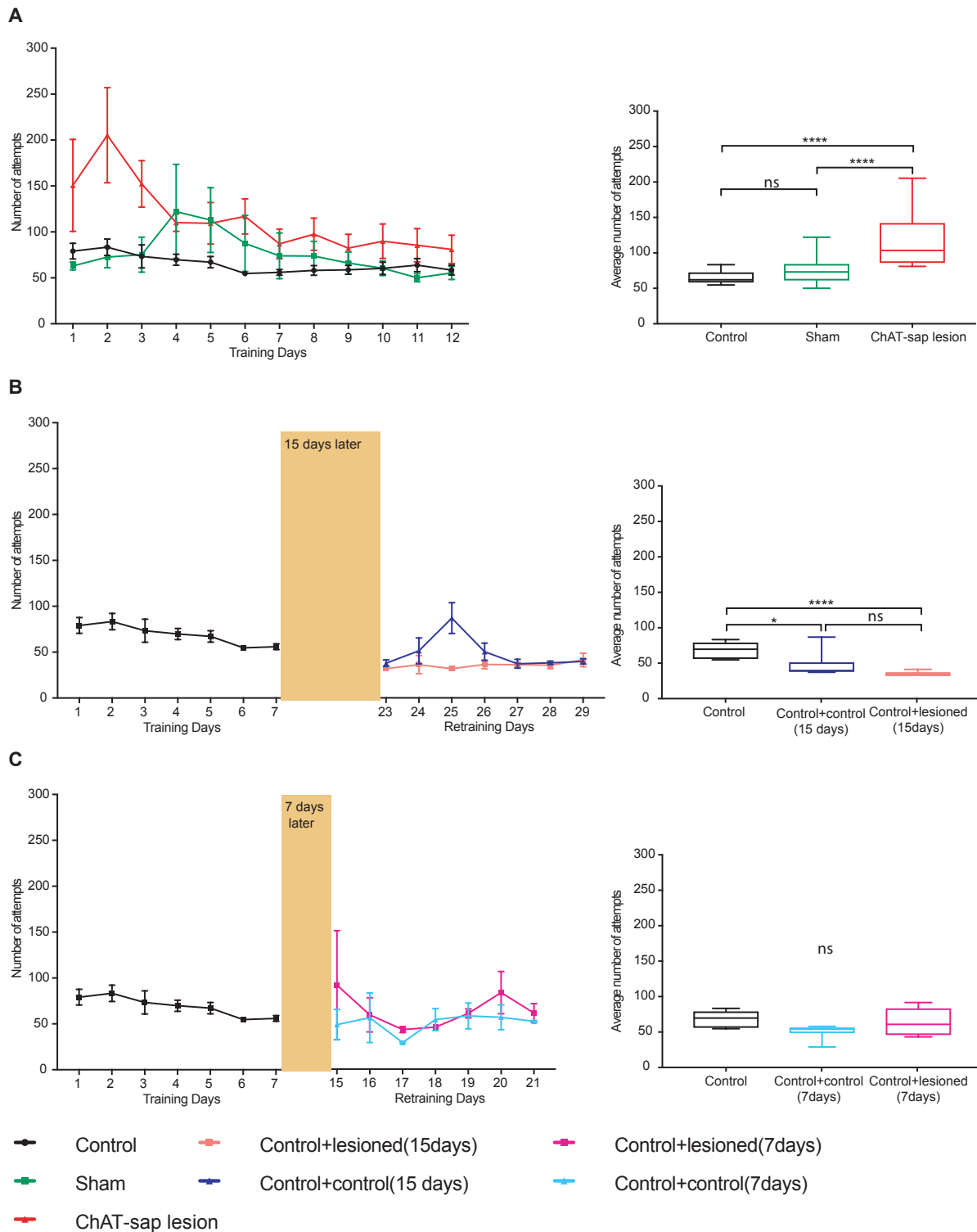


**Figure 3. 14 The reach-to-grasp attempts**

**A.** Intact control, sham, and ChAT-sap lesioned groups reaching attempts. **B.** The reaching attempts for pellets before and after the toxin lesion with 15 days resting period. **C.** The reaching attempts for pellets before and after the toxin lesion with 7 days resting period. The reaching attempts of each group drawn with different colors. All data shown in the figure is (Mean±SEM). The box

plot on the right is summary data from left (\*  $P \leq 0.05$ ; \*\*  $P < 0.01$ ; \*\*\*  $P < 0.001$ ; \*\*\*\*  $P < 0.0001$ ).

### 3.3.10 The number of pellets achieved with a single reach-to-grasp action

Based on earlier research, there are many ways or parameters that can be used to evaluate the reach-to-grasp task. A successful pellet reach with a single reach-to-grasp action improves during the daily sessions and is commonly used in successfully obtained food pellets analysis (Field & Whishaw, 2005; Marques & Olsson, 2010; Lopez-Huerta *et al.*, 2016). In the present study, the number of pellets achieved with a single reach-to-grasp-action in all three different behavior paradigms were counted and analyzed.

There are significant differences among ChAT-sap lesioned, intact control and sham groups on overall pellets obtained with a single reach-to-grasp action (control vs ChAT-sap lesioned:  $p \leq 0.0001$ ; sham vs ChAT-sap:  $p \leq 0.0001$ ). Intact control and sham groups were not different (control vs sham:  $p \leq 0.76$ ) in their likelihood of obtain a pellet with single reach-to-grasp (**Figure 3. 15. A**).

The Control+lesioned (15 days) and control+control (15 days) (**Figure 3. 15. B**) groups, the overall pellets obtained with a single reach to grasp were different before and after the lesion (control (D1-7) vs lesioned group (D23-29):  $p \leq 0.0024$ ; control (D1-7) vs control group (D23-29):  $p \leq 0.0016$ ). During the retraining session (D23-29) the number of pellets obtained with single reach-to-grasp increased in both lesioned and control groups. There was no statistical difference between lesioned and control groups ( $p=0.95$ ).

Finally, for control+lesioned (7 days) and control+control (7 days) groups the number of pellets achieved with a single reach-to-grasp were analyzed (**Figure 3. 15. C**). At retraining stage, the control+lesioned (7 days) group achieved fewer pellets with a single reach-to-grasp compared to control+control (7 days) ( $p \leq 0.0001$ ). The control (before 7 days resting) group was statistically not different from control+lesioned (7 days) ( $p=0.68$ ) but different from control+control (7 days) ( $p \leq 0.0001$ ).

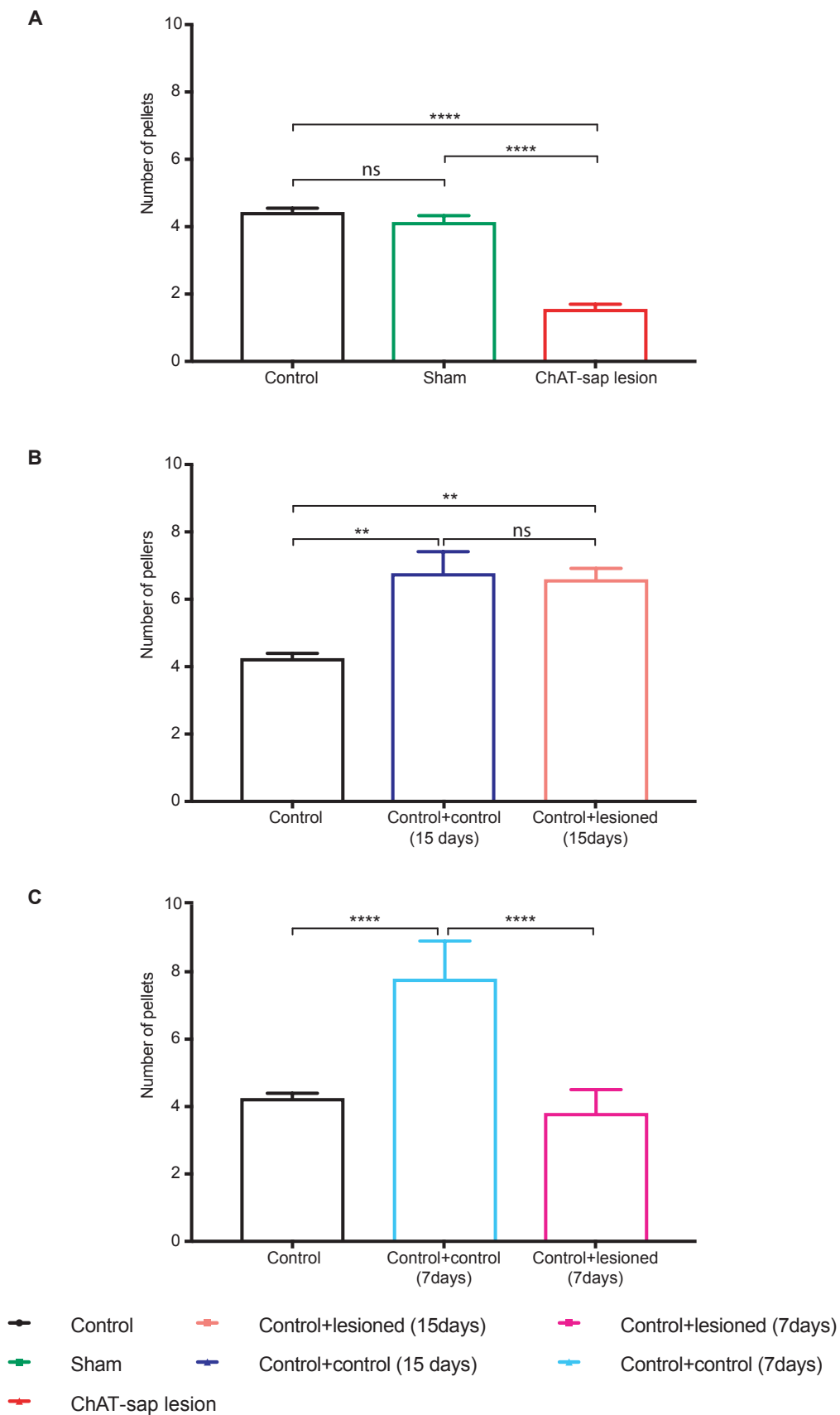


**Figure 3. 15** The number of pellets achieved with a single reach-to-grasp action.

**A.** The average number of pellets achieved per day with a single reach-to-grasp-action in consecutive trained groups (intact control, sham, ChAT-sap lesioned). **B.** The average number of pellets achieved per day with a single reach-to-grasp-action before and after the toxin lesion with 15 days resting period. **C.** The average number of pellets achieved per day with a single reach-to-grasp-action before and after the toxin lesion, with 7 days resting period. All data shown in the figure is (average data from 12 or 14 days) (\*  $P \leq 0.05$ ; \*\*  $P < 0.01$ ; \*\*\*  $P < 0.001$ ; \*\*\*\*  $P < 0.0001$ ).

### 3.3.11 The number of mice that did not attend to the reach-to-grasp task

We observed that there were 22.6% ( $n=21$ ) of mice not interested in the task and could not be trained. They were excluded from experiments (intact control  $n=14$ , sham  $n=4$ , ChAT-sap lesioned  $n=3$ ). The mice trained for behavior experiment is 77.4% ( $n=72$ ) (**Figure 3. 16**).

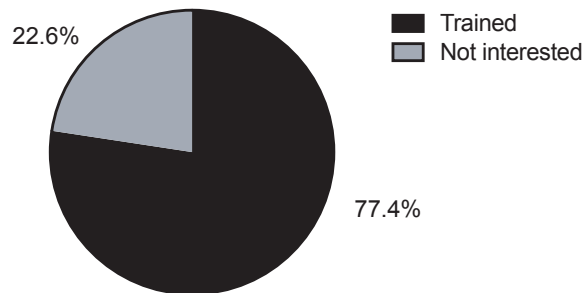


**Figure 3. 16 The number of animals used in task.**

The pie chart shows the percentage of trained and non-interested mice in total population.

### 3.3.12 Significant decrease of ChIs on lesioned compared to control side

To quantify the number of ChIs depleted with ChAT-sap toxin lesion in the mice used for behavior experiments, a stereological systematic random sampling method was used to count cells in lesion and intact hemispheres of toxin treated animals with two different methods after behavior experiments were completed.

ChIs showed a significant depletion with ChAT-sap toxin which is consistent with data shown in Chapter 2 and there was significant difference between lesioned and non-lesioned hemispheres in the striatum (non-lesioned vs lesioned:  $11590 \pm 375.2$  vs  $7075 \pm 457.6$   $p \leq 0.0001$ ,  $n=11$ ). The ChIs depletion was observed up to 3 weeks post lesion in lesioned mice used for

behavioral experiments and there was no evidence that the behavior experiments can impact on ChIs depletion during the experimental sessions (**Figure 3. 17. A**).

In addition, the mirror sampling method (for detailed description of method see section 3.2.2 and **Figure 3. 3. G**) was applied to count ChIs from sections to quantify the number of cells depleted in the region of toxin administration. Expectedly, there are significantly less ChIs in the striatum compared to non-lesioned hemisphere (non-lesioned vs lesioned:  $4922 \pm 534.3$  vs  $1474 \pm 181.8$ ,  $p \leq 0.0001$ ,  $n=11$ ) (**Figure 3. 17. B**).

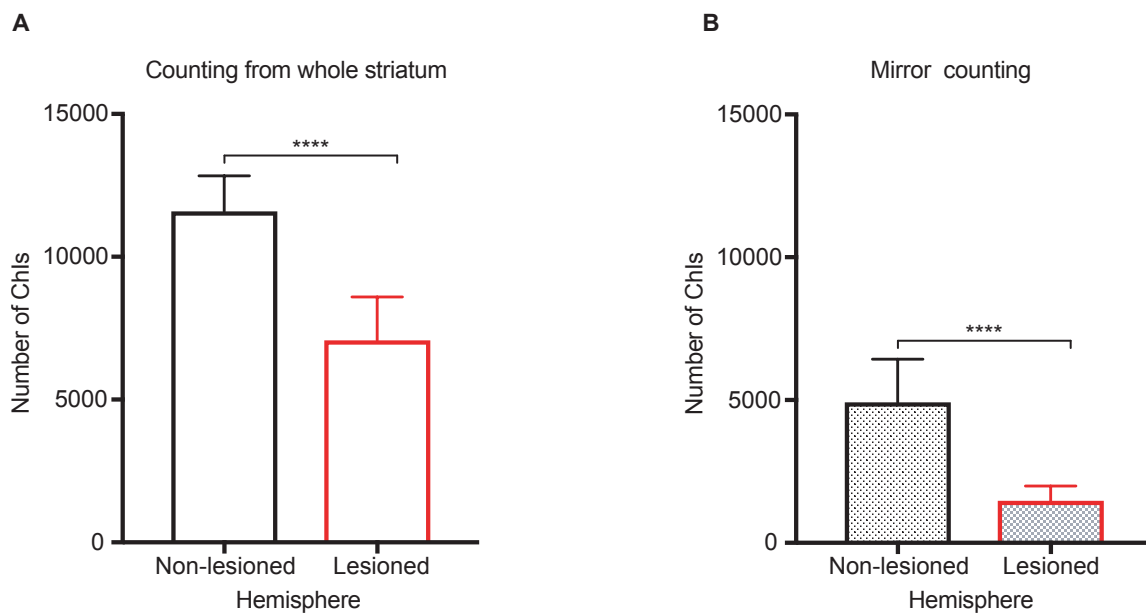


**Figure 3. 17 The confirmation of ChIs depletion in mice trained for behavior experiment.**

A. ChIs counting from whole striatum of lesioned and non-lesioned hemisphere of ChAT-sap injected groups. B. Mirror sampling method applied to quantify the number of cells missing in the toxin administrated region (\*  $P \leq 0.05$ ; \*\*  $P < 0.01$ ; \*\*\*  $P < 0.001$ ; \*\*\*\*  $P < 0.0001$ ).

### 3.3.12 The correlation of ChIs lesion and success rate

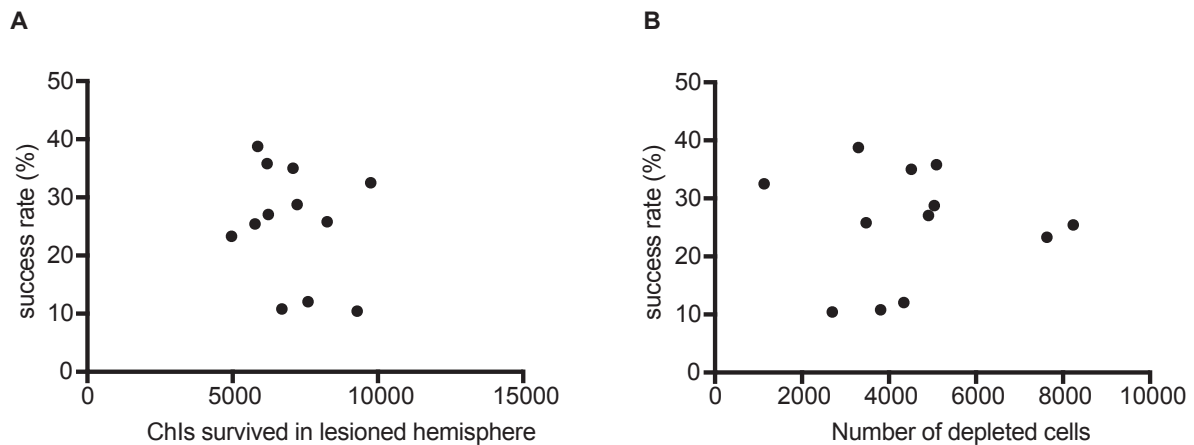


**Figure 3. 18 The correlation analysis of ChIs and the success rate.**

**A.**The number of ChIs counted from lesioned hemisphere and success rate correlation. **B.**The number of depleted cells and success rate correlation. (The number of depleted cells calculated by cells counted from lesioned hemisphere subtracted from the cells counted non-lesioned hemisphere of same animals).

To determine whether there is any correlation between ChIs lesion and success rate, we did two different kinds of analysis in which the number of ChIs surviving after the lesion and the number of lost cells was correlated with success rate of mice during the reach to grasp task.

There is insufficient evidence to determine whether there is a significant inverse linear correlation between the number of ChIs surviving from lesioned hemisphere and success rate, due to the fact that the correlation coefficient is not significantly different from zero ( $r = -0.237$ ,  $R^2 = 0.056$ ,  $p \leq 0.458$ , 5.6%,  $n = 11$ ) (**Figure 3. 18. A**).

Similarly, there is insufficient evidence to conclude there is a significant positive linear correlation between the number of ChIs depleted from lesioned hemisphere and success rate, because the correlation coefficient is not significantly different from zero ( $r = 0.00527$ ,  $R^2 = 2.8 \times 10^{-5}$ ,  $p \leq 0.9870$ , 0.002%,  $n = 9$ ) (**Figure 3. 18. B**).

Based on  $r$  value of both correlation analysis we concluded that there is not a significant relationship between ChIs number and success rate. Therefore, we cannot use the regression line to model a linear relationship between ChIs number and success rate in our present study.



### 3.3.14 Open field test

The open field test (OFT) is often used in mouse or rat studies to measure motor activity, exploratory behavior and the anxiety of animals in a new environment (**Figure 3. 4. A**). In the present study, to quantify the ChAT-sap injected mice exploratory features, OFT was conducted. The parameters analyzed were the total distance traveled, number of rearing, time spent in center region, average rearing duration, speed, and average circling. The tests were applied every day before the training session in the reach to grasp task for each individual mouse.

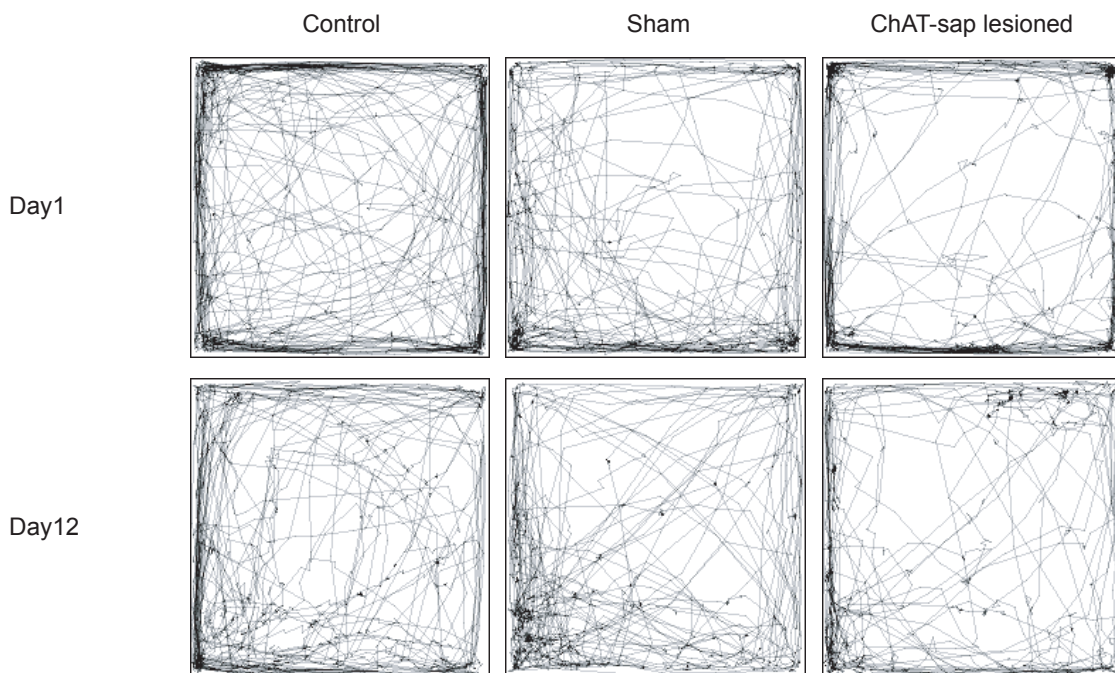


**Figure 3. 19** The path taken by individual mouse over a 15 minute testing session in the open field based on images taken from above.

The density of lines in a region correlated with time spent in that region, the mouse entered that area frequently.

The total distance traveled was measured for the ChAT-sap toxin injected mice, to identify the ChIs lesion impact on motor output. Based on the traces of mice in an open field (**Figure 3. 19**), there are significant differences between ChAT-sap lesioned, intact control and sham groups with respect to the overall distance traveled within the 15-minute test time (control vs sham:  $p \leq 0.0001$ ; sham vs ChAT-sap:  $p \leq 0.0037$ ). Interestingly, the ChIs lesioned mice traveled more compared to sham group mice, which implies that unilateral ChIs lesion changes

striatal microcircuitry in the brain region related to movement (**Figure 3. 20. A**). There were also significant interaction by days and groups variables ( $p \leq 0.0001$  and  $p \leq 0.0001$  respectively).

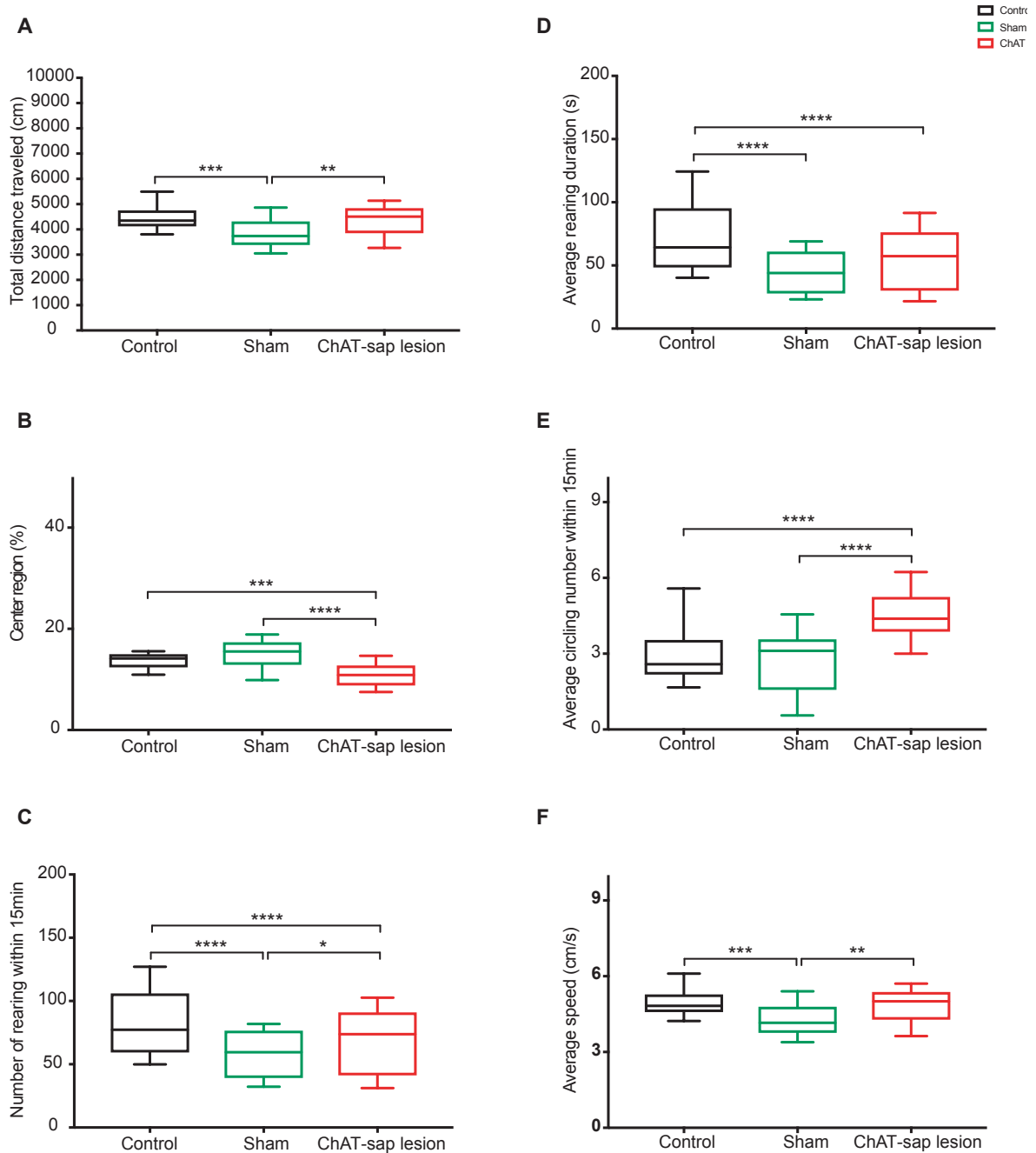


**Figure 3. 20 The exploratory behavior of mice in different conditions (1)**

**A.** Total distance traveled during open field test (cm). **B.** The time mice spend in center region (%). **C.** The number of rearings within 15min. **D.** Average total time spent in reared position (s). **E.** Average circling number within 15min. **F.** Average speed within 15min.

The anxiety of mice is often examined with time spent in the center region. ChAT-sap injected mice spent less time in the center region on average compared to intact control and

sham (control, sham, ChAT-sap respectively  $13.73 \pm 0.423\%$ ,  $15.28 \pm 0.8\%$ ,  $10.93 \pm 0.63\%$ ; ChAT-sap vs control:  $p \leq 0.0001$ , ChAT-sap vs sham:  $p \leq 0.0001$ ). Intact control and sham groups were not different (control vs sham:  $p \leq 0.11$ ) in their likelihood of anxiousness (**Figure 3. 20. B**) while the anxiety of ChAT-sap injected mice apparent from path trace (**Figure 3. 19**).

The measurement of rearing frequency in mice was considered to be a quantification of an aspect of exploratory behavior. From quantitative analysis on OFT data (**Figure 3. 20. C**), the control animals tend to explore more compared to sham and ChAT-sap lesioned animals on average ( $82.41 \pm 7.34$ ,  $57.81 \pm 5.19$  and  $67.9 \pm 7.018$  (s) respectively). In addition, the average total time spent rearing (**Figure 3. 20. D**) in controls is longer compared to sham and ChAT-sap and this is statistically significant (control vs sham: 0.0001, control vs ChAT-sap: 0.0001).

The average number of circling behaviors was measured as the ChAT-sap lesion was only made unilaterally which may cause imbalanced circuitry in the striatum. Interestingly, the ChAT-sap lesioned mice made almost two-fold more rotations than control and sham ( $2.94 \pm 0.3$ ,  $2.63 \pm 0.37$  and  $4.6 \pm 0.3$  respectively for control, sham and lesioned) which is statistically significant (**Figure 3. 20. E**).

Lastly, the average speed of mice in open field was measured in which sham treated mice speed is slower than control and ChAT-sap injected group (sham vs control:  $p \leq 0.0001$ . sham vs ChAT-sap injected:  $p \leq 0.0037$ ), these result support that control and ChAT-sap treated animal travels to longer distance and more frequent rearing behavior observed (**Figure 3. 20. F**).

### 3.4 Discussion

The ChIs are sparsely distributed in the striatum. It was only in recent years that the specific regulation (lesion, optogenetic control, in vivo labeling) of ChIs was possible, since then the ChIs related circuitry underlying striatal functions, has started to be uncovered. However, a previous study aimed to understand the impact of how nucleus accumbens ChIs lesions on DA-dependent behavior in rats they found that these treated rats were hyper-responsive to amphetamine (Laplante *et al.*, 2011). Another study focused on dorsomedial and ventral striatum ChIs role in strategy set shifting behavior using the same ChIs specific immunotoxin in rats. They found that neither of the lesions impairs learning of the task but the two brain regions can be distinguished based on a behavioral context (Aoki *et al.*, 2015). Additionally, the viral ablation of ChIs in the DLS of mice found a deficit in coordination on the rotorod behavioral task (Xu *et al.*, 2015). The IG17 line transgenic mice (expressing the fusion protein of GFP and human interleukin-2 receptor  $\alpha$  subunit) ChIs lesion study with multiple injections of immunotoxin showed impaired tone-cued procedural learning and spatial delayed alteration. But this study didn't show ChIs lesion effect on motor, spatial learning and fear response (Kitabatake *et al.*, 2003).

In the present study we employed the ChAT-sap immunotoxin targeting the ChIs in DLS. With this method, described in the second chapter, we were able to specifically lesion ChIs in DLS. The targeted lesion was confirmed by stereology and immunohistochemistry studies. To identify ChIs-depletion effects on behaviors, reach-to-grasp task and OFT were applied. This is the first study to describe the impairments in a skilled reach-to-grasp task in ChIs depleted mouse.

The behavioral experiment results clearly indicate that mice from 4 weeks of age can perform reach-to-grasp task and the ChAT-sap toxin injected mice can also perform reach-to-grasp task but with a statistically significantly lower success rate compared to intact control and sham groups. Because of incorrect paw placement, not fewer attempts or gross motor problems. ChIs depletion from DLS affects the performance of mice during the task which is demonstrated by different measurements, such as reaching accuracy, latency to retrieve 5 successful pellets, latency to retrieve first pellets and the number of reaching attempts. These results allow us to distinguish between groups of lesioned (ChAT-sap toxin injected) and non-

lesioned animals (intact control or sham) with different behavior paradigms in reach-to-grasp task performance.

We employed three different training paradigms – 12 days consecutive training after lesion, 15 days resting (control+control, control+lesioned), 7 days resting (control+control, control+lesioned)).

In 12 consecutive days training paradigm, all treatment groups learned to perform the task and improved performance throughout training days except the last couple of days where a slight decline was observed. The statistically significant difference in performances was found between controls (intact control and sham) and the ChAT-sap injected groups. The learning curve shaped from day 1-4 was very obvious and in most of the cases from day 5 on the learning curve did not increase exponentially by contrast a slightly declining trend was observed. The decreased response to conditioned cue (for example: chocolate pellet) in extended training can be explained with reward reevaluation process which was described by Dickinson (1985).

In 12 consecutive days training paradigm, the lesioned group started the task beginning 7 days after lesion. Apparently, there was poor performance from days 1- 6 and slight improvement from day 7 onwards (2 weeks after the ChAT-sap injection) which coincides with our observation of increased number of vAChT puncta at 2 weeks after the lesion. On the last day of performance, the lesioned group performance was similar to the sham group and there was no statistical difference ( $p=0.7349$ ).

In the 15 days resting paradigm, the control group improved performance after 15 days of resting, but there was no apparent improvement in the performance of the lesioned group. In 7 days resting paradigm, the control group improved in performance after 7 days of resting, however there was a huge decline in the performance of the lesioned group.

For the 12 consecutive days training paradigm groups (control, sham and ChAT-sap lesioned groups) the test was conducted on mice starting at 4 weeks of age till 5.7 weeks. While 7 days resting groups (control+control and control+lesioned) were tested from 4-7 weeks and 15 days resting groups (control+control and control+lesioned) were tested from 4-8 weeks. Among these three different training paradigms, the control groups with 7 days and 15 days

resting period, the performance of mice improved (the baseline shifted up) in the retraining period. These results are coincident with the onset of sexual maturity in control group mice. These results are consistent with previous research reports and observations (Marques & Olsson, 2010).

Control+lesioned (15 days) and control+lesioned (7 days) groups performance were not improved as extensively as controls in terms of success rate, latency to retrieve 5 pellets, latency to 1st pellet, the number of reach-to-grasp attempts, and the number of pellets achieved with a single reach-to-grasp action.

Control+lesioned (15 days) group success rate after the lesion (from D23-29) was similar to before the lesion (D1-7) and there is no huge drop in their performance. In addition, the other reach-to-grasp parameters like the latency to retrieve 5 pellets, 1<sup>st</sup> pellet and the number of pellets retrieved with single reach-to-grasp were also similar to control period (D1-7). These findings coincide with elevated vAChT puncta number after 15 days as discussed in the second chapter of the thesis. Even though the ChIs were depleted with ChAT-sap toxin bases on ChAT immunolabeling, but the increased number of vAChT boutons was found at two weeks and gradually recovered to equal control level 4 weeks and 6 weeks after the lesion. By contrast, control+lesioned (7 days) group did have poor learning skills during the daily training sessions (from D15-21).

Therefore, the age of mice and sexual maturity during the reach-to-grasp task training is important when testing motor learning skills in intact control mice. In other words, the careful timing of behavioral experiments based on the age of mice is crucial for motor learning skills. In addition, the elevated vAChT after 2 weeks of the lesion may also contribute at certain level of performance of lesioned mice (control+lesioned (15days)).

The individual differences not only existing among humans but also exist in animals. Individual differences were found (normal learner, slow learners, and fast learners) in control groups in the present study, supported by previous research in which rats were used for reach-to-grasp task endpoint scoring and other different measurements (Gholamrezaei & Whishaw, 2009; Marques & Olsson, 2010). Based on the 12 consecutive days training paradigm in this thesis, it can be concluded that the individual differences were not related to training and slow learners were not improved with continued days of training. To quantify the skilled reaching

task there are multiple standard task measurements which we used including success rate, latency to 5 pellets, latency to retrieve 1<sup>st</sup> pellet, and reaching attempts. In addition, the individual differences by days and groups found in the present research are consistent with earlier studies. The possible explanations can be the examination of success rates at different stages of training, anatomical observation from cortical developmental abnormalities, brain size, and neurochemical levels (Schwartzkroin *et al.*, 2004; Goodman & Gilbert, 2007).

The concern of conducting food restricted task in toxin injected mice with stereotaxic surgery is a possible delay in the full recovery of the mice after surgery. Even though special daily care was provided to the mice such as easily digestible water-rich medical gel was provided, which were strongly suggested by the local animal health care providers. In addition, we did not discuss the possible impact of food restriction on the progressive depletion of ChIs in the striatum at the early nor later stage of the experiments. The highest amount of food was provided to guarantee the maintenance of 85% of body weight for growing mice based on published experimental reports (Marques & Olsson, 2010; Lopez-Huerta *et al.*, 2016). The next day there was no food left, which is enough to motivate the mice to perform the task and which is clear from lesioned group mice repetitive reach-to-grasp attempts as we discussed in result section. We did not investigate the possible impact of gender differences on lesioned and non-lesioned animals' performance since it has been done by many earlier researchers (Field & Whishaw, 2005; Marques & Olsson, 2010). In addition, female rats show unstable performance compared to males in a rat study (Field & Whishaw, 2005).

In order to reduce stress and anxiety, mice were allowed to habituate with their cage mates for 2-3 days in the test box followed by a 2-3-day pre-training period (Farr & Whishaw, 2002; Marques & Olsson, 2010; Lopez-Huerta *et al.*, 2016). The importance of a habituation period again was observed during the retraining session after 7 or 15 days of resting period. In the present study, home cage beddings and strong lights were avoided in the test chamber.

The number of ChIs depleted by the ChAT-sap toxin in mice trained for behavior was similar to the data reported in Chapter two. However, these trained animals' brain sections were not stained for vAChT and it is also unclear the amount of variation. Unexpectedly, there was no correlation between the number of ChIs depletion and success rate of mice which indicates that impairment of reach-to-grasp skill is not linearly dependent on the number of

ChIs depleted. The altered striatal microcircuitry due to ChIs depletion is enough to change the reach-to-grasp task performance.

Exploratory activity is age- and species- dependent and can be correlated with learning skills due to the high attention required to achieve success in the task. Earlier research reported that rats are more active at juvenile stage (20-30 PD) and mice at adolescent stage (45-60 PD) (Spear & Brake, 1983; Ba & Seri, 1995; Macri *et al.*, 2002). By contrast, a recent study observed that young juvenile mice tend to explore the surrounding environments more often than adult mice (Marques & Olsson, 2010).

In our study, the parameters related to exploratory behavior (total distance traveled, rearing, circling, speed, time spent on rearing and center region) showed that lesioned group mice were more prone to explore the surrounding environments compared to sham and control group.

Based on the OFT results it is clear that ChIs depletion can be measured with different sensitive parameters against toxin treatment such as anxiety and exploratory behavior of mice. The outcome of ChIs lesion in DLS not only impairs reach-to-grasp skills but also has a major impact on the emotionality (anxiety) of mice. We found that the lesion group mice spent shorter time in the center region compared to other groups. This suggests that ChIs lesion in the DLS region can cause anxiety at a certain level. In addition, the increased circling behavior in ChAT-sap lesioned mice can be explained by a unilateral lesion which changes the balance of striatal circuitry; the dopaminergic unilateral lesion studies have been discussed in previous studies (Iwamoto *et al.*, 1976; Jaidar *et al.*, 2010).

During the consecutive OFT sessions, we found that in all three group of mice, the rearing frequency, time spent on rearing and total distance traveled in the open field were gradually increased (**Figure 3.19**). The increments can be explained by incentive motivational (reinforcement-linked) stimuli, while the reward (for example, chocolate pellet for food deprived animals in reach-to-grasp task in our study) can raise the level of general activity (total distance, rearing, rearing time in OFT) and facilitate the occurrence of rearing or increase speed during the OFT. The mice show an increased activity in OFT which has been repeatedly associated with a chocolate pellet of reach-to-grasp task. The chocolate pellet is considered a positive reinforcement for mice because the OFT tests were conducted immediately before



reach-to-grasp task in our current research. The influence of incentive-motivational stimuli on behavior was explained and discussed in the earlier neurophysiological studies to interpret the effects of drive and incentive motivation on general activity. The increased general activity of mice undergoing training in a motivational task was supported by former research (Bacon & Bindra, 1967; Bindra, 1968; Trowill *et al.*, 1969).

In general, there is no grandmaster behavioral experiment which can identify all possible outcomes of the lesion. The application of different kinds of experimental design can help us to understand the altered brain circuitry. The measurement of ChIs lesioned mice behavior allows us to understand the possible stereotype behaviors, its impact on striatal microcircuits, and ChIs related motor learning skills variation in neurodegenerative disease.

In conclusion, this is the first study to document a detailed quantitative impairment in skilled reach-to-grasp movements after a ChIs specific lesion with immunotoxin in wild-type mice. The main results are that mice with different resting paradigms perform skilled reaching movements quite well, and the skilled reaching test is sensitive to damage to the ChIs in DLS even though it was a partial lesion. An advantage of the model is that it is able to provide a quantitative scope and a qualitative assessment of deficits with two different kinds of behavior tests, compensation, and recovery in DLS ChIs.

## Chapter 4 Conclusion

### 4.1 Thesis summary

We have discussed a number of techniques and methods used to understand the role of ChIs in the striatum, and their involvement in different brain functions to maintain normal physiological functions of striatal circuitry. In the anatomical study in Chapter 2 we used the stereological systematic random sampling method to count the number of ChIs in toxin treated vs control animals. In Chapter 3 we showed, behaviorally, how ChIs depletion could affect the animal's performance of skilled reach-to grasp task in mice and in open field test. This study could allow us to observe locomotion in open field, provided that ChIs partial depletion in striatum does not have significant impairment on locomotor behavior, which also showed to be possible from the skilled reach-to grasp task. Both of the behaviors were conducted to elucidate changes that occurred in animal's performance from different perspectives.

### 4.2 Impact and future work

Sparsely distributed ChIs are an indispensable part of striatum and BG circuits. This thesis focusses, in part, on approaches to push the boundaries to understand the properties of ChIs in experimental settings in mice. Without venturing into areas involving the higher technical methods such as *in vivo* recording or imaging from multiple cells from moving animals. Using detailed experimental methods, such as the stereological systematic random sampling of ChIs correlated to behavior tests help us to extend our knowledge in this field. However, if we want to explore and comprehend the online recording and manipulation of ChIs in moving alive animals it is fundamental to push the methodological limits to seek a way to enhance the field even further.

Currently, *in vivo* recording from the cortex of behaving transgenic animals with both the high speed and high resolutions, which indicates that with the improvement of technology in fluorescent imaging methodology enable us to record from variety of cell in deeper brain regions like striatum.

Subsequently, improvement in imaging technology and inventing new tools to detect the activity of cells *in vivo* conditions with less damage are crucial to the field of neuroscience. The application of advanced technique such as recording cells *in vivo* condition in moving animals, we can make predictions for human brain physiological and disease states. In the case of striatal microcircuitry analysis we hope to provide further scientific report about the properties of ChIs depleted striatum. However, the work needs to be perfected, but it paves the way for combining physiology and imaging to better understand the role of ChIs in different circuitry states.

In summary, the techniques and results outlined in the work of this thesis can be relatively easily adopted by many groups and interpret experimental results which potentially allow the investigation of interesting brain properties.

In the future, we hope to record from multiple cells with calcium imaging methods, which will enable us to explore hundreds of cells in vitro 250 $\mu$ m thick sections to image from over 100 cells at 960/830 $\mu$ m field simultaneously. The calcium imaging of striatal MSNs in ChIs depleted condition of this big size, will be the first to demonstrate in the community and this will demonstrate how it could be done and provide changes or modification of striatal circuitry made by ChIs depletion. In the future we would like to apply pharmacological agents to show how the plasticity could be changed and explore its correlation with neurological disorders in which ChIs are involved.

## References

- Abbott, L.F. & Nelson, S.B. (2000) Synaptic plasticity: taming the beast. *Nat Neurosci*, 3 Suppl, 1178-1183.
- Abudukeyoumu, N., Hernandez-Flores, T., Garcia-Munoz, M. & Arbuthnott, G.W. (2018) Cholinergic modulation of striatal microcircuits. *Eur J Neurosci*.
- Aceves Buendia, J.J., Tiroshi, L., Chiu, W.H. & Goldberg, J.A. (2017) Selective remodeling of glutamatergic transmission to striatal cholinergic interneurons after dopamine depletion. *Eur J Neurosci*.
- Akiba, I., Kubo, T., Maeda, A., Bujo, H., Nakai, J., Mishina, M. & Numa, S. (1988) Primary structure of porcine muscarinic acetylcholine receptor III and antagonist binding studies. *FEBS Lett*, 235, 257-261.
- Akins, P.T., Surmeier, D.J. & Kitai, S.T. (1990) Muscarinic modulation of a transient K<sup>+</sup> conductance in rat neostriatal neurons. *Nature*, 344, 240-242.
- Albin, R.L., Minderovic, C. & Koeppe, R.A. (2017) Normal Striatal Vesicular Acetylcholine Transporter Expression in Tourette Syndrome. *eNeuro*, 4.
- Albin, R.L., Young, A.B. & Penney, J.B. (1989) The functional anatomy of basal ganglia disorders. *Trends Neurosci*, 12, 366-375.
- Alcantara, A.A., Mrzljak, L., Jakab, R.L., Levey, A.I., Hersch, S.M. & Goldman-Rakic, P.S. (2001) Muscarinic m1 and m2 receptor proteins in local circuit and projection neurons of the primate striatum: anatomical evidence for cholinergic modulation of glutamatergic prefronto-striatal pathways. *J Comp Neurol*, 434, 445-460.
- Alexander, G.E. & Crutcher, M.D. (1990) Functional architecture of basal ganglia circuits: neural substrates of parallel processing. *Trends Neurosci*, 13, 266-271.

- Alexander, G.E., DeLong, M.R. & Strick, P.L. (1986) Parallel organization of functionally segregated circuits linking basal ganglia and cortex. *Annu Rev Neurosci*, 9, 357-381.
- Aliane, V., Perez, S., Bohren, Y., Deniau, J.M. & Kemel, M.L. (2011) Key role of striatal cholinergic interneurons in processes leading to arrest of motor stereotypies. *Brain*, 134, 110-118.
- Aoki, S., Liu, A.W., Zucca, A., Zucca, S. & Wickens, J.R. (2015) Role of Striatal Cholinergic Interneurons in Set-Shifting in the Rat. *J Neurosci*, 35, 9424-9431.
- Aosaki, T., Kimura, M. & Graybiel, A.M. (1995) Temporal and spatial characteristics of tonically active neurons of the primate's striatum. *J Neurophysiol*, 73, 1234-1252.
- Apicella, P. (2002) Tonically active neurons in the primate striatum and their role in the processing of information about motivationally relevant events. *Eur J Neurosci*, 16, 2017-2026.
- Apicella, P. (2017) The role of the intrinsic cholinergic system of the striatum: What have we learned from TAN recordings in behaving animals? *Neuroscience*, 360, 81-94.
- Arbuthnott, G.W. & Wickens, J. (2007) Space, time and dopamine. *Trends Neurosci*, 30, 62-69.
- Assous, M., Faust, T.W., Assini, R., Shah, F., Sidibe, Y. & Tepper, J.M. (2018) Identification and Characterization of a Novel Spontaneously Active Bursty GABAergic Interneuron in the Mouse Striatum. *Journal Neurosci*, 38, 5688-5699.
- Atallah, H.E., McCool, A.D., Howe, M.W. & Graybiel, A.M. (2014) Neurons in the ventral striatum exhibit cell-type-specific representations of outcome during learning. *Neuron*, 82, 1145-1156.
- Aznavour, N., Mechawar, N., Watkins, K.C. & Descarries, L. (2003) Fine structural features of the acetylcholine innervation in the developing neostriatum of rat. *J Comp Neurol*, 460, 280-291.

- Ba, A. & Seri, B.V. (1995) Psychomotor functions in developing rats: ontogenetic approach to structure-function relationships. *Neurosci Biobehav Rev*, 19, 413-425.
- Bacon, W.E. & Bindra, D. (1967) The generality of the incentive-motivational effects of classically conditioned stimuli in instrumental learning. *Acta Biol Exp (Warsz)*, 27, 185-197.
- Barbeau, A. (1962) The pathogenesis of Parkinson's disease: a new hypothesis. *Can Med Assoc J*, 87, 802-807.
- Beatty, J.A., Song, S.C. & Wilson, C.J. (2015) Cell-type-specific resonances shape the responses of striatal neurons to synaptic input. *J Neurophysiol*, 113, 688-700.
- Beatty, J.A., Sullivan, M.A., Morikawa, H. & Wilson, C.J. (2012) Complex autonomous firing patterns of striatal low-threshold spike interneurons. *J Neurophysiol*, 108, 771-781.
- Benarroch, E.E. (2016) Intrinsic circuits of the striatum: Complexity and clinical correlations. *Neurology*, 86, 1531-1542.
- Bennett, B.D. & Bolam, J.P. (1993) Characterization of calretinin-immunoreactive structures in the striatum of the rat. *Brain Res*, 609, 137-148.
- Bennett, B.D., Callaway, J.C. & Wilson, C.J. (2000) Intrinsic membrane properties underlying spontaneous tonic firing in neostriatal cholinergic interneurons. *J Neurosci*, 20, 8493-8503.
- Bennett, B.D. & Wilson, C.J. (1999) Spontaneous activity of neostriatal cholinergic interneurons in vitro. *J Neurosci*, 19, 5586-5596.
- Berke, J.D. (2008) Uncoordinated firing rate changes of striatal fast-spiking interneurons during behavioral task performance. *J Neurosci*, 28, 10075-10080.

- Bernacer, J., Prensa, L. & Gimenez-Amaya, J.M. (2007) Cholinergic interneurons are differentially distributed in the human striatum. *PloS one*, 2, e1174.
- Bernard, V., Laribi, O., Levey, A.I. & Bloch, B. (1998) Subcellular redistribution of m2 muscarinic acetylcholine receptors in striatal interneurons in vivo after acute cholinergic stimulation. *J Neurosci*, 18, 10207-10218.
- Bernard, V., Levey, A.I. & Bloch, B. (1999) Regulation of the subcellular distribution of m4 muscarinic acetylcholine receptors in striatal neurons in vivo by the cholinergic environment: evidence for regulation of cell surface receptors by endogenous and exogenous stimulation. *J Neurosci*, 19, 10237-10249.
- Bernard, V., Normand, E. & Bloch, B. (1992) Phenotypical characterization of the rat striatal neurons expressing muscarinic receptor genes. *Journal Neurosci*, 12, 3591-3600.
- Berridge, K.C. & Robinson, T.E. (1998) What is the role of dopamine in reward: hedonic impact, reward learning, or incentive salience? *Brain Res Brain Res Rev*, 28, 309-369.
- Betarbet, R., Turner, R., Chockkan, V., DeLong, M.R., Allers, K.A., Walters, J., Levey, A.I. & Greenamyre, J.T. (1997) Dopaminergic neurons intrinsic to the primate striatum. *J Neurosci*, 17, 6761-6768.
- Bindra, D. (1968) Neuropsychological interpretation of the effects of drive and incentive-motivation on general activity and instrumental behavior. *Psychological review*, 75, 1-22.
- Bishop, G.A., Chang, H.T. & Kitai, S.T. (1982) Morphological and physiological properties of neostriatal neurons: an intracellular horseradish peroxidase study in the rat. *Neuroscience*, 7, 179-191.
- Bock, A., Schrage, R. & Mohr, K. (2017) Allosteric modulators targeting CNS muscarinic receptors. *Neuropharmacology*.

- Bolam, J.P., Hanley, J.J., Booth, P.A. & Bevan, M.D. (2000) Synaptic organisation of the basal ganglia. *J Anat*, 196 ( Pt 4), 527-542.
- Bolam, J.P., Ingham, C.A. & Smith, A.D. (1984a) The section-Golgi-impregnation procedure-3. Combination of Golgi-impregnation with enzyme histochemistry and electron microscopy to characterize acetylcholinesterase-containing neurons in the rat neostriatum. *Neuroscience*, 12, 687-709.
- Bolam, J.P., Wainer, B.H. & Smith, A.D. (1984b) Characterization of cholinergic neurons in the rat neostriatum. A combination of choline acetyltransferase immunocytochemistry, Golgi-impregnation and electron microscopy. *Neuroscience*, 12, 711-718.
- Bonner, T.I., Young, A.C., Brann, M.R. & Buckley, N.J. (1988) Cloning and expression of the human and rat m5 muscarinic acetylcholine receptor genes. *Neuron*, 1, 403-410.
- Book, A.A., Wiley, R.G. & Schweitzer, J.B. (1992) Specificity of 192 IgG-saporin for NGF receptor-positive cholinergic basal forebrain neurons in the rat. *Brain Res*, 590, 350-355.
- Bosch-Bouju, C., Hyland, B.I. & Parr-Brownlie, L.C. (2013) Motor thalamus integration of cortical, cerebellar and basal ganglia information: implications for normal and parkinsonian conditions. *Front Comput Neurosci*, 7, 163.
- Bradfield, L.A., Bertran-Gonzalez, J., Chieng, B. & Balleine, B.W. (2013) The thalamostriatal pathway and cholinergic control of goal-directed action: interlacing new with existing learning in the striatum. *Neuron*, 79, 153-166.
- Bredt, D.S., Glatt, C.E., Hwang, P.M., Fotuhi, M., Dawson, T.M. & Snyder, S.H. (1991) Nitric oxide synthase protein and mRNA are discretely localized in neuronal populations of the mammalian CNS together with NADPH diaphorase. *Neuron*, 7, 615-624.
- Brichta, L., Greengard, P. & Flajolet, M. (2013) Advances in the pharmacological treatment of Parkinson's disease: targeting neurotransmitter systems. *Trends Neurosci*, 36, 543-554.



- Brimblecombe, K.R. & Cragg, S.J. (2017) The Striosome and Matrix Compartments of the Striatum: A Path through the Labyrinth from Neurochemistry toward Function. *ACS Chem Neurosci*, 8, 235-242.
- Brittain, J.S. & Brown, P. (2014) Oscillations and the basal ganglia: motor control and beyond. *Neuroimage*, 85 Pt 2, 637-647.
- Bronfeld, M., Yael, D., Belevsky, K. & Bar-Gad, I. (2013) Motor tics evoked by striatal disinhibition in the rat. *Front Syst Neurosci*, 7, 50.
- Bulman-Fleming, M.B., Bryden, M.P. & Rogers, T.T. (1997) Mouse paw preference: effects of variations in testing protocol. *Behav Brain Res*, 86, 79-87.
- Buot, A. & Yelnik, J. (2012) Functional anatomy of the basal ganglia: limbic aspects. *Rev Neurol (Paris)*, 168, 569-575.
- Burbulla, L.F., Song, P., Mazzulli, J.R., Zampese, E., Wong, Y.C., Jeon, S., Santos, D.P., Blanz, J., Obermaier, C.D., Strojny, C., Savas, J.N., Kiskinis, E., Zhuang, X., Kruger, R., Surmeier, D.J. & Krainc, D. (2017) Dopamine oxidation mediates mitochondrial and lysosomal dysfunction in Parkinson's disease. *Science*, 357, 1255-1261.
- Burke, R.E., Fahn, S. & Marsden, C.D. (1986) Torsion dystonia: a double-blind, prospective trial of high-dosage trihexyphenidyl. *Neurology*, 36, 160-164.
- Butcher, L.L. & Hodge, G.K. (1976) Postnatal development of acetylcholinesterase in the caudate-putamen nucleus and substantia nigra of rats. *Brain research*, 106, 223-240.
- Cachope, R. & Cheer, J.F. (2014) Local control of striatal dopamine release. *Front Behav Neurosci*, 8, 188.
- Cachope, R., Mateo, Y., Mathur, B.N., Irving, J., Wang, H.L., Morales, M., Lovinger, D.M. & Cheer, J.F. (2012) Selective activation of cholinergic interneurons enhances accumbal phasic dopamine release: setting the tone for reward processing. *Cell Rep*, 2, 33-41.

- Calabresi, P., Centonze, D., Gubellini, P., Pisani, A. & Bernardi, G. (1998) Blockade of M2-like muscarinic receptors enhances long-term potentiation at corticostriatal synapses. *Eur J Neurosci*, 10, 3020-3023.
- Calabresi, P., Centonze, D., Gubellini, P., Pisani, A. & Bernardi, G. (2000) Acetylcholine-mediated modulation of striatal function. *Trends Neurosci*, 23, 120-126.
- Calabresi, P., Picconi, B., Tozzi, A., Ghiglieri, V. & Di Filippo, M. (2014) Direct and indirect pathways of basal ganglia: a critical reappraisal. *Nat Neurosci*, 17, 1022-1030.
- Carrillo-Reid, L., Tecuapetla, F., Ibanez-Sandoval, O., Hernandez-Cruz, A., Galarraga, E. & Bargas, J. (2009a) Activation of the cholinergic system endows compositional properties to striatal cell assemblies. *J Neurophysiol*, 101, 737-749.
- Carrillo-Reid, L., Tecuapetla, F., Vautrelle, N., Hernandez, A., Vergara, R., Galarraga, E. & Bargas, J. (2009b) Muscarinic enhancement of persistent sodium current synchronizes striatal medium spiny neurons. *J Neurophysiol*, 102, 682-690.
- Caulfield, M.P. (1993) Muscarinic receptors--characterization, coupling and function. *Pharmacol Ther*, 58, 319-379.
- Cepeda, C., Wu, N., Andre, V.M., Cummings, D.M. & Levine, M.S. (2007) The corticostriatal pathway in Huntington's disease. *Prog Neurobiol*, 81, 253-271.
- Cha, J.H., Kosinski, C.M., Kerner, J.A., Alsdorf, S.A., Mangiarini, L., Davies, S.W., Penney, J.B., Bates, G.P. & Young, A.B. (1998) Altered brain neurotransmitter receptors in transgenic mice expressing a portion of an abnormal human huntington disease gene. *Proc Natl Acad Sci U S A*, 95, 6480-6485.
- Chen, C.C., Gilmore, A. & Zuo, Y. (2014) Study motor skill learning by single-pellet reaching tasks in mice. *J Vis Exp*.

- Chesselet, M.F. & Graybiel, A.M. (1986) Striatal neurons expressing somatostatin-like immunoreactivity: evidence for a peptidergic interneuronal system in the cat. *Neuroscience*, 17, 547-571.
- Chudasama, Y. & Robbins, T.W. (2006) Functions of frontostriatal systems in cognition: comparative neuropsychopharmacological studies in rats, monkeys and humans. *Biol Psychol*, 73, 19-38.
- Chuhma, N., Tanaka, K.F., Hen, R. & Rayport, S. (2011) Functional connectome of the striatal medium spiny neuron. *J Neurosci*, 31, 1183-1192.
- Contant, C., Umbriaco, D., Garcia, S., Watkins, K.C. & Descarries, L. (1996) Ultrastructural characterization of the acetylcholine innervation in adult rat neostriatum. *Neuroscience*, 71, 937-947.
- Coppola, J.J., Ward, N.J., Jadi, M.P. & Disney, A.A. (2016) Modulatory compartments in cortex and local regulation of cholinergic tone. *J Physiol Paris*, 110, 3-9.
- Crittenden, J.R. & Graybiel, A.M. (2011) Basal Ganglia disorders associated with imbalances in the striatal striosome and matrix compartments. *Front Neuroanat*, 5, 59.
- Crittenden, J.R., Lacey, C.J., Lee, T., Bowden, H.A. & Graybiel, A.M. (2014) Severe drug-induced repetitive behaviors and striatal overexpression of VAcHT in ChAT-ChR2-EYFP BAC transgenic mice. *Front Neural Circuits*, 8, 57.
- Crittenden, J.R., Lacey, C.J., Weng, F.J., Garrison, C.E., Gibson, D.J., Lin, Y. & Graybiel, A.M. (2017) Striatal Cholinergic Interneurons Modulate Spike-Timing in Striosomes and Matrix by an Amphetamine-Sensitive Mechanism. *Front Neuroanat*, 11, 20.
- Crittenden, J.R., Tillberg, P.W., Riad, M.H., Shima, Y., Gerfen, C.R., Curry, J., Housman, D.E., Nelson, S.B., Boyden, E.S. & Graybiel, A.M. (2016) Striosome-dendron bouquets highlight a unique striatonigral circuit targeting dopamine-containing neurons. *Proc Natl Acad Sci U S A*, 113, 11318-11323.

- Cubo, E., Fernandez Jaen, A., Moreno, C., Anaya, B., Gonzalez, M. & Kompoliti, K. (2008) Donepezil use in children and adolescents with tics and attention-deficit/hyperactivity disorder: an 18-week, single-center, dose-escalating, prospective, open-label study. *Clin Ther*, 30, 182-189.
- Cui, G., Jun, S.B., Jin, X., Pham, M.D., Vogel, S.S., Lovinger, D.M. & Costa, R.M. (2013) Concurrent activation of striatal direct and indirect pathways during action initiation. *Nature*, 494, 238-242.
- Dagani, F., Anderson, J.J. & Chase, T.N. (1992) Mitochondrial function in Parkinson's disease. *Ann Neurol*, 32, 226-227.
- Dautan, D., Huerta-Ocampo, I., Witten, I.B., Deisseroth, K., Bolam, J.P., Gerdjikov, T. & Mena-Segovia, J. (2014) A major external source of cholinergic innervation of the striatum and nucleus accumbens originates in the brainstem. *J Neurosci*, 34, 4509-4518.
- de la Monte, S.M., Vonsattel, J.P. & Richardson, E.P., Jr. (1988) Morphometric demonstration of atrophic changes in the cerebral cortex, white matter, and neostriatum in Huntington's disease. *J Neuropathol Exp Neurol*, 47, 516-525.
- Del Castillo, J., De Mello, W.C. & Morales, T. (1967) The initiation of action potentials in the somatic musculature of *Ascaris lumbricoides*. *J Exp Biol*, 46, 263-279.
- Delcastillo, J., Demello, W.C. & Morales, T. (1963) The Physiological Role of Acetylcholine in the Neuromuscular System of *Ascaris Lumbricoides*. *Arch Int Physiol Biochim*, 71, 741-757.
- Dencker, D., Thomsen, M., Wortwein, G., Weikop, P., Cui, Y., Jeon, J., Wess, J. & Fink-Jensen, A. (2012) Muscarinic Acetylcholine Receptor Subtypes as Potential Drug Targets for the Treatment of Schizophrenia, Drug Abuse and Parkinson's Disease. *ACS Chem Neurosci*, 3, 80-89.
- Deng, P., Zhang, Y. & Xu, Z.C. (2007) Involvement of I(h) in dopamine modulation of tonic firing in striatal cholinergic interneurons. *J Neuroscience*, 27, 3148-3156.

- Deng, Y.P., Albin, R.L., Penney, J.B., Young, A.B., Anderson, K.D. & Reiner, A. (2004) Differential loss of striatal projection systems in Huntington's disease: a quantitative immunohistochemical study. *J Chem Neuroanat*, 27, 143-164.
- Deng, Y.P. & Reiner, A. (2016) Cholinergic interneurons in the Q140 knockin mouse model of Huntington's disease: Reductions in dendritic branching and thalamostriatal input. *J Comp Neurol*, 524, 3518-3529.
- Deng, Y.P., Wong, T., Bricker-Anthony, C., Deng, B. & Reiner, A. (2013) Loss of corticostriatal and thalamostriatal synaptic terminals precedes striatal projection neuron pathology in heterozygous Q140 Huntington's disease mice. *Neurobiol Dis*, 60, 89-107.
- Descarries, L., Gisiger, V. & Steriade, M. (1997) Diffuse transmission by acetylcholine in the CNS. *Prog Neurobiol*, 53, 603-625.
- Dickinson, A. (1985) Actions and habits: the development of behavioural autonomy. *Philos. Trans. Royal Soc. B*, 308, 67-78.
- Di Filippo, M., Tozzi, A., Picconi, B., Ghiglieri, V. & Calabresi, P. (2007) Plastic abnormalities in experimental Huntington's disease. *Current opinion in pharmacology*, 7, 106-111.
- Diekelmann, S., Wilhelm, I. & Born, J. (2009) The whats and whens of sleep-dependent memory consolidation. *Sleep Med Rev*, 13, 309-321.
- DiFiglia, M. & Aronin, N. (1982) Ultrastructural features of immunoreactive somatostatin neurons in the rat caudate nucleus. *J Neurosci*, 2, 1267-1274.
- DiFiglia, M., Pasik, P. & Pasik, T. (1976) A Golgi study of neuronal types in the neostriatum of monkeys. *Brain Res*, 114, 245-256.
- Digby, G.J., Shirey, J.K. & Conn, P.J. (2010) Allosteric activators of muscarinic receptors as novel approaches for treatment of CNS disorders. *Mol BioSyst*, 6, 1345-1354.

- Ding, J., Guzman, J.N., Tkatch, T., Chen, S., Goldberg, J.A., Ebert, P.J., Levitt, P., Wilson, C.J., Hamm, H.E. & Surmeier, D.J. (2006) RGS4-dependent attenuation of M4 autoreceptor function in striatal cholinergic interneurons following dopamine depletion. *Nat Neurosci*, 9, 832-842.
- Doig, N.M., Magill, P.J., Apicella, P., Bolam, J.P. & Sharott, A. (2014) Cortical and thalamic excitation mediate the multiphasic responses of striatal cholinergic interneurons to motivationally salient stimuli. *J Neurosci*, 34, 3101-3117.
- Doig, N.M., Moss, J. & Bolam, J.P. (2010) Cortical and thalamic innervation of direct and indirect pathway medium-sized spiny neurons in mouse striatum. *J Neurosci*, 30, 14610-14618.
- Dolezal, V. & Tucek, S. (1999) Calcium channels involved in the inhibition of acetylcholine release by presynaptic muscarinic receptors in rat striatum. *Br J Pharmacol*, 127, 1627-1632.
- Donoghue, J.P., Leibovic, S. & Sanes, J.N. (1992) Organization of the forelimb area in squirrel monkey motor cortex: representation of digit, wrist, and elbow muscles. *Exp Brain Res*, 89, 1-19.
- Dubach, M., Schmidt, R., Kunkel, D., Bowden, D.M., Martin, R. & German, D.C. (1987) Primate neostriatal neurons containing tyrosine hydroxylase: immunohistochemical evidence. *Neurosci Lett*, 75, 205-210.
- Dunant, Y. & Gisiger, V. (2017) Ultrafast and Slow Cholinergic Transmission. Different Involvement of Acetylcholinesterase Molecular Forms. *Molecules*, 22.
- Dure, L.S., Young, A.B. & Penney, J.B. (1991) Excitatory amino acid binding sites in the caudate nucleus and frontal cortex of Huntington's disease. *Ann Neurol*, 30, 785-793.
- Duvoisin, R.C. (1967) Cholinergic-anticholinergic antagonism in parkinsonism. *Arch Neurol*, 17, 124-136.

- Eglen, R.M. (2006) Muscarinic receptor subtypes in neuronal and non-neuronal cholinergic function. *Auton Autacoid Pharmacol*, 26, 219-233.
- English, D.F., Ibanez-Sandoval, O., Stark, E., Tecuapetla, F., Buzsaki, G., Deisseroth, K., Tepper, J.M. & Koos, T. (2012) GABAergic circuits mediate the reinforcement-related signals of striatal cholinergic interneurons. *Nat Neurosci*, 15, 123-130.
- Eskow Jaunarajs, K.L., Bonsi, P., Chesselet, M.F., Standaert, D.G. & Pisani, A. (2015) Striatal cholinergic dysfunction as a unifying theme in the pathophysiology of dystonia. *Prog Neurobiol*, 127-128, 91-107.
- Exley, R. & Cragg, S.J. (2008) Presynaptic nicotinic receptors: a dynamic and diverse cholinergic filter of striatal dopamine neurotransmission. *Br J Pharmacol*, 153 Suppl 1, S283-297.
- Fahn, S. (2014) The medical treatment of Parkinson disease from James Parkinson to George Cotzias. *Mov Disord*, 30, 4-18.
- Farr, T.D. & Whishaw, I.Q. (2002) Quantitative and qualitative impairments in skilled reaching in the mouse (*Mus musculus*) after a focal motor cortex stroke. *Stroke*, 33, 1869-1875.
- Faust, T.W., Assous, M., Shah, F., Tepper, J.M. & Koos, T. (2015) Novel fast adapting interneurons mediate cholinergic-induced fast GABAA inhibitory postsynaptic currents in striatal spiny neurons. *Eur J Neurosci*, 42, 1764-1774.
- Feingold, J., Gibson, D.J., DePasquale, B. & Graybiel, A.M. (2015) Bursts of beta oscillation differentiate postperformance activity in the striatum and motor cortex of monkeys performing movement tasks. *Proc Natl Acad Sci U S A*, 112, 13687-13692.
- Ferrante, R.J., Beal, M.F., Kowall, N.W., Richardson, E.P., Jr. & Martin, J.B. (1987) Spraying of acetylcholinesterase-containing striatal neurons in Huntington's disease. *Brain Res*, 411, 162-166.

- Field, E.F. & Whishaw, I.Q. (2005) Sexually dimorphic postural adjustments are used in a skilled reaching task in the rat. *Behav Brain Res*, 163, 237-245.
- Figueredo-Cardenas, G., Morello, M., Sancesario, G., Bernardi, G. & Reiner, A. (1996) Colocalization of somatostatin, neuropeptide Y, neuronal nitric oxide synthase and NADPH-diaphorase in striatal interneurons in rats. *Brain Res*, 735, 317-324.
- Figuroa, A., Galarraga, E. & Bargas, J. (2002) Muscarinic receptors involved in the subthreshold cholinergic actions of neostriatal spiny neurons. *Synapse*, 46, 215-223.
- Floresco, S.B., St Onge, J.R., Ghods-Sharifi, S. & Winstanley, C.A. (2008) Cortico-limbic-striatal circuits subserving different forms of cost-benefit decision making. *Cogn Affect Behav Neurosci*, 8, 375-389.
- Fonnum, F. (1984) Glutamate: a neurotransmitter in mammalian brain. *J Neurochem*, 42, 1-11.
- Fonnum, F., Gottesfeld, Z. & Grofova, I. (1978) Distribution of glutamate decarboxylase, choline acetyl-transferase and aromatic amino acid decarboxylase in the basal ganglia of normal and operated rats. Evidence for striatopallidal, striatoentopeduncular and striatonigral GABAergic fibres. *Brain Res*, 143, 125-138.
- Foster, D.J., Gentry, P.R., Lizardi-Ortiz, J.E., Bridges, T.M., Wood, M.R., Niswender, C.M., Sulzer, D., Lindsley, C.W., Xiang, Z. & Conn, P.J. (2014) M5 receptor activation produces opposing physiological outcomes in dopamine neurons depending on the receptor's location. *J Neurosci: the official journal of the Society for Neuroscience*, 34, 3253-3262.
- Fuccillo, M.V. (2016) Striatal Circuits as a Common Node for Autism Pathophysiology. *Front Neurosci*, 10, 27.
- Fujiyama, F., Sohn, J., Nakano, T., Furuta, T., Nakamura, K.C., Matsuda, W. & Kaneko, T. (2011) Exclusive and common targets of neostriatofugal projections of rat striosome neurons: a single neuron-tracing study using a viral vector. *Eur J Neurosci*, 33, 668-677.



- Fukuda, T. (2009) Network architecture of gap junction-coupled neuronal linkage in the striatum. *J Neurosci*, 29, 1235-1243.
- Fuxe, K., Borroto-Escuela, D.O., Romero-Fernandez, W., Diaz-Cabiale, Z., Rivera, A., Ferraro, L., Tanganelli, S., Tarakanov, A.O., Garriga, P., Narvaez, J.A., Ciruela, F., Guescini, M. & Agnati, L.F. (2012) Extrasynaptic neurotransmission in the modulation of brain function. Focus on the striatal neuronal-glia networks. *Front Physiol*, 3, 136.
- Gage, F.H., Armstrong, D.M., Williams, L.R. & Varon, S. (1988) Morphological response of axotomized septal neurons to nerve growth factor. *J Comp Neurol*, 269, 147-155.
- Gage, F.H., Batchelor, P., Chen, K.S., Chin, D., Higgins, G.A., Koh, S., Deputy, S., Rosenberg, M.B., Fischer, W. & Bjorklund, A. (1989) NGF receptor reexpression and NGF-mediated cholinergic neuronal hypertrophy in the damaged adult neostriatum. *Neuron*, 2, 1177-1184.
- Galarraga, E., Hernandez-Lopez, S., Reyes, A., Miranda, I., Bermudez-Rattoni, F., Vilchis, C. & Bargas, J. (1999) Cholinergic modulation of neostriatal output: a functional antagonism between different types of muscarinic receptors. *J Neurosci*, 19, 3629-3638.
- Gerfen, C.R. (1984) The neostriatal mosaic: compartmentalization of corticostriatal input and striatonigral output systems. *Nature*, 311, 461-464.
- Gerfen, C.R. (1989) The neostriatal mosaic: striatal patch-matrix organization is related to cortical lamination. *Science*, 246, 385-388.
- Gerfen, C.R. & Surmeier, D.J. (2011) Modulation of striatal projection systems by dopamine. *Annu Rev Neurosci*, 34, 441-466.
- Gholamrezaei, G. & Whishaw, I.Q. (2009) Individual differences in skilled reaching for food related to increased number of gestures: evidence for goal and habit learning of skilled reaching. *Behav Neurosci*, 123, 863-874.

- Gimenez-Amaya, J.M. & Graybiel, A.M. (1991) Modular organization of projection neurons in the matrix compartment of the primate striatum. *J Neurosci*, 11, 779-791.
- Girasole, A.E. & Nelson, A.B. (2015) Probing striatal microcircuitry to understand the functional role of cholinergic interneurons. *Mov Disord*, 30, 1306-1318.
- Girgis, J., Merrett, D., Kirkland, S., Metz, G.A., Verge, V. & Fouad, K. (2007) Reaching training in rats with spinal cord injury promotes plasticity and task specific recovery. *Brain*, 130, 2993-3003.
- Goldberg, J.A., Ding, J.B. & Surmeier, D.J. (2012) Muscarinic modulation of striatal function and circuitry. *Handb Exp Pharmacol*, 223-241.
- Goldberg, J.A. & Reynolds, J.N. (2011) Spontaneous firing and evoked pauses in the tonically active cholinergic interneurons of the striatum. *Neuroscience*, 198, 27-43.
- Goldberg, J.A. & Wilson, C.J. (2005) Control of spontaneous firing patterns by the selective coupling of calcium currents to calcium-activated potassium currents in striatal cholinergic interneurons. *J Neurosci*, 25, 10230-10238.
- Gonzales, K.K., Pare, J.F., Wichmann, T. & Smith, Y. (2013) GABAergic inputs from direct and indirect striatal projection neurons onto cholinergic interneurons in the primate putamen. *J Comp Neurol*, 521, 2502-2522.
- Gonzales, K.K. & Smith, Y. (2015) Cholinergic interneurons in the dorsal and ventral striatum: anatomical and functional considerations in normal and diseased conditions. *Ann N Y Acad Sci*, 1349, 1-45.
- Goodman, J.H. & Gilbert, M.E. (2007) Modest thyroid hormone insufficiency during development induces a cellular malformation in the corpus callosum: a model of cortical dysplasia. *Endocrinology*, 148, 2593-2597.

- Gotti, C., Clementi, F., Fornari, A., Gaimarri, A., Guiducci, S., Manfredi, I., Moretti, M., Pedrazzi, P., Pucci, L. & Zoli, M. (2009) Structural and functional diversity of native brain neuronal nicotinic receptors. *Biochem Pharmacol*, 78, 703-711.
- Grace, A.A. & Onn, S.P. (1989) Morphology and electrophysiological properties of immunocytochemically identified rat dopamine neurons recorded in vitro. *J Neurosci*, 9, 3463-3481.
- Graveland, G.A. & DiFiglia, M. (1985) The frequency and distribution of medium-sized neurons with indented nuclei in the primate and rodent neostriatum. *Brain Res*, 327, 307-311.
- Graybiel, A.M. (1995) Building action repertoires: memory and learning functions of the basal ganglia. *Curr Opin Neurobiol*, 5, 733-741.
- Graybiel, A.M., Aosaki, T., Flaherty, A.W. & Kimura, M. (1994) The basal ganglia and adaptive motor control. *Science*, 265, 1826-1831.
- Graybiel, A.M. & Ragsdale, C.W., Jr. (1978) Histochemically distinct compartments in the striatum of human, monkeys, and cat demonstrated by acetylthiocholinesterase staining. *Proc Natl Acad Sci U S A*, 75, 5723-5726.
- Greenamyre, J.T. (2018) What's wrong with mitochondria in Parkinson's disease? *Mov Disord*, 33, 1515-1517.
- Gundersen, H.J. & Jensen, E.B. (1987) The efficiency of systematic sampling in stereology and its prediction. *J Microsc*, 147, 229-263.
- Gundersen, H.J., Jensen, E.B., Kieu, K. & Nielsen, J. (1999) The efficiency of systematic sampling in stereology--reconsidered. *J Microsc*, 193, 199-211.
- Gundersen, H.J.G. (1977) Notes on the estimation of the numerical density of arbitrary profiles: the edge effect. *J Microsc*, 111, 219-223.

- Haber, S.N., Fudge, J.L. & McFarland, N.R. (2000) Striatonigrostriatal pathways in primates form an ascending spiral from the shell to the dorsolateral striatum. *J Neurosci*, 20, 2369-2382.
- Haga, T. (2013) Molecular properties of muscarinic acetylcholine receptors. *Proc Jpn Acad Ser B Phys Biol Sci*, 89, 226-256.
- Hagg, T., Fass-Holmes, B., Vahlsing, H.L., Manthorpe, M., Conner, J.M. & Varon, S. (1989) Nerve growth factor (NGF) reverses axotomy-induced decreases in choline acetyltransferase, NGF receptor and size of medial septum cholinergic neurons. *Brain Res*, 505, 29-38.
- Havekes, R., Abel, T. & Van der Zee, E.A. (2011) The cholinergic system and neostriatal memory functions. *Behav Brain Res*, 221, 412-423.
- Herculano-Houzel, S., von Bartheld, C.S., Miller, D.J. & Kaas, J.H. (2015) How to count cells: the advantages and disadvantages of the isotropic fractionator compared with stereology. *Cell Tissue Res*, 360, 29-42.
- Herkenham, M. & Pert, C.B. (1981) Mosaic distribution of opiate receptors, parafascicular projections and acetylcholinesterase in rat striatum. *Nature*, 291, 415-418.
- Hernandez-Flores, T., Hernandez-Gonzalez, O., Perez-Ramirez, M.B., Lara-Gonzalez, E., Arias-Garcia, M.A., Duhne, M., Perez-Burgos, A., Prieto, G.A., Figueroa, A., Galarraga, E. & Bargas, J. (2015) Modulation of direct pathway striatal projection neurons by muscarinic M(4)-type receptors. *Neuropharmacology*, 89, 232-244.
- Herrero, M.T., Barcia, C. & Navarro, J.M. (2002) Functional anatomy of thalamus and basal ganglia. *Childs Nerv Syst*, 18, 386-404.
- Hersch, S.M., Gutekunst, C.A., Rees, H.D., Heilman, C.J. & Levey, A.I. (1994) Distribution of m1-m4 muscarinic receptor proteins in the rat striatum: light and electron microscopic immunocytochemistry using subtype-specific antibodies. *J Neurosci*, 14, 3351-3363.

- Hersch, S.M. & Levey, A.I. (1995) Diverse pre- and post-synaptic expression of m1-m4 muscarinic receptor proteins in neurons and afferents in the rat neostriatum. *Life Sci*, 56, 931-938.
- Hikosaka, O., Nakamura, K., Sakai, K. & Nakahara, H. (2002) Central mechanisms of motor skill learning. *Curr Opin Neurobiol*, 12, 217-222.
- Hikosaka, O., Takikawa, Y. & Kawagoe, R. (2000) Role of the basal ganglia in the control of purposive saccadic eye movements. *Physiol Rev*, 80, 953-978.
- Hilario, M.R. & Costa, R.M. (2008) High on habits. *Front Neurosci*, 2, 208-217.
- Hokfelt, T., Skirboll, L., Rehfeld, J.F., Goldstein, M., Markey, K. & Dann, O. (1980) A subpopulation of mesencephalic dopamine neurons projecting to limbic areas contains a cholecystokinin-like peptide: evidence from immunohistochemistry combined with retrograde tracing. *Neuroscience*, 5, 2093-2124.
- Holt, D.J., Herman, M.M., Hyde, T.M., Kleinman, J.E., Sinton, C.M., German, D.C., Hersh, L.B., Graybiel, A.M. & Saper, C.B. (1999) Evidence for a deficit in cholinergic interneurons in the striatum in schizophrenia. *Neuroscience*, 94, 21-31.
- Hulme, E.C., Birdsall, N.J. & Buckley, N.J. (1990) Muscarinic receptor subtypes. *Annu Rev Pharmacol Toxicol*, 30, 633-673.
- Huot, P. & Parent, A. (2007) Dopaminergic neurons intrinsic to the striatum. *J Neurochem*, 101, 1441-1447.
- Hurst, R., Rollema, H. & Bertrand, D. (2013) Nicotinic acetylcholine receptors: from basic science to therapeutics. *Pharmacol Ther*, 137, 22-54.
- Ibanez-Sandoval, O., Tecuapetla, F., Unal, B., Shah, F., Koos, T. & Tepper, J.M. (2010) Electrophysiological and morphological characteristics and synaptic connectivity of

tyrosine hydroxylase-expressing neurons in adult mouse striatum. *J Neurosci*, 30, 6999-7016.

Ibanez-Sandoval, O., Tecuapetla, F., Unal, B., Shah, F., Koos, T. & Tepper, J.M. (2011) A novel functionally distinct subtype of striatal neuropeptide Y interneuron. *J Neurosci*, 31, 16757-16769.

Ibanez-Sandoval, O., Xenias, H.S., Tepper, J.M. & Koos, T. (2015) Dopaminergic and cholinergic modulation of striatal tyrosine hydroxylase interneurons. *Neuropharmacology*, 95, 468-476.

Inokawa, H., Yamada, H., Matsumoto, N., Muranishi, M. & Kimura, M. (2010) Juxtacellular labeling of tonically active neurons and phasically active neurons in the rat striatum. *Neuroscience*, 168, 395-404.

Inoue, R., Suzuki, T., Nishimura, K. & Miura, M. (2016) Nicotinic acetylcholine receptor-mediated GABAergic inputs to cholinergic interneurons in the striosomes and the matrix compartments of the mouse striatum. *Neuropharmacology*, 105, 318-328.

Iribe, Y., Moore, K., Pang, K.C. & Tepper, J.M. (1999) Subthalamic stimulation-induced synaptic responses in substantia nigra pars compacta dopaminergic neurons in vitro. *J Neurophysiol*, 82, 925-933.

Ishii, M. & Kurachi, Y. (2006) Muscarinic acetylcholine receptors. *Curr Pharm Des*, 12, 3573-3581.

Iwamoto, E.T., Loh, H.H. & Way, E.L. (1976) Circling behavior in rats with 6-hydroxydopamine or electrolytic nigral lesions. *Eur J Pharmacol*, 37, 339-356.

Jaidar, O., Carrillo-Reid, L., Hernandez, A., Drucker-Colin, R., Bargas, J. & Hernandez-Cruz, A. (2010) Dynamics of the Parkinsonian striatal microcircuit: entrainment into a dominant network state. *J Neurosci*, 30, 11326-11336.

- Jaidar, O., Carrillo-Reid, L., Nakano, Y., Lopez-Huerta, V.G., Hernandez-Cruz, A., Bargas, J., Garcia-Munoz, M. & Arbuthnott, G.W. (2019) Synchronized activation of striatal direct and indirect pathways underlies the behavior in unilateral dopamine-depleted mice. *Eur J Neurosci*.
- Janickova, H., Prado, V.F., Prado, M.A.M., El Mestikawy, S. & Bernard, V. (2017) Vesicular acetylcholine transporter (VAChT) over-expression induces major modifications of striatal cholinergic interneuron morphology and function. *J Neurochem*.
- Jerusalinsky, D., Kornisiuk, E., Alfaro, P., Quillfeldt, J., Ferreira, A., Rial, V.E., Duran, R. & Cervenansky, C. (2000) Muscarinic toxins: novel pharmacological tools for the muscarinic cholinergic system. *Toxicon*, 38, 747-761.
- Johnston, J.G., Gerfen, C.R., Haber, S.N. & van der Kooy, D. (1990) Mechanisms of striatal pattern formation: conservation of mammalian compartmentalization. *Brain Res Dev Brain Res*, 57, 93-102.
- Jones, E.G., Coulter, J.D., Burton, H. & Porter, R. (1977) Cells of origin and terminal distribution of corticostriatal fibers arising in the sensory-motor cortex of monkeys. *J Comp Neurol*, 173, 53-80.
- Kalia, L.V., Brotchie, J.M. & Fox, S.H. (2013) Novel nondopaminergic targets for motor features of Parkinson's disease: review of recent trials. *Mov Disord*, 28, 131-144.
- Karlsson, E., Jolkkonen, M., Mulugeta, E., Onali, P. & Adem, A. (2000) Snake toxins with high selectivity for subtypes of muscarinic acetylcholine receptors. *Biochimie*, 82, 793-806.
- Kataoka, Y., Kalanithi, P.S., Grantz, H., Schwartz, M.L., Saper, C., Leckman, J.F. & Vaccarino, F.M. (2010) Decreased number of parvalbumin and cholinergic interneurons in the striatum of individuals with Tourette syndrome. *J Comp Neurol*, 518, 277-291.

- Kawaguchi, Y. (1992) Large aspiny cells in the matrix of the rat neostriatum in vitro: physiological identification, relation to the compartments and excitatory postsynaptic currents. *J Neurophysiol*, 67, 1669-1682.
- Kawaguchi, Y. (1993) Physiological, morphological, and histochemical characterization of three classes of interneurons in rat neostriatum. *J Neurosci*, 13, 4908-4923.
- Kawaguchi, Y. (1997) Neostriatal cell subtypes and their functional roles. *Neurosci Res*, 27, 1-8.
- Kawaguchi, Y., Wilson, C.J., Augood, S.J. & Emson, P.C. (1995) Striatal interneurons: chemical, physiological and morphological characterization. *Trends Neurosci*, 18, 527-535.
- Kawaguchi, Y., Wilson, C.J. & Emson, P.C. (1989) Intracellular recording of identified neostriatal patch and matrix spiny cells in a slice preparation preserving cortical inputs. *J Neurophysiol*, 62, 1052-1068.
- Kawaguchi, Y., Wilson, C.J. & Emson, P.C. (1990) Projection subtypes of rat neostriatal matrix cells revealed by intracellular injection of biocytin. *J Neuroscience*, 10, 3421-3438.
- Kawai, R., Markman, T., Poddar, R., Ko, R., Fantana, A.L., Dhawale, A.K., Kampff, A.R. & Olveczky, B.P. (2015) Motor cortex is required for learning but not for executing a motor skill. *Neuron*, 86, 800-812.
- Kelley, A.E., Domesick, V.B. & Nauta, W.J. (1982) The amygdalostriatal projection in the rat—an anatomical study by anterograde and retrograde tracing methods. *Neuroscience*, 7, 615-630.
- Kemp, J.M. & Powell, T.P. (1971) The structure of the caudate nucleus of the cat: light and electron microscopy. *Philos Trans R Soc Lond B Biol Sci*, 262, 383-401.



- Kempster, P.A., Williams, D.R., Selikhova, M., Holton, J., Revesz, T. & Lees, A.J. (2007) Patterns of levodopa response in Parkinson's disease: a clinico-pathological study. *Brain*, 130, 2123-2128.
- Kepecs, A. & Fishell, G. (2014) Interneuron cell types are fit to function. *Nature*, 505, 318-326.
- Kimura, H., McGeer, P.L., Peng, J.H. & McGeer, E.G. (1981) The central cholinergic system studied by choline acetyltransferase immunohistochemistry in the cat. *J Comp Neurol*, 200, 151-201.
- Kimura, M., Kato, M. & Shimazaki, H. (1990) Physiological properties of projection neurons in the monkey striatum to the globus pallidus. *Exp Brain Res*, 82, 672-676.
- Kimura, M., Kato, M., Shimazaki, H., Watanabe, K. & Matsumoto, N. (1996) Neural information transferred from the putamen to the globus pallidus during learned movement in the monkey. *J Neurophysiol*, 76, 3771-3786.
- Kimura, M., Rajkowski, J. & Evarts, E. (1984) Tonicly discharging putamen neurons exhibit set-dependent responses. *Proc Natl Acad Sci U S A*, 81, 4998-5001.
- Kita, H. & Kitai, S.T. (1988) Glutamate decarboxylase immunoreactive neurons in rat neostriatum: their morphological types and populations. *Brain Res*, 447, 346-352.
- Kita, H., Kosaka, T. & Heizmann, C.W. (1990) Parvalbumin-immunoreactive neurons in the rat neostriatum: a light and electron microscopic study. *Brain Res*, 536, 1-15.
- Kita, T., Kita, H. & Kitai, S.T. (1986) Electrical membrane properties of rat substantia nigra compacta neurons in an in vitro slice preparation. *Brain Res*, 372, 21-30.
- Kitabatake, Y., Hikida, T., Watanabe, D., Pastan, I. & Nakanishi, S. (2003) Impairment of reward-related learning by cholinergic cell ablation in the striatum. *Proc Natl Acad Sci U S A*, 100, 7965-7970.

- Kitai, S.T. & Surmeier, D.J. (1993) Cholinergic and dopaminergic modulation of potassium conductances in neostriatal neurons. *Adv Neurol*, 60, 40-52.
- Klein, A. & Dunnett, S.B. (2012) Analysis of skilled forelimb movement in rats: the single pellet reaching test and staircase test. *Curr Protoc Neurosci/ editorial board, Jacqueline N. Crawley ... [et al.]*, Chapter 8, Unit8 28.
- Klein, C. & Fahn, S. (2013) Translation of Oppenheim's 1911 paper on dystonia. *Mov Disord*, 28, 851-862.
- Kondabolu, K., Roberts, E.A., Bucklin, M., McCarthy, M.M., Kopell, N. & Han, X. (2016) Striatal cholinergic interneurons generate beta and gamma oscillations in the corticostriatal circuit and produce motor deficits. *Proc Natl Acad Sci U S A*, 113, E3159-3168.
- Koob, G.F. (1992) Neural mechanisms of drug reinforcement. *Ann N Y Acad Sci*, 654, 171-191.
- Koos, T. & Tepper, J.M. (1999) Inhibitory control of neostriatal projection neurons by GABAergic interneurons. *Nat Neurosci*, 2, 467-472.
- Kreitzer, A.C. (2009) Physiology and pharmacology of striatal neurons. *Annu Rev Neurosci*, 32, 127-147.
- Kreitzer, A.C. & Malenka, R.C. (2008) Striatal plasticity and basal ganglia circuit function. *Neuron*, 60, 543-554.
- Kubota, Y., Mikawa, S. & Kawaguchi, Y. (1993) Neostriatal GABAergic interneurons contain NOS, calretinin or parvalbumin. *Neuroreport*, 5, 205-208.
- Lams, B.E., Isacson, O. & Sofroniew, M.V. (1988) Loss of transmitter-associated enzyme staining following axotomy does not indicate death of brainstem cholinergic neurons. *Brain Res*, 475, 401-406.

- Laplante, F., Lappi, D.A. & Sullivan, R.M. (2011) Cholinergic depletion in the nucleus accumbens: effects on amphetamine response and sensorimotor gating. *Prog Neuropsychopharmacol Biol Psychiatry*, 35, 501-509.
- Laplante, F., Zhang, Z.W., Huppe-Gourgues, F., Dufresne, M.M., Vaucher, E. & Sullivan, R.M. (2012) Cholinergic depletion in nucleus accumbens impairs mesocortical dopamine activation and cognitive function in rats. *Neuropharmacology*, 63, 1075-1084.
- Leckman, J.F., Riddle MA, Hardin MT, Ort SI, Swartz KL, Stevenson J & DJ., C. (1989a) The Yale Global Tic Severity Scale: initial testing of a clinician-rated scale of tic severity. *J Am Acad Child Adolesc Psychiatry*, 28, 566-573.
- Leckman, J.F., Riddle, M.A., Hardin, M.T., Ort, S.I., Swartz, K.L., Stevenson, J. & Cohen, D.J. (1989b) The Yale Global Tic Severity Scale: initial testing of a clinician-rated scale of tic severity. *J Am Acad Child Adolesc Psychiatry*, 28, 566-573.
- Lee, K., Dixon, A.K., Freeman, T.C. & Richardson, P.J. (1998) Identification of an ATP-sensitive potassium channel current in rat striatal cholinergic interneurons. *J Physiol*, 510 ( Pt 2), 441-453.
- Lehmann, J., Fibiger, H.C. & Butcher, L.L. (1979) The localization of acetylcholinesterase in the corpus striatum and substantia nigra of the rat following kainic acid lesion of the corpus striatum: a biochemical and histochemical study. *Neuroscience*, 4, 217-225.
- Lemon, R.N. (1993) The G. L. Brown Prize Lecture. Cortical control of the primate hand. *Exp Physiol*, 78, 263-301.
- Lenington, J.B., Coppola, G., Kataoka-Sasaki, Y., Fernandez, T.V., Palejev, D., Li, Y., Huttner, A., Pletikos, M., Sestan, N., Leckman, J.F. & Vaccarino, F.M. (2016) Transcriptome Analysis of the Human Striatum in Tourette Syndrome. *Biol Psychiatry*, 79, 372-382.

- Lewis, P.R., Jones, P.B., Breathnach, S.M. & Navaratnam, V. (1972) Regenerative capacity of visceral preganglionic neurones. *Nat New Biol*, 236, 181-182.
- Li, Q., Ko, H., Qian, Z.M., Yan, L.Y.C., Chan, D.C.W., Arbuthnott, G., Ke, Y. & Yung, W.H. (2017) Refinement of learned skilled movement representation in motor cortex deep output layer. *Nat Commun*, 8, 15834.
- Liao, C.F., Themmen, A.P., Joho, R., Barberis, C., Birnbaumer, M. & Birnbaumer, L. (1989) Molecular cloning and expression of a fifth muscarinic acetylcholine receptor. *J Biol Chem*, 264, 7328-7337.
- Lim, S.A., Kang, U.J. & McGehee, D.S. (2014) Striatal cholinergic interneuron regulation and circuit effects. *Front Synaptic Neurosci*, 6, 22.
- Loewi, O. (1921) Über humorale übertragbarkeit der Herznervenwirkung. *Pflüger's Archiv für die gesamte Physiologie des Menschen und der Tiere*, 189, 239-242.
- Lopez-Huerta, V.G., Nakano, Y., Bausenwein, J., Jaidar, O., Lazarus, M., Cherasse, Y., Garcia-Munoz, M. & Arbuthnott, G. (2016) The neostriatum: two entities, one structure? *Brain Struct Funct*, 221, 1737-1749.
- Lopez-Real, A., Rodriguez-Pallares, J., Guerra, M.J. & Labandeira-Garcia, J.L. (2003) Localization and functional significance of striatal neurons immunoreactive to aromatic L-amino acid decarboxylase or tyrosine hydroxylase in rat Parkinsonian models. *Brain Res*, 969, 135-146.
- Lovinger, D.M. (2008) Communication networks in the brain: neurons, receptors, neurotransmitters, and alcohol. *Alcohol Res Health*, 31, 196-214.
- Lynch, G.S., Lucas, P.A. & Deadwyler, S.A. (1972) The demonstration of acetylcholinesterase containing neurones within the caudate nucleus of the rat. *Brain Res*, 45, 617-621.

- Macri, S., Adriani, W., Chiarotti, F. & Laviola, G. (2002) Risk taking during exploration of a plus-maze is greater in adolescent than in juvenile or adult mice. *Anim Behav*, 64, 541-546.
- Malach, R. & Graybiel, A.M. (1986) Mosaic architecture of the somatic sensory-recipient sector of the cat's striatum. *J Neurosci*, 6, 3436-3458.
- Mamaligas, A.A. & Ford, C.P. (2016) Spontaneous Synaptic Activation of Muscarinic Receptors by Striatal Cholinergic Neuron Firing. *Neuron*, 91, 574-586.
- Manyam, B.V. (1990) Paralysis agitans and levodopa in "Ayurveda": ancient Indian medical treatise. *Mov Disord*, 5, 47-48.
- Marques, J.M. & Olsson, I.A. (2010) Performance of juvenile mice in a reach-to-grasp task. *J Neurosci Methods*, 193, 82-85.
- Matamales, M., Skrbis, Z., Hatch, R.J., Balleine, B.W., Gotz, J. & Bertran-Gonzalez, J. (2016) Aging-Related Dysfunction of Striatal Cholinergic Interneurons Produces Conflict in Action Selection. *Neuron*, 90, 362-373.
- McCairn, K.W., Bronfeld, M., Bebelovsky, K. & Bar-Gad, I. (2009) The neurophysiological correlates of motor tics following focal striatal disinhibition. *Brain*, 132, 2125-2138.
- McFarland, N.R. & Haber, S.N. (2002) Thalamic relay nuclei of the basal ganglia form both reciprocal and nonreciprocal cortical connections, linking multiple frontal cortical areas. *J Neurosci*, 22, 8117-8132.
- McGeer, P.L., McGeer, E.G., Fibiger, H.C. & Wickson, V. (1971) Neostriatal choline acetylase and cholinesterase following selective brain lesions. *Brain Res*, 35, 308-314.
- McGeorge, A.J. & Faull, R.L. (1989) The organization of the projection from the cerebral cortex to the striatum in the rat. *Neuroscience*, 29, 503-537.

- McKiernan, B.J., Marcario, J.K., Karrer, J.H. & Cheney, P.D. (1998) Corticomotoneuronal postspike effects in shoulder, elbow, wrist, digit, and intrinsic hand muscles during a reach and prehension task. *J Neurophysiol*, 80, 1961-1980.
- Mellanby, H. (1955) The identification and estimation of acetylcholine in three parasitic nematodes (*Ascaris lumbricoides*, *Litomosoides carinii*, and the microfilariae of *Dirofilaria repens*). *Parasitology*, 45, 287-294.
- Mena-Segovia, J. & Bolam, J.P. (2017) Rethinking the Pedunculopontine Nucleus: From Cellular Organization to Function. *Neuron*, 94, 7-18.
- Meredith, G.E., Farrell, T., Kellaghan, P., Tan, Y., Zahm, D.S. & Totterdell, S. (1999) Immunocytochemical characterization of catecholaminergic neurons in the rat striatum following dopamine-depleting lesions. *Eur J Neurosci*, 11, 3585-3596.
- Miklyaeva, E.I., Castaneda, E. & Whishaw, I.Q. (1994) Skilled reaching deficits in unilateral dopamine-depleted rats: impairments in movement and posture and compensatory adjustments. *J Neurosci*, 14, 7148-7158.
- Munoz-Manchado, A.B., Foldi, C., Szydlowski, S., Sjulson, L., Farries, M., Wilson, C., Silberberg, G. & Hjerling-Leffler, J. (2016) Novel Striatal GABAergic Interneuron Populations Labeled in the 5HT3a(EGFP) Mouse. *Cereb Cortex*, 26, 96-105.
- Narushima, M., Uchigashima, M., Fukaya, M., Matsui, M., Manabe, T., Hashimoto, K., Watanabe, M. & Kano, M. (2007) Tonic enhancement of endocannabinoid-mediated retrograde suppression of inhibition by cholinergic interneuron activity in the striatum. *J Neurosci*, 27, 496-506.
- Nathanson, N.M. (2000) A multiplicity of muscarinic mechanisms: enough signaling pathways to take your breath away. *Proc Natl Acad Sci U S A*, 97, 6245-6247.
- Nelson, A.B., Hammack, N., Yang, C.F., Shah, N.M., Seal, R.P. & Kreitzer, A.C. (2014) Striatal cholinergic interneurons Drive GABA release from dopamine terminals. *Neuron*, 82, 63-70.

- Niciu, M.J., Kelmendi, B. & Sanacora, G. (2012) Overview of glutamatergic neurotransmission in the nervous system. *Pharmacol Biochem Behav*, 100, 656-664.
- Niittykoski, M., Ruotsalainen, S., Haapalinna, A., Larson, J. & Sirvio, J. (1999) Activation of muscarinic M3-like receptors and beta-adrenoceptors, but not M2-like muscarinic receptors or alpha-adrenoceptors, directly modulates corticostriatal neurotransmission in vitro. *Neuroscience*, 90, 95-105.
- Oldenburg, I.A. & Ding, J.B. (2011) Cholinergic modulation of synaptic integration and dendritic excitability in the striatum. *Curr Opin Neurobiol*, 21, 425-432.
- Olesen, M.V., Needham, E.K. & Pakkenberg, B. (2017) The Optical Fractionator Technique to Estimate Cell Numbers in a Rat Model of Electroconvulsive Therapy. *J Vis Exp*.
- Oorschot, D.E. (1996) Total number of neurons in the neostriatal, pallidal, subthalamic, and substantia nigral nuclei of the rat basal ganglia: a stereological study using the cavalieri and optical disector methods. *J Comp Neurol*, 366, 580-599.
- Ovsepian, S.V., O'Leary, V.B. & Zaborszky, L. (2016) Cholinergic Mechanisms in the Cerebral Cortex: Beyond Synaptic Transmission. *Neuroscientist*, 22, 238-251.
- Packard, M.G. & Knowlton, B.J. (2002) Learning and memory functions of the Basal Ganglia. *Annu Rev Neurosci*, 25, 563-593.
- Palfi, S., Leventhal, L., Chu, Y., Ma, S.Y., Emborg, M., Bakay, R., Deglon, N., Hantraye, P., Aebischer, P. & Kordower, J.H. (2002) Lentivirally delivered glial cell line-derived neurotrophic factor increases the number of striatal dopaminergic neurons in primate models of nigrostriatal degeneration. *J Neurosci*, 22, 4942-4954.
- Pan, W.X., Mao, T. & Dudman, J.T. (2010) Inputs to the dorsal striatum of the mouse reflect the parallel circuit architecture of the forebrain. *Front Neuroanat*, 4, 147.

- Pancani, T., Bolarinwa, C., Smith, Y., Lindsley, C.W., Conn, P.J. & Xiang, Z. (2014) M4 mAChR-mediated modulation of glutamatergic transmission at corticostriatal synapses. *ACS Chem Neurosci*, 5, 318-324.
- Penney, J.B., Jr. & Young, A.B. (1982) Quantitative autoradiography of neurotransmitter receptors in Huntington disease. *Neurology*, 32, 1391-1395.
- Peralta, E.G., Winslow, J.W., Peterson, G.L., Smith, D.H., Ashkenazi, A., Ramachandran, J., Schimerlik, M.I. & Capon, D.J. (1987) Primary structure and biochemical properties of an M2 muscarinic receptor. *Science*, 236, 600-605.
- Percheron, G., François, C. & Yelnik, J. (Year) Spatial Organization and Information Processing in the Core of the Basal Ganglia. *Proceedings of the The Basal Ganglia II*. Springer US, City. p. 205-226.
- Perez-Burgos, A., Perez-Rosello, T., Salgado, H., Flores-Barrera, E., Prieto, G.A., Figueroa, A., Galarraga, E. & Bargas, J. (2008) Muscarinic M(1) modulation of N and L types of calcium channels is mediated by protein kinase C in neostriatal neurons. *Neuroscience*, 155, 1079-1097.
- Perez-Burgos, A., Prieto, G.A., Galarraga, E. & Bargas, J. (2010) CaV2.1 channels are modulated by muscarinic M1 receptors through phosphoinositide hydrolysis in neostriatal neurons. *Neuroscience*, 165, 293-299.
- Perez-Ramirez, M.B., Laville, A., Tapia, D., Duhne, M., Lara-Gonzalez, E., Bargas, J. & Galarraga, E. (2015) KV7 Channels Regulate Firing during Synaptic Integration in GABAergic Striatal Neurons. *Neural plasticity*, 2015, 472676.
- Perez-Rosello, T., Figueroa, A., Salgado, H., Vilchis, C., Tecuapetla, F., Guzman, J.N., Galarraga, E. & Bargas, J. (2005) Cholinergic control of firing pattern and neurotransmission in rat neostriatal projection neurons: role of CaV2.1 and CaV2.2 Ca<sup>2+</sup> channels. *J Neurophysiol*, 93, 2507-2519.



- Peterson, B., Riddle, M.A., Cohen, D.J., Katz, L.D., Smith, J.C., Hardin, M.T. & Leckman, J.F. (1993) Reduced basal ganglia volumes in Tourette's syndrome using three-dimensional reconstruction techniques from magnetic resonance images. *Neurology*, 43, 941-949.
- Peterson, D.A., Sejnowski, T.J. & Poizner, H. (2010) Convergent evidence for abnormal striatal synaptic plasticity in dystonia. *Neurobiol Dis*, 37, 558-573.
- Pineda, J.C.,argas, J., Flores-Hernandez, J. & Galarraga, E. (1995) Muscarinic receptors modulate the afterhyperpolarizing potential in neostriatal neurons. *Eur J Pharmacol*, 281, 271-277.
- Pisani, A., Bernardi, G., Ding, J. & Surmeier, D.J. (2007) Re-emergence of striatal cholinergic interneurons in movement disorders. *Trends Neurosci*, 30, 545-553.
- Prensa, L., Gimenez-Amaya, J.M. & Parent, A. (1999) Chemical heterogeneity of the striosomal compartment in the human striatum. *J Comp Neurol*, 413, 603-618.
- Qin, K., Dong, C., Wu, G. & Lambert, N.A. (2011) Inactive-state preassembly of G(q)-coupled receptors and G(q) heterotrimers. *Nat Chem Biol*, 7, 740-747.
- Quik, M. & Wonnacott, S. (2011)  $\alpha_6\beta_2^*$  and  $\alpha_4\beta_2^*$  nicotinic acetylcholine receptors as drug targets for Parkinson's disease. *Pharmacol Rev*, 63, 938-966.
- Rakic, P., Bourgeois, J.P., Eckenhoff, M.F., Zecevic, N. & Goldman-Rakic, P.S. (1986) Concurrent overproduction of synapses in diverse regions of the primate cerebral cortex. *Science*, 232, 232-235.
- Redgrave, P., Prescott, T.J. & Gurney, K. (1999) The basal ganglia: a vertebrate solution to the selection problem? *Neuroscience*, 89, 1009-1023.
- Reiner, A., Albin, R.L., Anderson, K.D., D'Amato, C.J., Penney, J.B. & Young, A.B. (1988) Differential loss of striatal projection neurons in Huntington disease. *Proc Natl Acad Sci U S A*, 85, 5733-5737.

- Reiner, A., Medina, L. & Veenman, C.L. (1998) Structural and functional evolution of the basal ganglia in vertebrates. *Brain Res Brain Res Rev*, 28, 235-285.
- Reynolds, J.N., Hyland, B.I. & Wickens, J.R. (2004) Modulation of an afterhyperpolarization by the substantia nigra induces pauses in the tonic firing of striatal cholinergic interneurons. *J Neurosci*, 24, 9870-9877.
- Rosas, H.D., Goodman, J., Chen, Y.I., Jenkins, B.G., Kennedy, D.N., Makris, N., Patti, M., Seidman, L.J., Beal, M.F. & Koroshetz, W.J. (2001) Striatal volume loss in HD as measured by MRI and the influence of CAG repeat. *Neurology*, 57, 1025-1028.
- Rowan, E.G. & Harvey, A.L. (2011) Snake toxins from mamba venoms: unique tools for the physiologist. *Acta chimica Slovenica*, 58, 689-692.
- Royce, G.J. (1982) Laminar origin of cortical neurons which project upon the caudate nucleus: a horseradish peroxidase investigation in the cat. *J Comp Neurol*, 205, 8-29.
- Rymar, V.V., Sasseville, R., Luk, K.C. & Sadikot, A.F. (2004) Neurogenesis and stereological morphometry of calretinin-immunoreactive GABAergic interneurons of the neostriatum. *J Comp Neurol*, 469, 325-339.
- Salahudeen, M.S., Duffull, S.B. & Nishtala, P.S. (2015) Anticholinergic burden quantified by anticholinergic risk scales and adverse outcomes in older people: a systematic review. *BMC Geriatr*, 15, 31.
- Sanchez, G., Rodriguez, M.J., Pomata, P., Rela, L. & Murer, M.G. (2011) Reduction of an afterhyperpolarization current increases excitability in striatal cholinergic interneurons in rat parkinsonism. *J Neurosci*, 31, 6553-6564.
- Santiago, M.P. & Potter, L.T. (2001) Biotinylated m4-toxin demonstrates more M4 muscarinic receptor protein on direct than indirect striatal projection neurons. *Brain Res*, 894, 12-20.

- Scarduzio, M., Zimmerman, C.N., Jaunarajs, K.L., Wang, Q., Standaert, D.G. & McMahon, L.L. (2017) Strength of cholinergic tone dictates the polarity of dopamine D2 receptor modulation of striatal cholinergic interneuron excitability in DYT1 dystonia. *Exp Neurol*, 295, 162-175.
- Schmitz, C. & Hof, P.R. (2000) Recommendations for straightforward and rigorous methods of counting neurons based on a computer simulation approach. *J Chem Neuroanat*, 20, 93-114.
- Schulz, J.M. & Reynolds, J.N. (2013) Pause and rebound: sensory control of cholinergic signaling in the striatum. *Trends Neurosci*, 36, 41-50.
- Schwartzkroin, P.A., Roper, S.N. & Wenzel, H.J. (2004) Cortical dysplasia and epilepsy: animal models. *Adv Exp Med Biol*, 548, 145-174.
- Sciamanna, G., Hollis, R., Ball, C., Martella, G., Tassone, A., Marshall, A., Parsons, D., Li, X., Yokoi, F., Zhang, L., Li, Y., Pisani, A. & Standaert, D.G. (2012) Cholinergic dysregulation produced by selective inactivation of the dystonia-associated protein torsinA. *Neurobiol Dis*, 47, 416-427.
- Sciamanna, G., Tassone, A., Martella, G., Mandolesi, G., Puglisi, F., Cuomo, D., Madeo, G., Ponterio, G., Standaert, D.G., Bonsi, P. & Pisani, A. (2011) Developmental profile of the aberrant dopamine D2 receptor response in striatal cholinergic interneurons in DYT1 dystonia. *PLoS one*, 6, e24261.
- Servent, D., Blanchet, G., Mourier, G., Marquer, C., Marcon, E. & Fruchart-Gaillard, C. (2011) Muscarinic toxins. *Toxicon*, 58, 455-463.
- Shapiro, R.A., Scherer, N.M., Habecker, B.A., Subers, E.M. & Nathanson, N.M. (1988) Isolation, sequence, and functional expression of the mouse M1 muscarinic acetylcholine receptor gene. *J Biol Chem*, 263, 18397-18403.

- Sharott, A., Doig, N.M., Mallet, N. & Magill, P.J. (2012) Relationships between the firing of identified striatal interneurons and spontaneous and driven cortical activities in vivo. *J Neurosci*, 32, 13221-13236.
- Sharott, A., Vinciati, F., Nakamura, K.C. & Magill, P.J. (2017) A Population of Indirect Pathway Striatal Projection Neurons Is Selectively Entrained to Parkinsonian Beta Oscillations. *J Neurosci*, 37, 9977-9998.
- Shen, W., Hamilton, S.E., Nathanson, N.M. & Surmeier, D.J. (2005) Cholinergic suppression of KCNQ channel currents enhances excitability of striatal medium spiny neurons. *J Neurosci*, 25, 7449-7458.
- Shen, W., Plotkin, J.L., Francardo, V., Ko, W.K., Xie, Z., Li, Q., Fieblinger, T., Wess, J., Neubig, R.R., Lindsley, C.W., Conn, P.J., Greengard, P., Bezard, E., Cenci, M.A. & Surmeier, D.J. (2015) M4 Muscarinic Receptor Signaling Ameliorates Striatal Plasticity Deficits in Models of L-DOPA-Induced Dyskinesia. *Neuron*, 88, 762-773.
- Shen, W., Tian, X., Day, M., Ulrich, S., Tkatch, T., Nathanson, N.M. & Surmeier, D.J. (2007) Cholinergic modulation of Kir2 channels selectively elevates dendritic excitability in striatopallidal neurons. *Nat Neurosci*, 10, 1458-1466.
- Shepherd, G.M. (2013) Corticostriatal connectivity and its role in disease. *Nat Rev Neurosci*, 14, 278-291.
- Silberberg, G. & Bolam, J.P. (2015) Local and afferent synaptic pathways in the striatal microcircuitry. *Curr Opin Neurobiol*, 33, 182-187.
- Singh, A., Zhi, L. & Zhang, H. (2019) LRRK2 and mitochondria: Recent advances and current views. *Brain Res*, 1702, 96-104.
- Smith, R., Chung, H., Rundquist, S., Maat-Schieman, M.L., Colgan, L., Englund, E., Liu, Y.J., Roos, R.A., Faull, R.L., Brundin, P. & Li, J.Y. (2006) Cholinergic neuronal defect without cell loss in Huntington's disease. *Hum Mol Genet*, 15, 3119-3131.

- Spear, L.P. & Brake, S.C. (1983) Periadolescence: age-dependent behavior and psychopharmacological responsivity in rats. *Dev Psychobiol*, 16, 83-109.
- Starr, P.A., Kang, G.A., Heath, S., Shimamoto, S. & Turner, R.S. (2008) Pallidal neuronal discharge in Huntington's disease: support for selective loss of striatal cells originating the indirect pathway. *Exp Neurol*, 211, 227-233.
- Steiner, H. & Tseng, K.-Y. (2010) Handbook of basal ganglia structure and function *Handbook of behavioral neuroscience vol 20*. Elsevier,, Amsterdam.
- Stirpe, F., Gasperi-Campani, A., Barbieri, L., Falasca, A., Abbondanza, A. & Stevens, W.A. (1983) Ribosome-inactivating proteins from the seeds of *Saponaria officinalis* L. (soapwort), of *Agrostemma githago* L. (corn cockle) and of *Asparagus officinalis* L. (asparagus), and from the latex of *Hura crepitans* L. (sandbox tree). *Biochem J*, 216, 617-625.
- Stocco, A., Lebiere, C. & Anderson, J.R. (2010) Conditional routing of information to the cortex: a model of the basal ganglia's role in cognitive coordination. *Psychol Rev*, 117, 541-574.
- Stuber, G.D., Hnasko, T.S., Britt, J.P., Edwards, R.H. & Bonci, A. (2010) Dopaminergic terminals in the nucleus accumbens but not the dorsal striatum corelease glutamate. *J Neurosci*, 30, 8229-8233.
- Surmeier, D.J., Reiner, A., Levine, M.S. & Ariano, M.A. (1993) Are neostriatal dopamine receptors co-localized? *Trends Neurosci*, 16, 299-305.
- Takagi, H., Somogyi, P., Somogyi, J. & Smith, A.D. (1983) Fine structural studies on a type of somatostatin-immunoreactive neuron and its synaptic connections in the rat neostriatum: a correlated light and electron microscopic study. *J Comp Neurol*, 214, 1-16.
- Tan, U. (1987) Paw preferences in dogs. *Int J Neurosci*, 32, 825-829.

- Tan, U., Yaprak, M. & Kutlu, N. (1990) Paw preference in cats: distribution and sex differences. *Int J Neurosci*, 50, 195-208.
- Tande, D., Hoglinger, G., Debeir, T., Freundlieb, N., Hirsch, E.C. & Francois, C. (2006) New striatal dopamine neurons in MPTP-treated macaques result from a phenotypic shift and not neurogenesis. *Brain*, 129, 1194-1200.
- Tanimura, A., Pancani, T., Lim, S.A.O., Tubert, C., Melendez, A.E., Shen, W. & Surmeier, D.J. (2017) Striatal cholinergic interneurons and Parkinson's disease. *Eur J Neurosci*.
- Taverna, S., Canciani, B. & Pennartz, C.M. (2007) Membrane properties and synaptic connectivity of fast-spiking interneurons in rat ventral striatum. *Brain Res*, 1152, 49-56.
- Taylor, J.R., Morshed, S.A., Parveen, S., Mercadante, M.T., Scahill, L., Peterson, B.S., King, R.A., Leckman, J.F. & Lombroso, P.J. (2002) An animal model of Tourette's syndrome. *Am J Psychiatry*, 159, 657-660.
- Tepper, J.M. & Bolam, J.P. (2004) Functional diversity and specificity of neostriatal interneurons. *Curr Opin Neurobiol*, 14, 685-692.
- Tepper, J.M., Tecuapetla, F., Koos, T. & Ibanez-Sandoval, O. (2010) Heterogeneity and diversity of striatal GABAergic interneurons. *Front Neuroanat*, 4, 150.
- Threlfell, S. & Cragg, S.J. (2011) Dopamine signaling in dorsal versus ventral striatum: the dynamic role of cholinergic interneurons. *Front Syst Neurosci*, 5, 11.
- Threlfell, S., Lalic, T., Platt, N.J., Jennings, K.A., Deisseroth, K. & Cragg, S.J. (2012) Striatal dopamine release is triggered by synchronized activity in cholinergic interneurons. *Neuron*, 75, 58-64.
- Tippett, L.J., Waldvogel, H.J., Thomas, S.J., Hogg, V.M., van Roon-Mom, W., Synek, B.J., Graybiel, A.M. & Faull, R.L. (2007) Striosomes and mood dysfunction in Huntington's disease. *Brain*, 130, 206-221.

- Tops, M., Koole, S.L., H, I.J. & Buisman-Pijlman, F.T. (2014) Why social attachment and oxytocin protect against addiction and stress: Insights from the dynamics between ventral and dorsal corticostriatal systems. *Pharmacol Biochem Behav*, 119, 39-48.
- Trowill, J.A., Panksepp, J. & Gandelman, R. (1969) An incentive model of rewarding brain stimulation. *Psychol Rev*, 76, 264-281.
- Tubert, C., Taravini, I.R.E., Flores-Barrera, E., Sanchez, G.M., Prost, M.A., Avale, M.E., Tseng, K.Y., Rela, L. & Murer, M.G. (2016) Decrease of a Current Mediated by Kv1.3 Channels Causes Striatal Cholinergic Interneuron Hyperexcitability in Experimental Parkinsonism. *Cell Rep*, 16, 2749-2762.
- Tucci, V., Achilli, F., Blanco, G., Lad, H.V., Wells, S., Godinho, S. & Nolan, P.M. (2007) Reaching and grasping phenotypes in the mouse (*Mus musculus*): a characterization of inbred strains and mutant lines. *Neuroscience*, 147, 573-582.
- Unzai, T., Kuramoto, E., Kaneko, T. & Fujiyama, F. (2017) Quantitative Analyses of the Projection of Individual Neurons from the Midline Thalamic Nuclei to the Striosome and Matrix Compartments of the Rat Striatum. *Cereb Cortex*, 27, 1164-1181.
- Usunoff, K.G., Hassler, R., Romansky, K., Usunova, P. & Wagner, A. (1976) The nigrostriatal projection in the cat. Part 1. Silver impregnation study. *J Neurol Sci*, 28, 265-288.
- Valente, E.M., Warner, T.T., Jarman, P.R., Mathen, D., Fletcher, N.A., Marsden, C.D., Bhatia, K.P. & Wood, N.W. (1998) The role of DYT1 in primary torsion dystonia in Europe. *Brain*, 121 ( Pt 12), 2335-2339.
- Vertes, R.P., Linley, S.B. & Hoover, W.B. (2015) Limbic circuitry of the midline thalamus. *Neurosci Biobehav Rev*, 54, 89-107.
- Vonsattel, J.P. & DiFiglia, M. (1998) Huntington disease. *J Neuropathol Exp Neurol*, 57, 369-384.

- Voorn, P., Vanderschuren, L.J., Groenewegen, H.J., Robbins, T.W. & Pennartz, C.M. (2004) Putting a spin on the dorsal-ventral divide of the striatum. *Trends Neurosci*, 27, 468-474.
- Wamsley, B. & Fishell, G. (2017) Genetic and activity-dependent mechanisms underlying interneuron diversity. *Nat Rev Neurosci*, 18, 299-309.
- Wang, Z., Kai, L., Day, M., Ronesi, J., Yin, H.H., Ding, J., Tkatch, T., Lovinger, D.M. & Surmeier, D.J. (2006) Dopaminergic control of corticostriatal long-term synaptic depression in medium spiny neurons is mediated by cholinergic interneurons. *Neuron*, 50, 443-452.
- Watabe-Uchida, M., Zhu, L., Ogawa, S.K., Vamanrao, A. & Uchida, N. (2012) Whole-brain mapping of direct inputs to midbrain dopamine neurons. *Neuron*, 74, 858-873.
- Wenk, G.L. & Olson, D.S. (1984) Recovery of neocortical choline acetyltransferase activity following ibotenic acid injection into the nucleus basalis of Meynert in rats. *Brain Research*, 293, 184-186.
- West, M.J. (2012) *Basic stereology for biologists and neuroscientists*. Cold Spring Harbor Laboratory Press, Cold Spring Harbor.
- West, M.J., Slomianka, L. & Gundersen, H.J. (1991) Unbiased stereological estimation of the total number of neurons in the subdivisions of the rat hippocampus using the optical fractionator. *Anat Rec*, 231, 482-497.
- White, N.M. & Hiroi, N. (1998) Preferential localization of self-stimulation sites in striosomes/patches in the rat striatum. *Proc Natl Acad Sci U S A*, 95, 6486-6491.
- Wichmann, T. & DeLong, M.R. (1996) Functional and pathophysiological models of the basal ganglia. *Curr Opin Neurobiol*, 6, 751-758.
- Wichmann, T. & DeLong, M.R. (2003) Functional neuroanatomy of the basal ganglia in Parkinson's disease. *Adv Neurol*, 91, 9-18.



Wickens, J. (1993) *A theory of the striatum*. Pergamon, Oxford.

Wickens, J.R., Begg, A.J. & Arbuthnott, G.W. (1996) Dopamine reverses the depression of rat corticostriatal synapses which normally follows high-frequency stimulation of cortex in vitro. *Neuroscience*, 70, 1-5.

Wiley, R.G., Oeltmann, T.N. & Lappi, D.A. (1991) Immunolesioning: selective destruction of neurons using immunotoxin to rat NGF receptor. *Brain Res*, 562, 149-153.

Wilson, C.J. (2005) The mechanism of intrinsic amplification of hyperpolarizations and spontaneous bursting in striatal cholinergic interneurons. *Neuron*, 45, 575-585.

Wilson, C.J. (2013) Active decorrelation in the basal ganglia. *Neuroscience*, 250, 467-482.

Wilson, C.J., Chang, H.T. & Kitai, S.T. (1990) Firing patterns and synaptic potentials of identified giant aspiny interneurons in the rat neostriatum. *J Neurosci*, 10, 508-519.

Wilson, C.J. & Goldberg, J.A. (2006) Origin of the slow afterhyperpolarization and slow rhythmic bursting in striatal cholinergic interneurons. *J Neurophysiol*, 95, 196-204.

Wilson, C.J. & Groves, P.M. (1980) Fine structure and synaptic connections of the common spiny neuron of the rat neostriatum: a study employing intracellular inject of horseradish peroxidase. *J Comp Neurol*, 194, 599-615.

Wilson, C.J. & Groves, P.M. (1981) Spontaneous firing patterns of identified spiny neurons in the rat neostriatum. *Brain Res*, 220, 67-80.

Wouterlood, F.G., Hartig, W., Groenewegen, H.J. & Voorn, P. (2012) Density gradients of vesicular glutamate- and GABA transporter-immunoreactive boutons in calbindinand mu-opioid receptor-defined compartments in the rat striatum. *J Comp Neurol*, 520, 2123-2142.

- Wu, Y. & Parent, A. (2000) Striatal interneurons expressing calretinin, parvalbumin or NADPH-diaphorase: a comparative study in the rat, monkey and human. *Brain Res*, 863, 182-191.
- Xenias, H.S., Ibanez-Sandoval, O., Koos, T. & Tepper, J.M. (2015) Are striatal tyrosine hydroxylase interneurons dopaminergic? *J Neurosci*, 35, 6584-6599.
- Xu, M., Kobets, A., Du, J.C., Lenington, J., Li, L., Banasr, M., Duman, R.S., Vaccarino, F.M., DiLeone, R.J. & Pittenger, C. (2015) Targeted ablation of cholinergic interneurons in the dorsolateral striatum produces behavioral manifestations of Tourette syndrome. *Proce Natl Acad Sci U S A*, 112, 893-898.
- Yael, D., Vinner, E. & Bar-Gad, I. (2015) Pathophysiology of tic disorders. *Mov Disord*, 30, 1171-1178.
- Yan, Z., Flores-Hernandez, J. & Surmeier, D.J. (2001) Coordinated expression of muscarinic receptor messenger RNAs in striatal medium spiny neurons. *Neuroscience*, 103, 1017-1024.
- Yan, Z. & Surmeier, D.J. (1996) Muscarinic (m2/m4) receptors reduce N- and P-type Ca<sup>2+</sup> currents in rat neostriatal cholinergic interneurons through a fast, membrane-delimited, G-protein pathway. *J Neurosci*, 16, 2592-2604.
- Yin, H.H. & Knowlton, B.J. (2006) The role of the basal ganglia in habit formation. *Nature reviews. Neuroscience*, 7, 464-476.
- Zhang, W., Yamada, M., Gomeza, J., Basile, A.S. & Wess, J. (2002) Multiple muscarinic acetylcholine receptor subtypes modulate striatal dopamine release, as studied with M1-M5 muscarinic receptor knock-out mice. *J Neurosci*, 22, 6347-6352.
- Zheng, T. & Wilson, C.J. (2002) Corticostriatal combinatorics: the implications of corticostriatal axonal arborizations. *J Neurophysiol*, 87, 1007-1017.

- Zhou, F.M., Liang, Y. & Dani, J.A. (2001) Endogenous nicotinic cholinergic activity regulates dopamine release in the striatum. *Nat Neurosci*, 4, 1224-1229.
- Zhou, F.M., Wilson, C.J. & Dani, J.A. (2002) Cholinergic interneuron characteristics and nicotinic properties in the striatum. *J Neurobiol*, 53, 590-605.
- Ztaou, S., Maurice, N., Camon, J., Guiraudie-Capraz, G., Kerkerian-Le Goff, L., Beurrier, C., Liberge, M. & Amalric, M. (2016) Involvement of Striatal Cholinergic Interneurons and M1 and M4 Muscarinic Receptors in Motor Symptoms of Parkinson's Disease. *J Neurosci*, 36, 9161-9172.